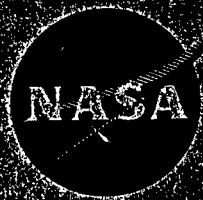NASA
SPACE VEHICLE
DESIGN CRITERIA
(CHEMICAL PROPULSION)

NASA SP-8113

LIQUID ROCKET ENGINE

COMBUSTION STABILIZATION DEVICES

NASA

NOVEMBER 1974

NATIONAL AERONAUTICS AND SPACE ADMINISTRATION

FOREWORD

NASA experience has indicated a need for uniform criteria for the design of space vehicles. Accordingly, criteria are being developed in the following areas of technology:

> Environment
> Structures
> Guidance and Control
> Chemical Propulsion

Individual components of this work will be issued as separate monographs as soon as they are completed. This document, part of the series on Chemical Propulsion, is one such monograph. A list of all monographs issued prior to this one can be found on the final pages of this document.

These monographs are to be regarded as guides to design and not as NASA requirements, except as may be specified in formal project specifications. It is expected, however, that these documents, revised as experience may indicate to be desirable, eventually will provide uniform design practices for NASA space vehicles.

This monograph, "Liquid Rocket Engine Combustion Stabilization Devices," was prepared under the direction of Howard W. Douglass, Chief, Design Criteria Office, Lewis Research Center; project management was by Harold Schmidt assisted by Lionel Levinson. The monograph was written by L. P. Combs, C. L. Oberg, T. A. Coultas, and W. H. Evers, Jr., Rocketdyne Division, Rockwell International Corporation, and was edited by Russell B. Keller, Jr. of Lewis. To assure technical accuracy of this document, scientists and engineers throughout the technical community participated in interviews, consultations, and critical reviews of the text. In particular, G. D. Garrison of Pratt & Whitney Aircraft Division of United Aircraft Corporation; D. T. Harrje of Princeton University; J. M. McBride of Aerojet Liquid Rocket Company; R. R. Weiss of the Air Force Rocket Propulsion Laboratory; and R. J. Priem of the Lewis Research Center individually and collectively reviewed the monograph in detail.

Comments concerning the technical content of this monograph will be welcomed by the National Aeronautics and Space Administration, Lewis Research Center (Design Criteria Office), Cleveland, Ohio 44135.

November 1974

i

GUIDE TO THE USE OF THIS MONOGRAPH

The purpose of this monograph is to organize and present, for effective use in design, the significant experience and knowledge accumulated in development and operational programs to date. It reviews and assesses current design practices, and from them establishes firm guidance for achieving greater consistency in design, increased reliability in the end product, and greater efficiency in the design effort. The monograph is organized into two major sections that are preceded by a brief introduction and complemented by a set of references.

The State of the Art, section 2, reviews and discusses the total design problem, and identifies which design elements are involved in successful design. It describes succinctly the current technology pertaining to these elements. When detailed information is required, the best available references are cited. This section serves as a survey of the subject that provides background material and prepares a proper technological base for the *Design Criteria* and Recommended Practices.

The *Design Criteria*, shown in italics in section 3, state clearly and briefly what rule, guide, limitation, or standard must be imposed on each essential design element to assure successful design. The *Design Criteria* can serve effectively as a checklist of rules for the project manager to use in guiding a design or in assessing its adequacy.

The Recommended Practices, also in section 3, state how to satisfy each of the criteria. Whenever possible, the best procedure is described; when this cannot be done concisely, appropriate references are provided. The Recommended Practices, in conjunction with the *Design Criteria,* provide positive guidance to the practicing designer on how to achieve successful design.

Both sections have been organized into decimally numbered subsections so that the subjects within similarly numbered subsections correspond from section to section. The format for the Contents displays this continuity of subject in such a way that a particular aspect of design can be followed through both sections as a discrete subject.

The design criteria monograph is not intended to be a design handbook, a set of specifications, or a design manual. It is a summary and a systematic ordering of the large and loosely organized body of existing successful design techniques and practices. Its value and its merit should be judged on how effectively it makes that material available to and useful to the designer.

CONTENTS

vi

LIST OF FIGURES

vii

viii

LIST OF TABLES

LIQUID ROCKET ENGINE

COMBUSTION STABILIZATION DEVICES

1. INTRODUCTION

The problem of combustion instability, or oscillatory combustion, has been encountered in nearly all rocket engine development programs. Combustion instability severely impairs the operation of both the engine and the vehicle system, and considerable effort therefore has been directed toward solving the instability problem. In general, combustion instability results from a coupling of the combustion process and the fluid dynamics of the engine system. By this coupling, the combustion process delivers energy to pressure and velocity oscillations in the combustion chamber. Consequently, combustion instability may be significantly reduced or eliminated either by reducing the coupling of the oscillations and the driving combustion process or by increasing the damping inherent in the engine system. This monograph discusses the design of devices that are assumed to reduce coupling – combustion chamber baffles – and devices that are assumed to increase damping – acoustic absorbers. Methods of modifying the combustion process (e.g., changing injection element characteristics) as a means of achieving combustion stability are not considered to be within the scope of the monograph.

The basic objective in approaching the combustion instability problem, with either baffles or absorbers, is to achieve adequate stabilization as simply as possible. Thus, for example, designs using simple, uncooled baffle structures are fully explored before designs using complicated, internally cooled baffle structures are considered. At present, however, few well-defined, established criteria exist for selection of baffle configurations, lengths, or spacings that will lead to stable operation of the engine. Most designs in use today were based on experience with similar combustion-chamber configurations, propellant combinations, and operating conditions. Analytical approaches to baffle design are quite new and, although not yet well established, show considerable promise. Baffle design as treated in this monograph therefore makes use of both empirical and analytical methods.

During normal operation and, in particular, during unstable combustion, baffles may be subjected to large transient stresses, high heat loads, and corrosive environments. Again,

1

both analytical and empirical techniques for static and dynamic stress analyses, thermal analyses, and chemical compatibility analyses are discussed.

Baffles can affect existing engine configurations. For example, the use of baffles necessitates discontinuities in injection patterns that, in turn, produce irregularities in the combustion-product flowfields and thereby produce poor performance. Baffle designs, therefore, interact directly with injector and combustion-chamber designs. Less direct interactions with propellant feed systems, thrust vector control systems, stability rating devices, and instrumentation systems may also be encountered. As shown in the monograph, early recognition of potential interactions is essential to minimization of deleterious effects.

Acoustic absorber design is based on increasing the damping inherent in the engine system. As in the case of baffles, few well-established guides for design exist. Analytical techniques for calculating and optimizing the absorber damping contribution are discussed, and empirical results are presented. The analytical calculations have shown good qualitative correlation with test results and are considered reliable. Since the damping provided by an acoustic absorber is strongly dependent on the acoustic impedance properties of the absorber, considerable emphasis is placed on proper measurement and calculation of those properties. Detailed methods for calculating acoustic impedance are given in Appendix A.

For both baffles and absorbers, the monograph treats the problem of converting the results of analysis, observation, and test into useful structures that will provide the desired combustion stability over the required lifetime of the rocket engine. To this end, the details of configuration selection, construction, thermal control, and confirmation testing are presented in terms of the practices that have been used successfully in the design of baffles and absorbers for combustion chambers in operational engines.

2

2. STATE OF THE ART

The state of the art of the design and use of combustion stabilization devices in liquid propellant rocket engines is discussed in the sections that follow. Both baffles and acoustic absorbers are treated in detail. A complete description of the phenomenon of combustion instability may be found in the major reference book on the subject (ref. 1); there, the theory and much detail on the work to date on combustion instability is presented. However, much of the material in reference 1 must be considered advanced technology and to some extent unproved. The emphasis in this monograph is on proved techniques that produced successful hardware.

2.1 BAFFLES

Baffles have been used successfully to prevent transverse acoustic modes of combustion instability; baffles have little if any effect on feed-system-coupled modes or longitudinal acoustic modes of instability. The transverse modes (i.e., tangential and radial), for which baffles have been found effective, are characterized by oscillatory pressure waves and gas-particle motion parallel to the propellant injector face. Pressure waves and gas motion affect the propellant combustion processes in a manner such that transient energy addition to each wave exceeds that wave's energy losses.

Several theories have been postulated to describe the method by which combustion-chamber baffles can bring about stable combustion. These theories can be grouped into two general classes. The first class postulates that baffles affect combustion instability by reducing the coupling of the combustion process and the oscillatory gas motion. One theory in this class presumes that baffles function by disrupting transverse gas motions; an allied theory proposes that they work by shielding certain sensitive regions of the combustion. Another theory in this class claims that the higher acoustic frequencies associated with baffle compartments result in lowered coupling. The second class of theories postulates that baffles function by increasing damping in the combustion chamber. One theory considers that oscillatory energy is dissipated by baffle tip vortices. Other theories in this class presume that baffles produce a drag on the flow over baffles and thereby increase the dissipation of oscillatory energy.

The most important, and least understood, aspect of baffle design is how to ensure that the baffles will eliminate the instability. This elimination in fact entails using an adequate number of sufficiently long baffles to achieve the proper baffle compartment size as related to chamber acoustics. The other major aspects of baffle design deal with materials, structural design, thermal adequacy, and baffle interaction with other engine components.

3

Since the discussion of baffles (and acoustic absorbers as well) will make frequent references to the acoustics of the combustion chamber, as approximated by the acoustic modes of a corresponding closed chamber, a short discussion of classical acoustics will open the next section. This general background will prove helpful in understanding subsequent sections.

2.1.1 Combustion Chamber Acoustics

The simplest and most widely used approach for the design of baffles is to place them near the gas velocity antinodes of the appropriate chamber acoustic resonance. This procedure requires knowledge of the acoustic resonance characteristics, which are usually estimated from the acoustics of a corresponding closed chamber. Consideration has usually been confined to the acoustics of the unbaffled combustion chamber. Acoustic analyses of the baffled combustion chamber are sometimes attempted to give semi-quantitative indications of (1) degree of attenuation produced and (2) changes in modal frequencies and pressure distribution patterns; alternatively, similar information may be obtained from acoustic bench experiments with baffled model chambers. The more complicated and more costly analytical approaches are still qualitative, falling short of quantitative validity.

A recent program (refs. 2, 3, and 4) aimed at developing methods for predicting the stabilizing effects of baffles has not yet been successful; however, it was demonstrated that the acoustics of baffled chambers may be calculated.

Acoustic analysis. — Analysis of the acoustics of a closed unbaffled chamber corresponding to the combustion chamber is based on solving the wave equation with boundary conditions appropriate to the particular chamber configuration. For conventional cylindrical chambers, for example, solutions for simple right circular cylindrical cavities with both ends closed and with no through-flow are commonly used. The mathematical approach (separation of variables) and typical results are given in references 5 and 6; also given are solutions for annular cylindrical chambers.

The resonant frequency and the locations of the maximum amplitude pressure and velocities vary with the acoustic mode. The transverse (tangential and radial) eigenvalues $\beta_{m,n}$ and longitudinal eigenvalues q give the oscillation frequency f in Hz as

$$f_{m,n,q} = c \sqrt{\left(\frac{\beta_{m,n}}{D_{ch}}\right)^2 + \left(\frac{q}{L_{ch}}\right)^2} \tag{1}$$

4

where

f = oscillation frequency

c = velocity of sound

$\beta_{m,n}$ = transverse eigenvalue from table I

m,n = tangential and radial mode numbers (0, 1, 2. . . .)

q = longitudinal eigenvalue (longitudinal mode number), q = 0, 1, 2. . . .

D_{ch} = chamber diameter

L_{ch} = chamber length

The pressure and velocity profiles for the fundamental tangential-mode traveling wave are shown in figure 1 (ref. 5). Baffles in the chamber, unless they are inordinately short, interfere with the traveling waves. This effect is an indication of the prime mechanism by which baffles are believed to work: the prevention of transverse gas displacement by the baffle surfaces. An integral part of this mechanism is reflection of pressure waves from the baffles. For greatest effectiveness, therefore, baffles have been located in regions of maximum acoustic particle displacement; i.e., positioned at velocity antinodal planes (for tangential and longitudinal modes, the pressure nodal planes). These positions may then become pressure antinodes for a new wave. Conversely, a baffle positioned at an established pressure antinodal plane normally has very little effect on oscillation amplitudes.

Acoustic model experiments. — Some indications of baffle effectiveness have been obtained by performing acoustic bench experiments (refs. 1 and 8) with scale models of combustion chambers. Care must be exercised in interpreting the results of such experiments because the test amplitudes are relatively low. The models are usually constructed as closed chambers, with solid plates representing the injector and sonic plane at the nozzle throat. Small electromagnetic speakers are positioned at appropriate locations in the model to drive the chamber's acoustic resonances. Resonant characteristics are discerned with strategically located or movable probe-type microphones (ref. 8). Typically, sound pressure level and phase at a given point are compared with values at a reference point.

One very useful application of this technique is to identify the acoustic resonances that can be driven in a complicated chamber configuration. The frequency of driver oscillation is gradually changed, and the frequency and sound pressure level (SPL) at fixed points in the chamber are recorded as functions of time. Resonances are easily seen as peaks on the SPL records. Many resonances can be identified immediately from their frequencies and the

5

Table I. – Transverse Eigenvalues in a Cylindrical
Chamber (ref. 7)

Mode	m	n	$\beta_{m,n}$
1st Tangential	1	0	0.586
2nd Tangential	2	0	0.972
3rd Tangential	3	0	1.34
4th Tangential	4	0	1.69
5th Tangential	5	0	2.04
6th Tangential	6	0	2.39
7th Tangential	7	0	2.73
8th Tangential	8	0	3.07
1st Radial	0	1	1.22
2nd Radial	0	2	2.23
3rd Radial	0	3	3.24
4th Radial	0	4	4.24
Combined	1	1	1.70
Combined	2	1	2.13
Combined	3	1	2.55
Combined	4	1	2.95
Combined	5	1	3.35
Combined	1	2	2.71
Combined	2	2	3.17
Combined	3	2	3.61
Combined	1	3	3.73

$\beta_{m,0} \approx m/\pi$ when $m \gg 1$

$\beta_{m,n} \approx n + \dfrac{m}{2} + \dfrac{1}{4}$ when $n \gg 1, n > m$

6
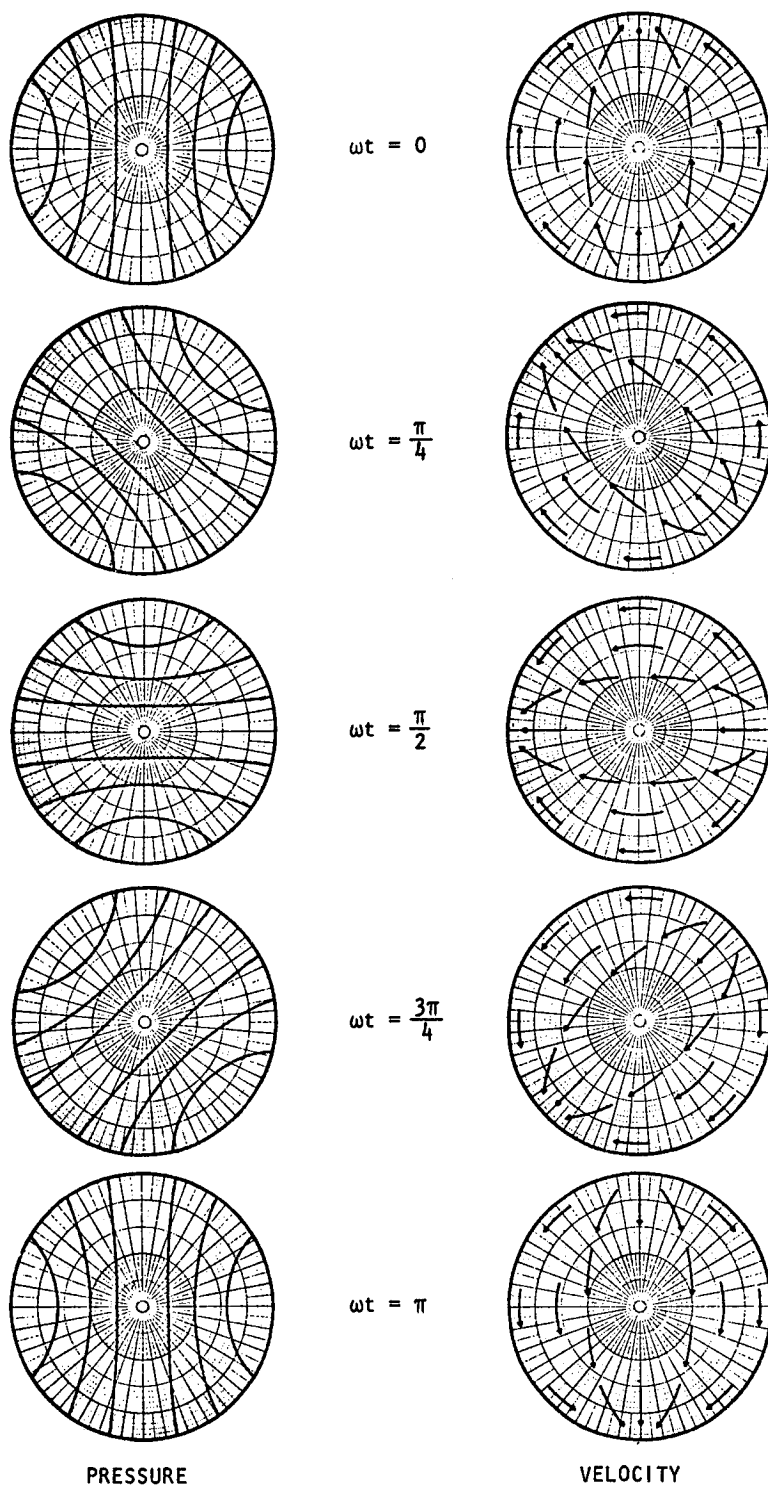
Figure 1. — Pressure and velocity profiles for fundamental tangential-mode traveling wave (ref. 5).

7

recorded SPL's at various positions. For others, subsequent experiments may need to be conducted in which driver frequency is held constant at that of the resonance while more detailed spatial amplitude and phase measurements are made. If desired, particle velocity characteristics may also be measured with hot-wire anemometers. The experimental techniques are described in references 8 and 9.

Baffle effectiveness is studied in acoustic models primarily by comparing sound pressure levels for chambers with and without baffles. Potential baffle effectiveness is presumed to be proportional to the attenuation of the modes of interest. This attenuation does not reflect the effects of high-amplitude waves that occur in the combustion chamber. For modes that are attenuated but not completely eliminated, a measurable parameter is the acoustic decay coefficient. Decay coefficients are obtained from acoustic model experiments by abruptly stopping the oscillatory power to the acoustic driver and monitoring the temporal decay in amplitude of a particular resonance that was being driven. Part (a) of figure 2 (ref. 9) shows
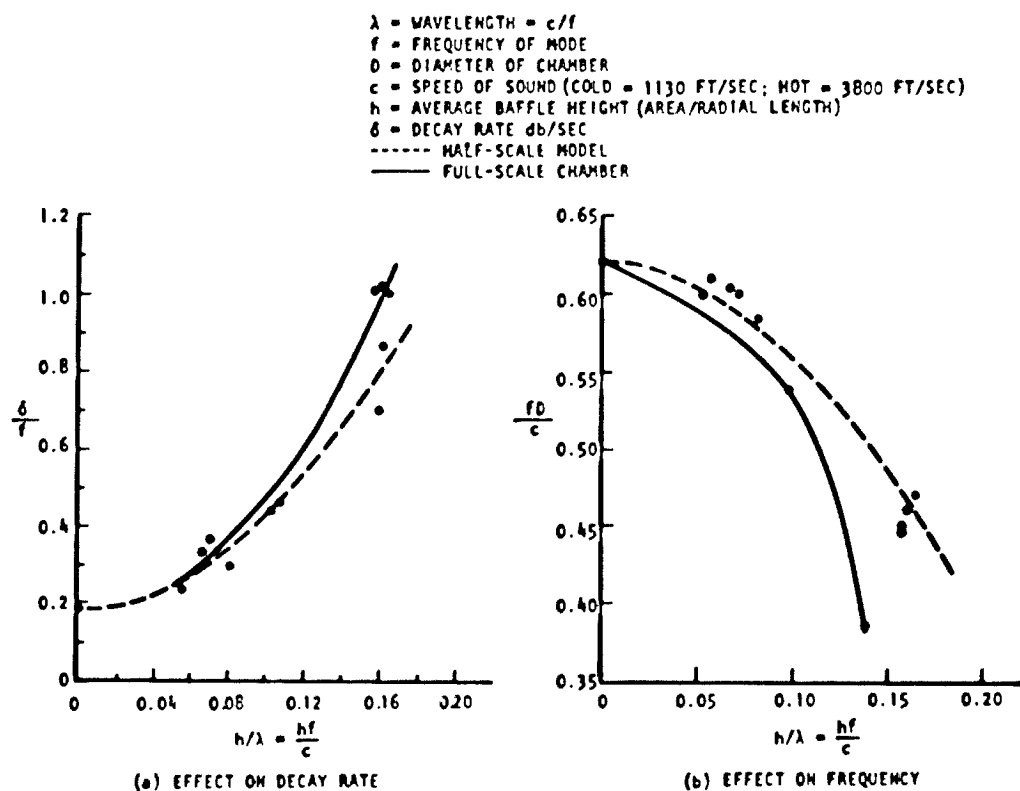
Figure 2. – Experimental results on effect of baffle height on first tangential mode (ref. 9).

8

typical results of this type of model experiment and presents comparable data from studies with full-scale chambers. Care must be exercised in setting the driver frequencies because baffles lower the resonant frequencies of the modes that they affect most strongly. Examples of such reduction are shown in figure 2(b) *, which also shows that these model effects are comparable to actual combustion-chamber behavior.

2.1.2 Baffle Geometry

2.1.2.1 TRANSVERSE COMPARTMENT DIMENSIONS

Although the baffle length (sec. 2.1.2.2) may be adequate to prevent resonances of the entire combustion chamber, the baffle compartments themselves can sustain a compartment mode of instability. The probability of this kind of instability lies in the response of the combustion processes to a compartment resonance. Generally, the likelihood of instability decreases as the resonant frequency decreases. This relation, in turn, implies that small transverse spaces between baffles are beneficial. In practice, there are several limitations on the number of baffles that can be used and on how closely they may be spaced. To minimize the likelihood of compartment modes, the compartment dimensions are minimized within limits set by structure, thermal environment, interactions with injection ports, and similar parameters.

Baffle spacings that provide adequate stabilization most often have been arrived at by cut-and-try development testing. Personnel engaged in such developmental work have accumulated a body of experience that, although useful for a particular project, may not be applicable to new or different injector or chamber designs. Further, this experience is difficult to impart quantitatively to other designers. Recently, some success has been achieved in the application of analytical methods to the design of baffles. Because this approach can be (1) more nearly accurate quantitatively, (2) applied with greater confidence to situations outside the range of existing design experience, and (3) more readily imparted to other designers than can empirical knowledge, it is discussed first.

Nonlinear combustion analysis for compartment sizing. — Analytical models of combustion instability have been recognized for some time as desirable aids in designing baffles. An analytical approach to baffle design has been employed in some recent engine development programs (refs. 10 and 11). Limited experimental evaluations of the results look promising enough to warrant including an analytical examination of baffle spacing and length in any baffle design effort.

---

*The limiting nondimensional frequency as $h \to 0$ in a cylindrical chamber is $fD/c = 0.586$ (table I). The higher value in figure 2(b) apparently results from the noncylindrical chamber shape used for the test.

9

The analytical procedure makes use of a nonlinear combustion-instability model such as Priem's (ref. 12). A version of the Priem model for a linear chamber (ref. 13) is particularly appropriate for baffle compartment study and has been used in several design analyses (refs. 10 and 11). The general approach is as follows:

(1) Develop a detailed description of the steady-state-spray combustion field existing in the combustion chamber. Translate injection-element type and geometry, propellant velocities, and propellant properties into predicted propellant spray characteristics at some axial starting plane downstream of the injector face (ref. 14). Use a one-dimensional steady-state combustion model (ref. 15) to predict the nature of the combustion field downstream of the starting plane during stable operation; the results are input for the instability model. The output of this steady-state combustion model allows the calculation of parameters such as burning rate, liquid and gas velocities, and gas mixture ratio as a function of axial distance from the injector. From these data, determine a "most sensitive" axial location; this location is defined as the point at which the smallest pressure perturbation will cause an instability. Generally, at this point, the liquid and gas velocities are nearly equal and the burning rate is highest (ref. 11).

(2) Perform instability model calculations (refs. 11, 12, and 13) at the "most sensitive" zone to determine whether baffles are needed. If they are found necessary, the baffles must extend past the most sensitive zone. Perform sequential calculations with various model combustion widths (which now represent the spacing between adjacent baffles) to find a maximum baffle-compartment dimension that is predicted to afford adequate stability.

(3) Now, assume that the baffle compartments are sized to avert compartment modes of instability, and examine the stability of the combustion space downstream of the baffle tips. Using a diameter for the model chamber equal to that of the unbaffled chamber and starting from the most-sensitive-zone location, increase axial distance from the injector sequentially until some plane that is predicted to have adequate stability is reached. This plane is interpreted as defining a minimum baffle length for stabilization.

The analytical procedure assumes that there is no acoustic interaction between the baffle compartments and the unbaffled remainder of the chamber. Actual coupling should provide additional damping, so that the predicted compartment dimensions and baffle lengths should be conservatively small and long, respectively.

Experience guidelines for compartment sizing. — For many cylindrical chambers, burning a variety of propellants, adequate stabilization has been achieved with baffles spaced and oriented to produce maximum transverse compartment dimensions ranging between 6 in.

10

and 15 in. (15.2 cm and 38.1 cm)*. The data have been summarized by McBride (ref. 1, secs. 8.2.2 and 8.2.3) by comparing compartment dimensions to the wavelength of a particular instability. The recommendation derived from the study was that the maximum transverse dimension w_{max} (measured along baffle or chamber surfaces) should lie in the range

$$0.2 \lambda < w_{max} < 0.4 \lambda \qquad (2)$$

where λ is the instability wavelength. The lower limit appears to have been based largely on LO_2/LH_2** data of reference 16.

Now consider a hub- and-spoke baffle design (sec. 2.1.2.3) such that $w_\theta > w_r$:
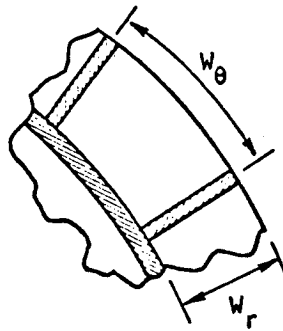
Then the tangential baffle spacing for suppressing tangential modes becomes

$$w_{\theta\ max} = (const) \lambda = (const) \frac{D_{ch}}{\beta_{m,0}} \qquad (3)$$

The tangential spacing is also related to the number of radial baffles N_B by

$$w_{\theta max} = \frac{\pi D_{ch}}{N_B} \qquad (4)$$

Hence, the quoted limits of $w_{\theta max}$ result in

---

*Parenthetical units here and elsewhere in the monograph are in the International System of Units (SI units). See Mechtly, E. A.: The International System of Units. Physical Constants and Conversion Factors, Second Revision. NASA SP-7012, 1973.

**Materials, symbols, and abbreviations are identified or defined in Appendix B.

$$\frac{\pi\beta_{m,0}}{0.2} > N_B \geq \frac{\pi\beta_{m,0}}{0.4} \qquad (5)$$

For the first tangential resonance ($\beta_{1,0} = 0.586$), the result is approximately

$$10 \geq N_B \geq 5 \text{ baffles}$$

Similarly, if $w_r > w_\theta$, the number of cylindrical baffle cans N_{CC} may be found to be approximately

$$\frac{1}{2}\left(\frac{\beta_{0,n}}{0.2} - 1\right) > N_{CC} > \frac{1}{2}\left(\frac{\beta_{0,n}}{0.4} - 1\right) \qquad (6)$$

where $\beta_{0,n}$ is the nth radial resonance.

Rounding off to the next larger integer for the first radial mode ($\beta_{0,1} = 1.22$),

$$3 > N_{CC} \geq 1 \qquad (7)$$

The values thus derived give wide ranges of design choice that must be narrowed for specific combustion chamber applications. Not only is a wide choice of the number of baffles given by the empirical equation for w_{max}, but it is obviously incorrect in the case of small combustion chambers, because the number of baffles is shown to be independent of chamber diameter. Such a relationship is obviously absurd since it would require tiny (1 in. diam.) chambers to have at least five baffles. The empirical process of narrowing the choice depends heavily upon past experience. Recitation of some general guidelines, none of which is infallible, and citation of some specific examples may be helpful.

Generally, the larger the chamber, the greater the possibility that more than the minimum number of baffles will be needed to accomplish adequate stabilization, as indicated in table II. The tabulation, although not complete or totally consistent since different propellants and injector types are included, shows that the average value for the parameter D_{ch}/N_B is about 3. Although the ratio D_{ch}/N_B is often used in the literature as a measure of baffle requirements, it appears that the ratio $D_{ch}/(N_B - 2)$ would be a considerably better parameter. The use of a single diametral or radial baffle does nothing to the first tangential mode except require that it stand instead of spin. Thus, the addition of one or two radial baffles has virtually no effect on the most common mode of instability. It is only when three baffles are used (i.e., $N_B = 3$ or $N_B - 2 = 1$) that a change is made in the instability mode.

12

Table II. – Relation of Chamber Diameter to Number of Baffles in Dynamically Stable Operational Engines

Engine	Chamber diameter, D_{ch}		Number of radial baffles, N_B	D_{ch}/N_B		$D_{ch}/(N_B - 2)$	
	in.	cm		in.	cm	in.	cm
RS-14*	3.2	8.1	3	1.1	2.8	3.2	8.1
LM Ascent*'	7.79	19.8	3	2.6	6.6	7.8	19.8
Titan Stage II	14.5	36.8	7	2.1	5.3	2.9	7.4
Apollo Service Module	17.6	44.7	5	3.5	8.9	5.9	14.9
Titan Stage I	20.0	50.8	7	2.9	7.4	4.0	10.2
Atlas Booster and H-1	20.4	51.8	6	3.4	8.6	5.1	13.0
F-1	39.0	99.1	8	4.9	12.4	6.5	16.5

*Also used absorber

In addition, it can be seen that by the use of $N_B - 2$ the ratio of maximum to minimum values for the parameter has been reduced from about 4.5 to about 2.7. Further, the two engines with the high numbers, the F-1 and the LM Ascent, are noted for extremely stable injectors; the former derives its stability from very large fuel orifices, the latter from a highly effective acoustic absorber. Thus, if one is to achieve a rule of thumb from this experience, it appears that a good empirical relationship worth remembering would indicate that when D_{ch} is expressed in inches the ratio $D_{ch}/(N_B - 2)$ should be not more than about 5.

However, D_{ch}/N_B or $D_{ch}/(N_B - 2)$ is almost totally dependent on the injector type and pattern and the propellant combination. Closer baffle spacing is required with injectors designed to produce good interpropellant mixing and finely atomized sprays than with "coarse" injectors (ref. 1, sec. 7.4.6, and ref. 17). Reference 17 presents minimum combustion response times determined for several injectors using LO_2/LH_2 propellants.

13

These values are indicative of maximum resonant frequencies allowable in a baffle cavity or combustion chamber. According to one theory, elaborated in references 18 and 19, if the period of the instability is less than the response time, the combustion will not respond to the instability wave and therefore will remain stable.

A rule of thumb sometimes applied is that there is little likelihood of instability if the baffle compartment transverse resonant frequency exceeds 5000 Hz. Many examples may be cited where stability was achieved with far lower frequencies (e.g., the even numbers of baffles in the foregoing list); most of these chambers had moderately coarse injection patterns and hole sizes. With very fine atomization and good interpropellant mixing, baffle compartment modes of instability at frequencies of over 9000 Hz have occurred. Design of baffle spacing to raise the lowest compartment resonances to even higher frequencies may be physically impractical. In that case, stabilization of the baffle compartment modes has sometimes been achieved by using some other device (e.g., an acoustic cavity) to provide auxiliary damping.

2.1.2.2 BAFFLE LENGTH

Baffle length is the distance downstream of the injector to which a baffle assembly extends. If the injector is curved or if baffle length is not constant across the injector face, it may be appropriate to define a mean baffle length. For example, with radial variation of baffle length, the expression

$$\overline{L}_B = \frac{1}{r_{ch}} \int_0^{r_{ch}} L_B(r)\, dr \qquad (7)$$

where

$\overline{L}_B$ = mean baffle length

r = radius, i.e., radial distance from chamber axis

$L_B(r)$ = baffle length at r

r_{ch} = radius of combustion chamber

has been used (refs. 1 and 9). For tangential modes, however, more influence is exerted on combustion stability by the outer portions of baffles than by the inner portions, so that such a definition appears incomplete. If baffles extend uniformly to a given chamber cross section, the baffle length at the chamber wall might be considered to be the appropriate minimum variable.

14

The length required to effect adequate stabilization varies among baffled liquid rocket engines by as much as an order of magnitude (½ in. [1.27 cm] for small storable-propellant engines to 5 in. [12.7 cm] for large toroidal aerospike engines). The requisite length appears to be influenced strongly by the propellant combination and the injector design and less strongly by combustion chamber design and operating conditions (see item 3 in the nonlinear combustion analysis previously described).

A recent experimental study of baffle spacing (ref. 20) indicates that it may be possible to determine the required baffle length from cold-flow analysis. Using cold-flow techniques originally developed by J. Rupe and described in references 14 and 15, Clayton found that the required baffle length for dynamic stability corresponded to the point of uniform propellant distribution in the chamber. This criterion was very successful in correlating baffle length with spray analysis.

Guidelines from hot-firing tests. — A majority of baffle lengths have been selected on the basis of past experience. Usually, experimental information with similar propellants, injector designs, and other parameters have served as a guide. Extension to designs or conditions beyond those for which direct experience has been established is always questionable, and experimental evaluation of new designs is essential.

Full-scale engine experience regarding baffle lengths frequently has agreed with results obtained in experiments with appropriate model chambers. For example, hot-firing tests with LOX/RP-1 propellants in the Atlas booster engine, the H-1 engine, and two-dimensional and annular model chambers consistently demonstrated that baffles 2.5 to 3 in. (6.3 to 7.6 cm) in length were needed to ensure stable operation. All the tests involved similar injector element types (self-impinging doublets) and design variables (hole sizes, spacings, impingement angles, etc.,) and essentially the same combustion-chamber contraction ratio and instability modal frequencies. Chamber pressure was varied from about 150 to 700 psi (1.03 to 4.83 MN/m²).

Subsequently, the combustion chamber for the F-1 engine was found to require about that same range of baffle lengths, even though this larger engine had sizeable increases in injection-element orifice sizes, chamber pressure, and maximum baffle compartment dimensions, while the chamber contraction ratio and acoustic frequencies were very appreciably decreased. There is a strong implication, based on the above LOX/RP-1 experience, that baffle length either is constant or depends on other parameters not varied in these tests, viz., injection element type and propellant combination. With LOX/RP-1 propellant, self-impinging element types (doublets and triplets) have nearly always been used. For experience with other injector types, other propellants must be investigated.

The variation of stability with baffle length was measured in a series of tests with Lunar Module Ascent Engine (LMAE) (ref. 21). For these tests, the injection elements in the baffles were plugged, and the baffle was sequentially shortened. The results from these tests are shown in figure 3 (ref. 21). For baffle lengths less than 0.75 in. (19 mm), instability was

15

	CAVITY DEPTH, IN.				RATING DEVICE
	NONE	1.1	1.5	1.75	
	●	○	◙	⊕	10-GRAIN PULSE GUN
	▲	△	◭	◮	20-GRAIN PULSE GUN
	■	□	◪	⊟	40-GRAIN PULSE GUN
	◆	◇	◈	⬗	6.5-GRAIN BOMB

NOTE:

1 IN. = 25.4 MM

DAMP TIME, MSEC
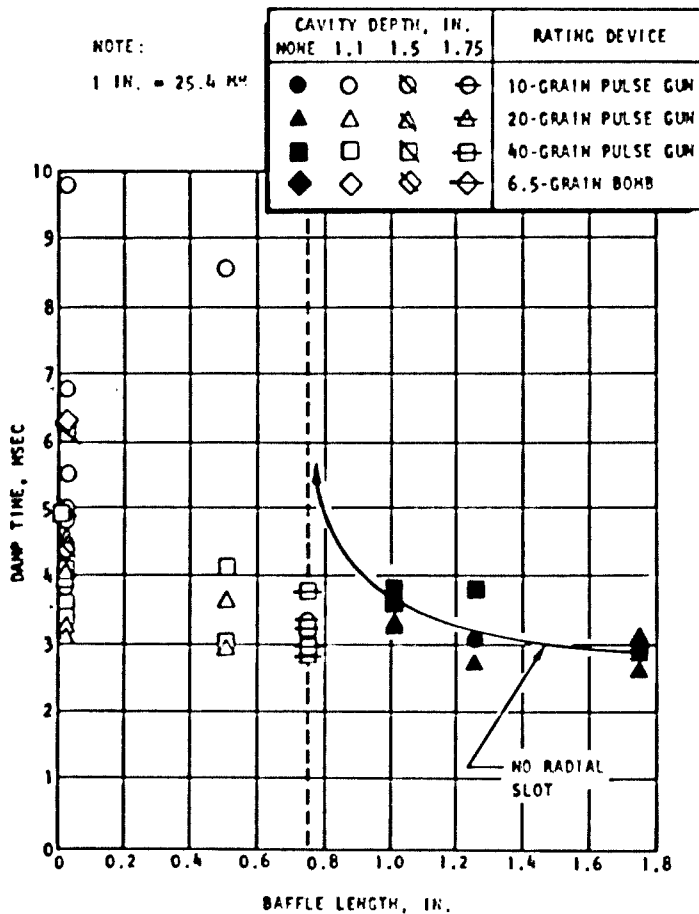
BAFFLE LENGTH, IN.

Figure 3. — Effect of baffle length and cavity depth on damp
time — Lunar Module Ascent Engine (ref. 21).

readily initiated without a quarterwave-type acoustic absorber. However, with the absorber, stability was maintained even when the baffle was removed entirely.

Baffles have sometimes been made too long because of improper diagnosis of instability problems. The two cases described below were annular chambers and had fairly large contraction ratios.

In the Extended Range Lance (XRL) booster engine (contraction ratio of three), baffles initially 3 in. (7.6 cm) long were insufficient to stop an anomalous first tangential mode.

16

This tangential mode was not clearly identified, but the frequency value was approximately that calculated for the first tangential. The decision was made to make the baffles 5 in. (12.7 cm) long. When this configuration was tested, the mode had a slightly lower frequency and the amplitude was decreased, but the instability remained. Later in the program, this particular instability was identified with resonance in the feed system and was completely eliminated by feed-system baffles. It is unlikely that the increase in baffle length provided much aid in instability suppression.

In a similar case, an aerospike engine (contraction ratio of 12, utilizing hydrogen and oxygen propellants) exhibited an eighth tangential mode of about 1500 Hz. The combustion chamber had baffles 3 in. (7.6 cm) long; they were extended to 5 in. (12.7 cm) with little change in results, as in the case above. It was later found that the instability that had been attributed to insufficient baffle length was actually a feed-system problem, and the problem was solved by modification of the feed system.

The proper approach, of course, is to be certain that the source of the instability lies in the combustion chamber before altering the chamber baffles.

Experimental guidelines. – Considerable experience has been accumulated with the cryogenic LO_2/LH_2 propellant combination and with the earth-storable propellants, primarily $N_2O_4/50{:}50$*. Some of these data were reviewed by McBride (ref. 1, secs. 8.2.2 and 8.2.3), who arrived at a conclusion that an optimum baffle length $L_{B\,opt}$ is proportional to chamber size for cylindrical chambers, i.e.,

$$L_{B\,opt} = (0.2 \text{ to } 0.3)D_{ch} \tag{8}$$

It has been frequently observed that there is a minimum effective baffle length below which stabilization cannot be ensured. Figure 4 (ref. 16) presents an example of a chamber in which baffles shorter than 1.0 in. were ineffective no matter how closely spaced. (It should be noted that the "McBride Criterion" (eq. (8)) appeared adequate for all baffles tested in reference 16 and thus would appear to give a generally conservative estimate.) When baffles longer than the minimum are used, a tradeoff of baffle length and maximum compartment size may be possible. It was proposed in reference 16 that, for baffles longer than the minimum effective, the maximum baffle compartment dimension could be as large as perhaps five times the baffle length. (This factor is just the slope of the stability boundary on the right hand side of figure 4, which happens to extrapolate nearly through the origin.) Considerably more data would be required to develop confidence in the approach, but it is interesting to consider the implications of the simple tradeoff relationship $L_B \geq \frac{1}{5} w_{max}$.

*50% N_2H_4: 50% UDMH, by weight.

17
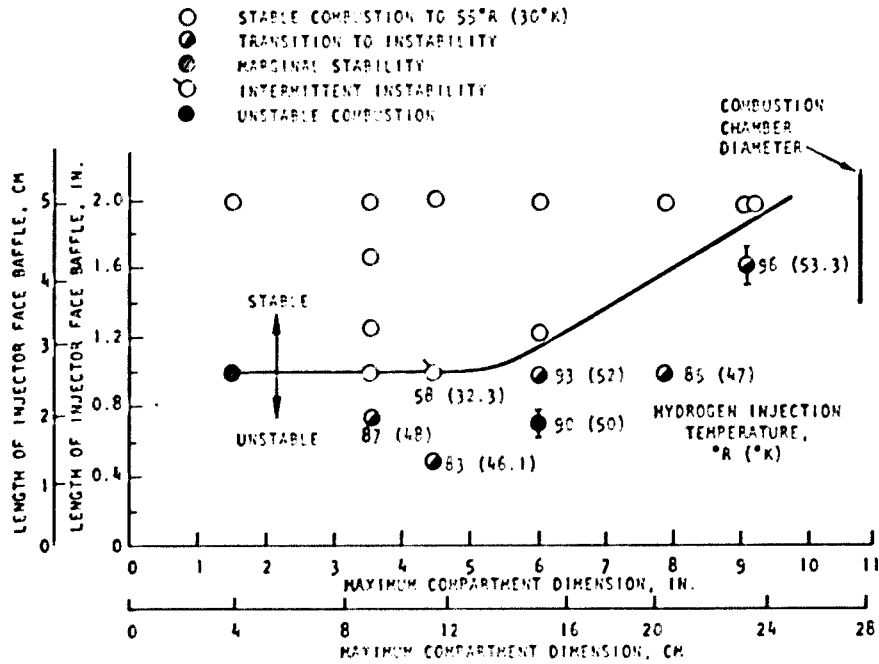
Figure 4. — Correlation of baffle length and maximum compartment dimension (LO_2/LH_2, coaxial jet, o'f = 5)(ref. 16).

If the largest compartment dimension is $w_{\theta\,max}$, the dimension is related to the number of radial baffle blades in a cylindrical combustion chamber by equation (4).

Then

$$\frac{l_B}{D_{ch}} \geq \frac{\pi}{5N_B} \qquad (9)$$

may be compared with McBride's recommendation (eq. (8)).

Denoting the baffle length (when the equality holds) by $l_{B\,min}$:

N_B	3	4	5	6
$L_{B\,min}/D_{ch}$	0.210	0.157	0.125	0.105

18

These values suggest that McBride's "optimum baffle length" could be appropriate only for three- or four-blade baffle configurations.

If the largest compartment dimension is $w_{r\,max}$, minimum baffle length may be related to the number of cylindrical cans by

$$\frac{L_{B\,min}}{D_{ch}} \approx \frac{1}{5(2\,N_{CC} + 1)}$$

$$\approx \frac{1}{15} \quad \text{for} \quad N_{CC} = 1 \tag{10}$$

$$\approx \frac{1}{25} \quad \text{for} \quad N_{CC} = 2$$

These numbers are appreciably smaller than the corresponding minimum blade lengths for a radial baffle. This difference suggests that a hub-and-spoke baffle configuration (sec. 2.1.2.3) with equal hub and spoke lengths may have hub lengths considerably in excess of the minimum when the spoke lengths are marginally larger than the minimum. This relation might partially account for the great preponderance of tangential modes among cases of instability observed with marginally adequate baffle designs.

2.1.2.3 CONFIGURATION

The nodal surfaces for the lower order modes in cylindrical and annular combustion chambers usually are radial planes or circular cylindrical surfaces. As a result, the plan view of common baffle shapes has continuous cylindrical cans positioned near the pressure nodes of the radial acoustic modes and plane radial vanes positioned to disrupt the tangential acoustic modes. These cans and vanes are combined to form a "hub-and-spoke" pattern. In other cases, only the tangential modes have been designed for, so that only radial vanes are employed. Both types of baffle design are illustrated in figure 5. On occasion, particularly in small chambers, the radial baffle blades have not extended to the center of the chamber; extreme examples of this are small baffle tabs extending only a fraction of a chamber radius from the chamber wall (sec. 2.1.2.3.1).

The number of radial vanes used depends largely upon the diameter of the combustion chamber as discussed in section 2.1.2.1. In general, an odd number of baffles is preferred over an even number, because an odd number (3, 5, 7, ...) of radial baffles can be aligned with the nodal pattern of the corresponding (3, 5, 7, ...) tangential mode, while an even number (4, 6, 8, ...) can be aligned with the nodes of the lower order (2, 3, 4, ...)

19

(a) RADIAL
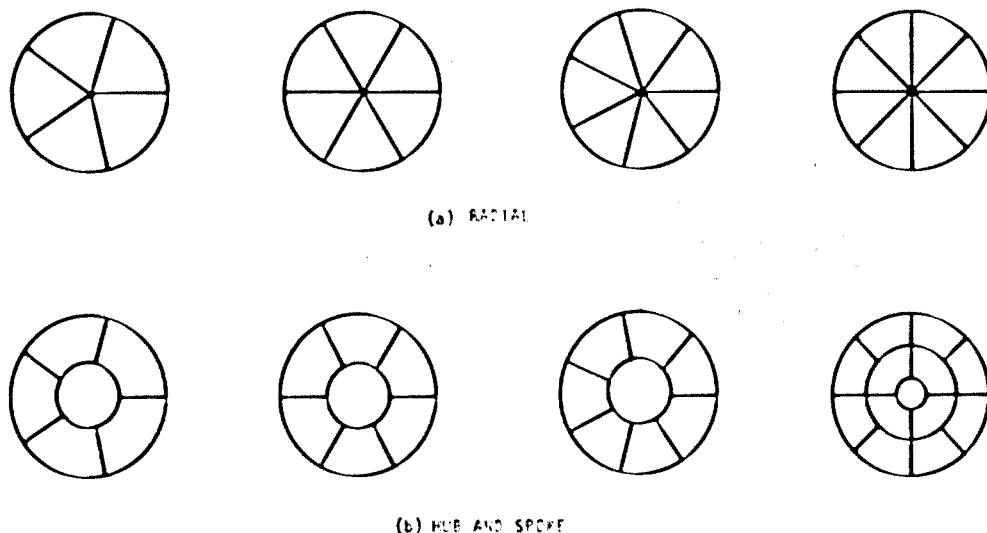
(b) HUB AND SPOKE

Figure 5. — Plan views of some typical radial blade and hub-and-spoke baffle designs.

tangential mode. There are occasional exceptions, but experience has shown that it is nearly axiomatic that lower order modes, if allowed, are more likely to be initiated and sustained than a higher frequency mode. Sometimes, however, structural convenience will insist on an even-number symmetrical baffle configuration.

Some examples of the results of a particular number of baffles illustrate the effects being discussed. A single radial baffle ensures only that the first tangential standing rather than traveling mode would be driven (fig. 6); two radial (one diametral) baffles have precisely the same effect. As shown in figure 7, three radial baffles are effective in eliminating the first- and second-order modes but have no effect on the third tangential mode, whereas four radial baffles are effective in eliminating the first- and third-order modes but the second and fourth would be unattenuated. Five radial baffles help prevent the occurrence of all modes having order lower than fifth, while six radial baffles affect the first, second, fourth, and fifth, but leave the third and sixth unattenuated; and so forth.

The foregoing discussion assumes that the baffles are long enough to be effective and that a given number of baffles is distributed with equal spaces between them. Nonuniform spacings and nonradial baffles have sometimes been advocated as a means of achieving greater stabilization with a given number of baffles. Some examples are sketched in figure 8. Experimental evaluations of such configurations rarely have been very extensive; however,

20
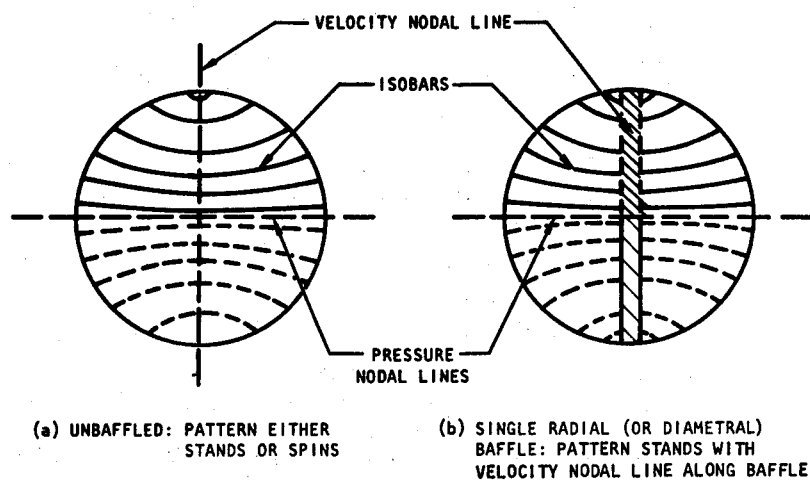
Figure 6. — Effect of a single baffle on first tangential mode.
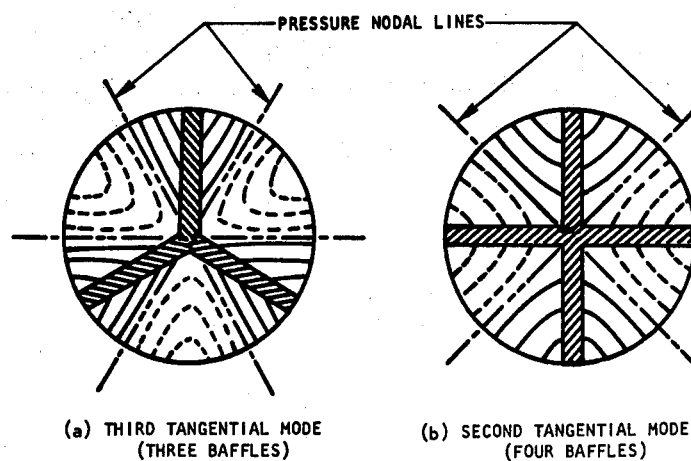
Figure 7. — Mode fitting: odd number of baffles, j, fits j^{th} tangential mode; even number of baffles, k, fits $(k/2)^{th}$ tangential mode.

21
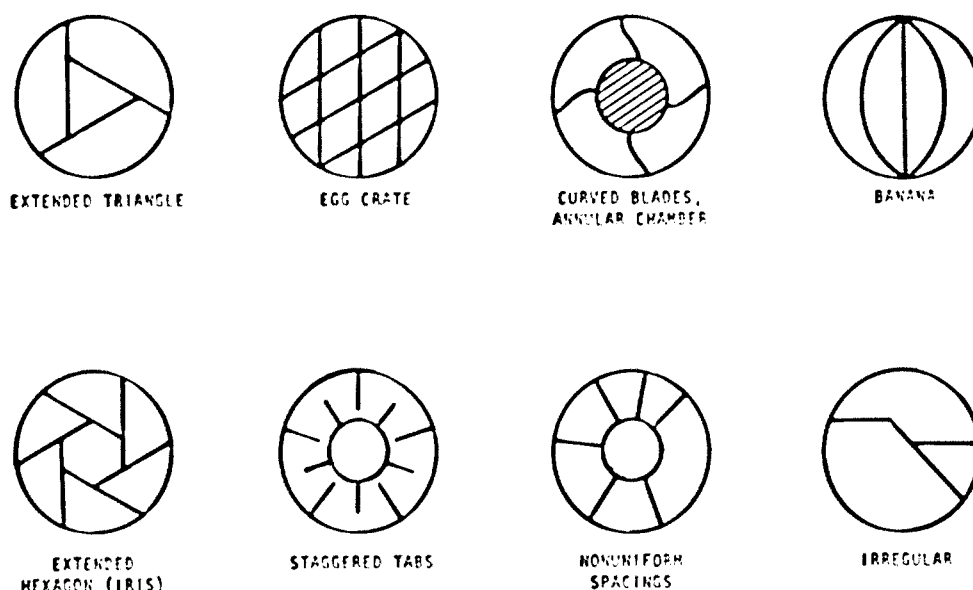
Figure 8. — Examples of nonradial baffles and baffle configurations with nonuniform spacing.

accumulated hot-firing experience generally has failed to indicate any stabilization advantages for such baffle orientations over the conventional uniformly spaced hub-and-spoke arrangement. The "banana baffle" conceived from results of acoustic analyses (ref. 22) did not prevent the first tangential mode (ref. 9). There may be valid reasons for using orientations of the sort sketched in figure 8 (e.g., avoiding excessive propellant splash, heating of baffles, or interaction with thrust-vector-control injectant), but no increases in stabilization have been demonstrated with these patterns compared with hub-and-spoke configuration.

An important subject, but beyond the scope of this monograph, is instability coupled to the feed system. This kind of combustion instability is discussed in detail in references 23, 24, and 25. It is important to mention here, however, that orientation of the baffles with respect to the feed system may be such as to anchor a feed-system oscillation. In the case of the F-1 engine, fuel-system oscillations generally were seen to occur with the fuel inlets as pressure anti-nodes. Similarly, the LOX-system oscillations preferred to stand around the LOX dome splitter. It would be nearly impossible to design a feed system that did not have a preferred orientation for a standing wave in the hydraulic side of the injector. As mentioned previously, feed-system-coupled oscillations have been mistaken for baffle problems.

22

To compound the problem, the injector symmetry usually makes it most convenient from a design standpoint to attach the baffles directly over one of these feed-system barriers, e.g., the LOX dome splitter. When this design practice is employed, the feed system and the combustion chamber can oscillate together (acoustic velocities in most liquids are very close to those in combustion gases) and thus easily reinforce each other. Unfortunately, no systematic study has been made of this coupling, so that there is no definite proof that the combustion gas and liquid side couple.

2.1.2.3.1 Profile

If one looks across the injector face to obtain a profile or elevation view normal to a baffle's surface, two key design points emerge: baffle conformity to instability modal velocity and pressure distribution, and continuity of baffle surfaces with adjacent surfaces. The profile of the baffle is shaped to obstruct acoustic particle displacement; this dictum follows directly from the preceding discussion. Although baffle location is based on the description of particle displacement patterns, baffle effectiveness also depends on the pressure oscillation pattern. This fact sometimes is used to modify the design, particularly the baffle profile.

The role of baffle profile is best illustrated with an example. For the first tangential traveling wave, the maximum amplitude of particle velocity occurs at the center of the chamber, where the pressure amplitude vanishes. Near the walls, pressure amplitude is at a maximum, whereas particle velocity is finite but has lower amplitude than at the center. It has sometimes been found that combustion-chamber stability to this mode is not impaired by removing the central portion of radial baffles. In the extreme, some small rockets have been stabilized with very small baffle tabs extending from the wall as shown in figure 9.

A less extreme example is the use of "wing-shaped" baffles (fig. 10) in stabilizing the Gemini engines (ref. 26). Truncated baffles, as in figure 9, have been used for engines that were only marginally unstable, so that only a small amount of disruption of wave travel was needed to effect stability.

Partial propagation of pressure waves and gas flows jetted through gaps between baffle and injector, between baffle and chamber wall, or between baffles may subvert the intended stabilization. With slowly reacting propellants, attachment of the baffle to the injector face may not be required for stability; reference 27 discusses a small rocket (with nitric acid oxidizer) that was stabilized by baffles several inches downstream rather than by baffles adjacent to the injector. However, very narrow cracks (0.010 in. [0.25 mm]) between baffle and injector face, which may not influence stability but do allow oscillatory hot-gas flows through them, have resulted in hardware erosion. These narrow cracks, even under stable combustion conditions, often result in erosion by steady gas flow; this steady flow is generated by pressure gradients caused by propellant maldistribution in adjacent baffle compartments. If injection density is maintained constant between compartments, this gas flow can be reduced.

23
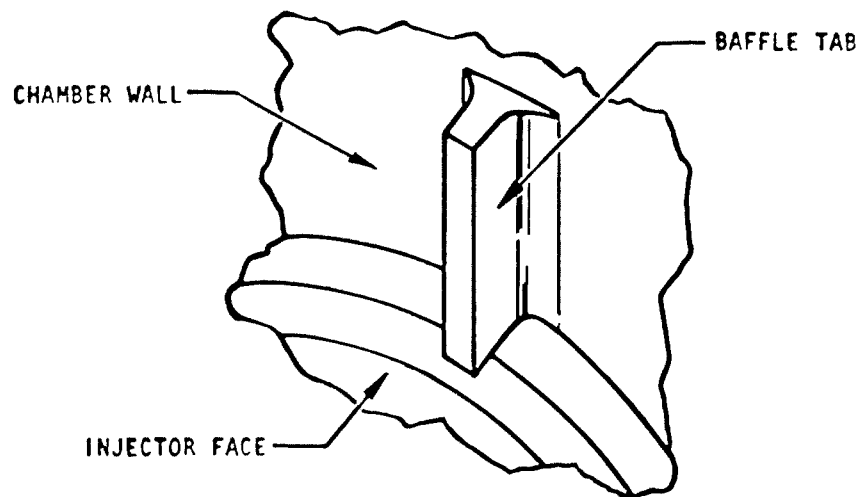
Figure 9. – Baffle tab.
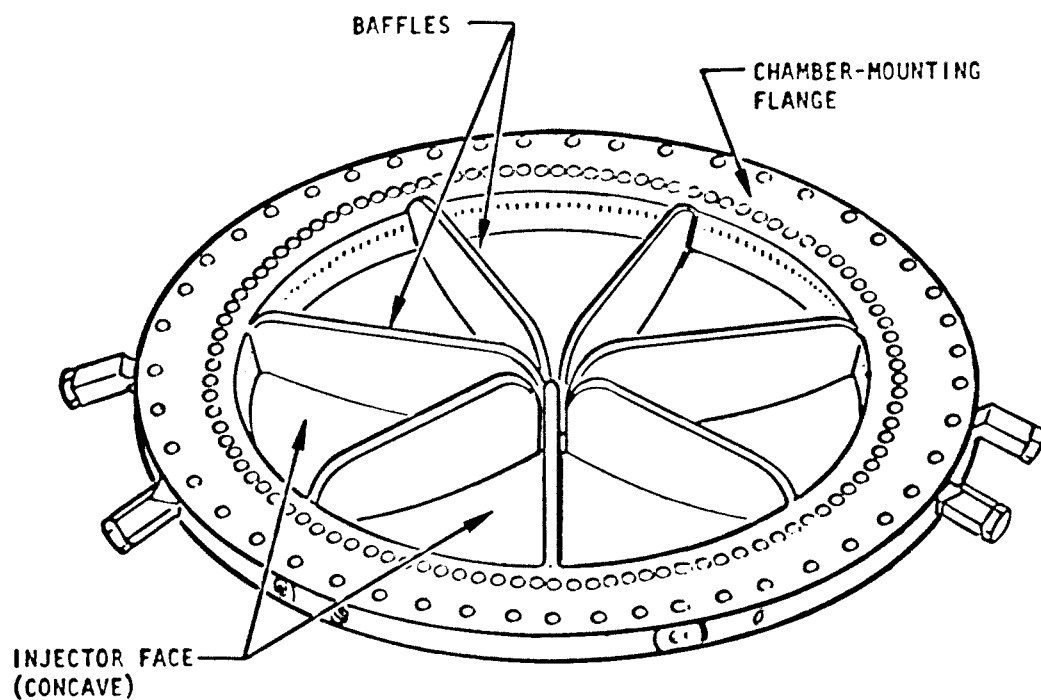
Figure 10. – Wing-shaped baffles used for stabilizing the Gemini engines (ref. 26).

24

2.1.2.3.2 Cross Section

Four examples of baffle design are presented in the cross-sectional views given in figure 11. The benefits or drawbacks to each design are discussed briefly below.

(a) BASIC BAFFLE DESIGN

(b) PLANE, RADIAL BAFFLE USED ON F-1 INJECTOR

(c) DESIGN INTENDED TO PREVENT PLUGGING OF INJECTOR ORIFICES WHEN IMPOSED ON EXISTING INJECTOR

(d) CONTOURED BAFFLE INTENDED TO HELP CONTROL GAS FLOW
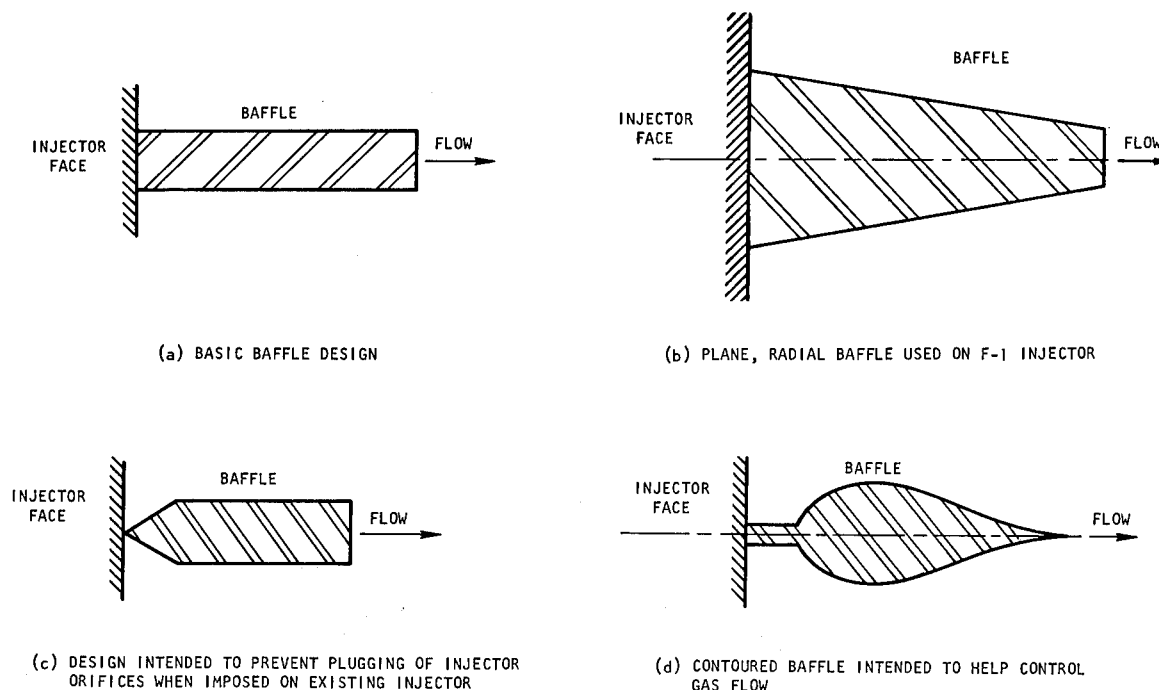
Figure 11. — Four types of baffle cross sections.

By far the majority of baffle designs has been based on a simple rectangular baffle cross section shown in figure 11(a). The thickness of such a baffle depends on the baffle cooling method and baffle strength required (secs. 2.1.4 and 2.1.3). In general, the thicker the baffle, the more likely the baffle will interact adversely with injector design, performance, chamber cooling, and so forth. In many cases, trapezoidal baffle cross sections have been employed in attempts to minimize such interactions (e.g., F-1 engine injector baffle shown in fig. 11(b)). Other variations include a rectangular section followed by a rounded or trapezoidal baffle tip (tapered tip). The method of baffle cooling influences the selection here.

25

There is some analytical evidence (ref. 11) that wedge-shaped baffles are better, from a stability standpoint, than rectangular baffles. This improvement was postulated on the basis of the baffles occupying a large percentage of the cross-sectional area of the chamber. Under these circumstances, the sudden deceleration of the combustion gases at the baffle tips allows the liquid propellants that remain unvaporized to overtake the gas and produce additional regions of very low relative velocity.

Generally, baffle designs having increasing thickness with increasing distance from the injector have been avoided. There have been exceptions, as follows:

(1) Sharpened or knife-edge baffles superimposed upon an existing injector design when it is desired to avoid plugging injection holes (fig. 11(c)). This design usually has been found undesirable because it lacks an adequate injector-to-baffle seal; injector face erosion may result from transverse gas flow under the baffle, even during stable combustion.

(2) Baffles intended to form "combustion cells" with geometrically controlled combustion-gas acceleration/deceleration characteristics. An example, studied in the F-1 engine development program, is shown in figure 11(d). The spacing of these contoured baffles was close enough that products of partial combustion in the cells were accelerated to high subsonic velocities in the convergent section. The idea was to enhance breakup of large propellant droplets or ligaments by imposing strong shear forces on them for a short while. In this particular case, however, combustion efficiency was reduced markedly because the oxidizer evaporated faster than did the fuel, so that oxidizer-rich gases expanded away from fuel-spray-rich core-streams in the divergent sections. When fuel and oxidizer vaporize at about the same rate, this technique has shown promise (ref. 28).

2.1.2.4 DESIGN CONFIRMATION AND RATING

In new design situations where the confidence in the analysis or empiricism on which the design is based is very low, it is possible to develop an effective baffle design by extensive hot-firing stability-rating tests. Ideally, the test series would be structured to determine sequentially (1) minimum effective baffle length, (2) maximum transverse dimension for which this minimum is effective, and (3) subsequent rate of increase of minimum effective length with increases in transverse dimension beyond the value found in (2). Such a program is described in references 29 and 30.

A given development effort will probably fall more or less short of this ideal, there usually being neither enough time nor money for such complete characterization. The degree of departure from ideal depends on many factors such as the severity of the instability problem, cost and difficulty involved in testing with varied compartment sizes, baffle

26

cooling method (if any), and test duration. A hot-firing design development can be made much more efficient by linking it with combustion analyses such as the method outlined in section 2.1.2.1 and with cold-flow acoustic experiments as discussed in section 2.1.1.

Regardless of the confidence in the analysis or in the design of the combustion chamber and its baffles, the resultant hardware is tested to demonstrate mission suitability. Rocket engines that are to be "man rated" (i.e., carry human passengers) must show dynamic stability. The purpose in requiring a dynamically stable rocket engine is to ensure that catastrophic loss of the engine or vehicle will not occur as a result of combustion instability. Dynamic stability considered in initial engine design minimizes the overall development cost of a reliable system.

Stability testing therefore preferably begins early in the development program and is extensive enough to provide high confidence in the stability margin of the evolving engine design; deferring extensive stability testing until the end of the development program can lead to major cost and schedule impacts if unacceptable stability characteristics are discovered at this late stage. References 29 and 30 describe the approach followed in a well-prepared stability rating program. Reference 29 also suggests that, to find the "design margin", tests be made at operating conditions under which the engine is never to be operated. This kind of test does little to rate an engine, because (as mentioned so often) only small design changes or operating condition changes may make large changes in the stability of an injector. There is a way, however, to determine a "stability margin"; but the method has not found much use because of its high cost. The margin may be expressed in either the length of the baffle or the number of baffles. Thus, if the design uses eight baffles 3 in. (7.6 cm) long and it can be demonstrated that six baffles 2.5 in. (6.3 cm) long are just marginal in stabilizing the engine, the "design margin" might be said to be two baffles and 0.5 in. (12.7 mm). The design margin can be stated more quantitatively in the case of acoustic absorber designs, where a damping coefficient can be calculated (sec. 2.2).

For engines that are not to be man rated, such an extensive rating procedure may not be justified but, as noted above, well-planned and systematic rating can help in making the development program more cost effective.

Artificial disturbance devices. – Currently, the two most effective devices for artificially triggering instability in a combustor are nondirectional explosive charges (bombs) mounted inside the combustion chamber and detonated during the test run, and pulse guns that direct a shock wave into the combustion chamber. Other techniques such as a short gas pulse into the engine, variation of operating conditions (not desirable), and feed-system pulsing have also been used as artificial disturbances. The various methods are discussed in great detail in reference 1, chapter 10. This reference also gives detailed information on the instrumentation to be used in concert with the triggering devices, where the device should be placed in the chamber, and the relative advantages of one to another.

A stability rating technique used prior to the introduction of the bomb or pulse gun was called the T-bar ($\bar{t}$). Engines were simply tested at their nominal rated operating conditions until they spontaneously became unstable. After many tests, the average time between occurrences of instability, $\bar{t}$, was determined. Presumably, the longer the time between periods of instability, the more stable the injector. Cost considerations for this type of testing make it an undesirable method of rating.

2.1.3 Structural and Mechanical Design

Problems attributed to the structural or mechanical design of baffles occur frequently, but these problems usually are caused in turn by poor cooling or functional design. Nonetheless, a sound structural design with appropriate materials is always required. In addition, poor quality control or inadequate inspection have caused difficulties in ensuring structural integrity. These problems are discussed in subsequent paragraphs.

2.1.3.1 MATERIAL SELECTION

The selection of the baffle material has depended to a great extent on the required baffle lifetime, the operating conditions, the rate of heat transfer to the baffles, and the individual test duration. Generally, the design procedure and philosophy depend very strongly on the required baffle lifetime, both total firing duration and number of starts of the engine. For very short firings, baffles are not exposed to hot combustion gases for a very long time, so the material may be selected primarily on the basis of the structural rather than thermal considerations. If repeated firings or long durations are important, thermal suitability and chemical compatibility become the dominant considerations in the choice of material.

Strength. — As mentioned, baffles seldom fail for structural reasons if the thermal problems have been properly considered. The largest loads that the baffle must withstand are the transient loads due to hard starts or bomb blasts within baffle compartments. Thus baffle materials are seldom selected on the basis of room-temperature strength alone. It is obvious that if other considerations (e.g., thermal loads, chemical compatibility, and thermal expansion) can be ignored, the material with the highest strength at the anticipated operating conditions will allow thinner baffles to be used, and thus interaction with injection sprays can be minimized (see. 2.1.5.1).

Thermal properties. — Most baffles have been made of high-thermal-conductivity material such as copper or aluminum. These materials act to diffuse any local hot spots that may occur on the baffle surface and thus prevent local melting or overheating. Further, the high conductivity allows heat to be transferred rapidly from the baffle surface to the baffle coolant without a large temperature drop between inner and outer baffle surface. These effects are discussed further in section 2.1.4.

28

A material possessing a low value for thermal diffusivity κ ($= k/\rho C_p$) and a high melting point often is useful for heat-sink baffles. The low value for κ delays the achievement of steady-state temperature in the baffle, and the baffle thus may maintain structural integrity, particularly if engine firing duration is short.

Theoretically, materials with high melting points would be desirable for all baffles, because they could be operated at high temperature. Thus, since the difference between gas temperature and allowable baffle surface temperature would be low, the heat flux to the baffles would be low, and cooling problems would be minimized. In practice, however, materials with very high melting points (e.g., the refractory metals molybdenum, tungsten, and columbium) have other properties that have thus far militated against their use. All of these materials are easily oxidized and often are very brittle. Unfortunately, satisfactory oxidation-resistant coatings for these materials have not yet been developed. Furthermore, refractory metals are quite expensive and difficult to fabricate. Ablative materials*, however, have been used for baffles and are discussed in section 2.1.3.5.

An interesting use was made of aluminum baffles in a LOX/RP-1 engine (ref. 31). The objective was to consume the baffles soon after ignition so that they would not interfere with engine operation during mainstage, but would be present during ignition to prevent a combustion instability triggered by a hard start.

Chemical compatibility. — Chemical attack by one or both propellants on the baffle material is a very real possibility. Generally the baffles will be relatively hot on the surface, and raw, unburned propellant splashing against them can cause severe and rapid corrosion. This corrosion has not been a severe problem in the past, since it is usually recognized early in the design phase that chemical compatibility is required. The use of aluminum and carbon steel with oxygen; copper with nitrogen tetroxide and nitric-acid-based oxidizers; and silica-based ablative materials with fluorine have been avoided (ref. 32).

If there are overwhelming reasons to utilize a particular baffle material, chemical compatibility can be attained by thin plating; e.g., gold plating of copper has stopped corrosion by IRFNA. Further, when the baffles are sufficiently cooled to reduce the rate of corrosion, an "incompatible" baffle material can be used for short times. Corrosion protection is highly coupled with injector mixture-ratio gradients and heat transfer to the baffles.

Quality control. — Assurance that baffle material meets specifications has been shown to be important. During F-1 engine development, for example, cracks were found in the outer ring baffle on three injectors. Dye-penetrant inspection showed a large number of cracks in the

---

*Materials that absorb or dissipate heat while being decomposed to gases and porous char. Ablative materials isolate underlying structural material from degrading effects of high-temperature environments.

ring baffle where radial baffles were attached. These baffles were removed and analyzed metallurgically. The analysis revealed that the baffle had been fabricated from a forging of oxygen-bearing copper. It was found that the oxygen-bearing copper had entered the baffle manufacturing process because there was insufficient sampling of the forging during receiving inspection to ensure OFHC (Oxygen Free High Conductivity) quality. It should be noted, however, that even OFHC copper, if allowed to heat above its recrystallization temperature, can also exhibit cracking and low strength.

2.1.3.2 STRESSES

Mechanical stresses have caused few problems in baffle design. Steady transverse loads are quite low and approach zero if the mass and mixture-ratio distributions are uniform among baffle compartments. Dynamic transverse stresses can, however, become appreciable. Axial loads on the baffles are also generally quite small and are imposed mainly by the coolant flow through the baffles. It has been found that axial drag forces are virtually negligible.

2.1.3.2.1 Thermal Stresses

Thermal stress, thermal fatigue, and long-term creep have been responsible for most baffle structural failures. These phenomena usually are produced by local overheating of the baffle. As mentioned, high-conductivity materials such as aluminum and copper have been used to minimize highly localized hot spots on the baffles, but if the area of overheating is more than a small fraction of an inch, this heat-spreading technique is of limited benefit. Further, the local hot spots may go unnoticed for long firings and may not be a problem if the baffle and engine lifetime is less than a few hundred seconds. In the case of the F-1 engine, all qualification injectors that accumulated firing time equal to or in excess of the required 2250 seconds exhibited distortion. Visual inspection revealed yielded or bulged radial baffles and pronounced deformation of the rings, lands, and orifices at radial baffle attach points. Figures 12 and 13 depict distortion of F-1 qualification injectors that had accumulated 3288 seconds during 57 engine tests (fig. 12) and 3048 seconds during 34 engine tests (fig. 13). Dimensional inspection of F-1 injectors that had accumulated over 2250 seconds of use disclosed other "normal" distortion.

After repeated testing of the injector, the inner radial baffles exhibit a swelling effect on the smooth baffle surface just downstream of the second oxidizer ring inside the outer ring baffle. The high heat flux in this area causes high baffle temperature, and because of the restraint at each end of the baffle, the thermal growth is manifested as compressive yielding. The yielding is inelastic and concentrated in the area of maximum metal temperatures. This yielding results in progressive permanent deformation called "bulge". The bulging starts in the area of the trailing-edge coolant passage and eventually extends from the trailing edge to the baffle base. The excessive bulging further aggravates the high baffle temperatures and has resulted in erosion of the baffles. These erosions cause a thinning of the wall of the

30
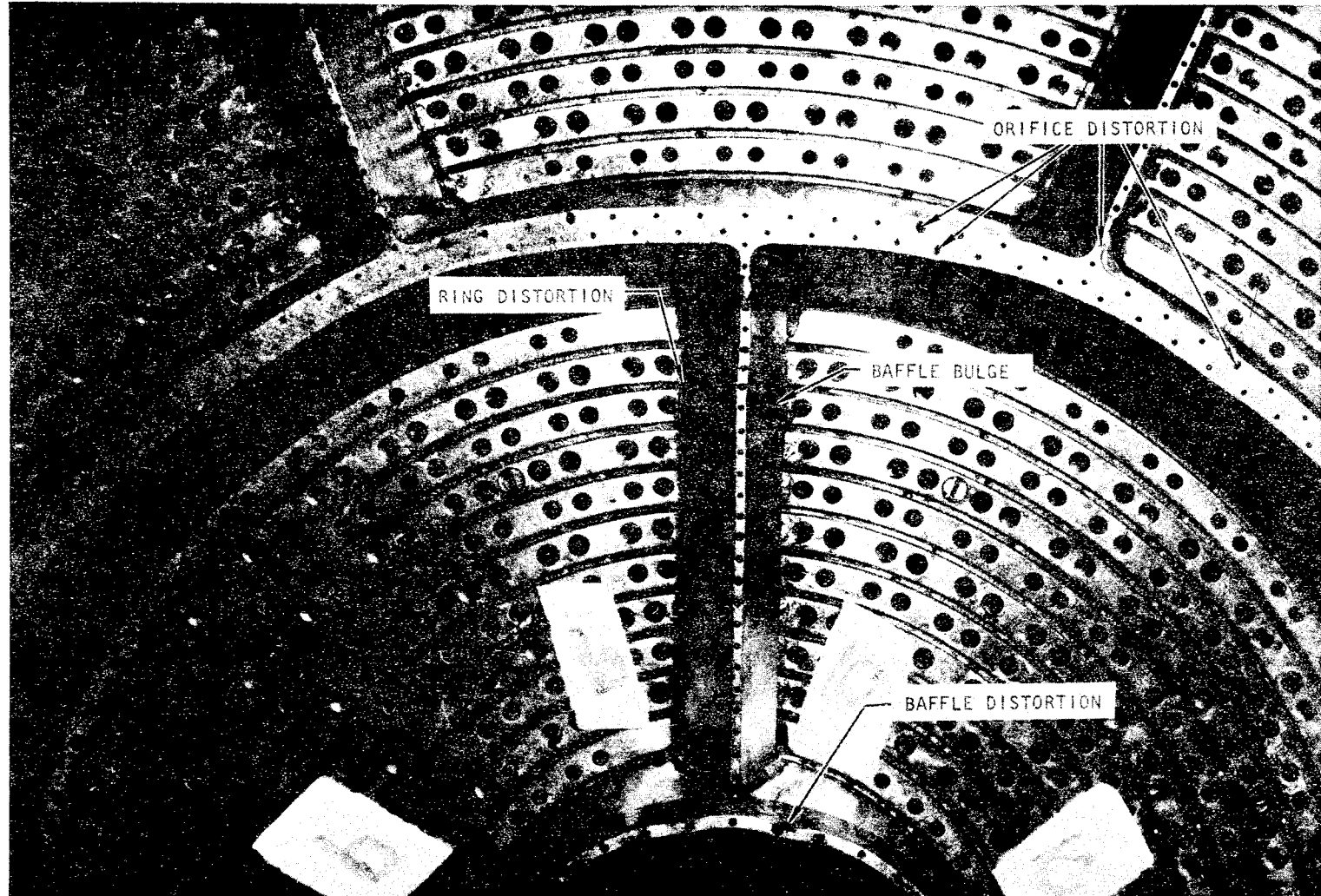
Figure 12. — Distortion of baffle injector on F-1 engine — inner radial baffle after 3288 seconds, 57 tests.

31
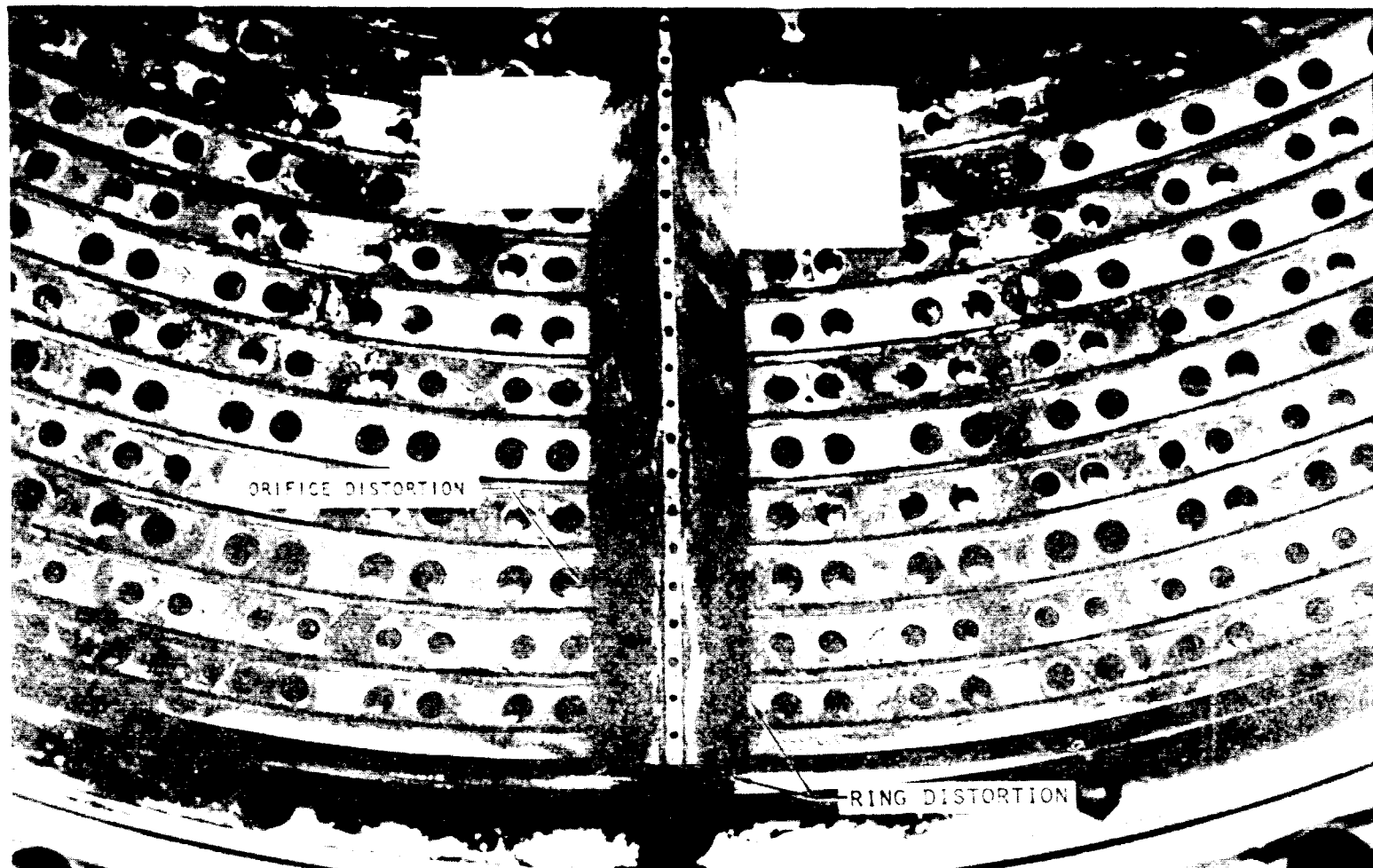
Figure 13. — Distortion of baffle injector on F-1 engine — outer radial baffle after 3048 seconds, 34 tests.

trailing-edge coolant passage and ultimately a combination erosion/pressure failure, which occurred on five injectors.

The bulging of the inner radial baffles also causes a reduction in the effective hole size at the entrance of the dump coolant orifices. To determine the rate of change, an inspection of the orifice sizes was made after each 150-second test. The maximum-diameter pin that could be inserted through the coolant hole was considered to represent the orifice size. The inspections revealed large reductions in orifice size near the outer ring. The orifices were reduced in diameter from an original value of 0.067 in. (1.7 mm) to 0.050 in. (1.3 mm) at 2250 seconds. This change is equivalent to a 40-percent decrease in coolant flow, which causes an increase in the surface temperature. This higher temperature, however, is an effect and not the cause of baffle bulging.

Periodic redrilling of the coolant holes was evaluated to determine the effects of more nearly constant flowrate on baffle overheating. Redrilling is difficult to perform with the injector in the engine. The small-diameter drill (0.067 in. (1.7 mm)) is very susceptible to breakage in the coolant holes. The removal of the broken drill is difficult, and notching the baffles to expose the broken portion usually is necessary. The frequency of drill breaking in the orifices makes this method of maintaining original orifice size undesirable.

2.1.3.2.2 Dynamic Stresses

Transverse loads to which baffles are exposed usually are dynamic or short-term loads. These loads have caused severe permanent distortion in many baffle systems. Even in the case of the F-1 engine, which utilized very strong baffles, the blades became permanently bowed after a few tests for dynamic stability (i.e., a bomb exploded in a baffle compartment). In the Gemini (Titan) engine development program, it was found that baffles that were unsupported at the tip (cantilevered from the injector face) suffered severe distortion from bomb blasts inside the chamber. In extreme cases of a sustained combustion instability, the baffles were not only distorted but were ejected from the chamber (ref. 29).

Engines that operate at relatively low chamber pressure (e.g., the LMAE and Apollo Service Module engine) have not experienced this distortion problem to such an extent. Although the steady-state pressure is not important directly in the loading of the baffles, it has been found that when a bomb is detonated in an engine the resulting overpressure is a strong function of chamber pressure. Thus the transverse load experienced by the baffles increases directly with chamber pressure.

In addition to bomb blasts, hard starts can also cause baffle deflection. Generally, hypergolic propellants ignite smoothly and do not cause an ignition spike or hard start. However, even with hypergolic propellants (and nonhypergolic propellants in very small chambers operating at vacuum conditions) severe ignition spikes occur under certain temperature and valve-timing conditions (ref. 33). In the case of propellants such as liquid

33

oxygen and either hydrogen or RP-1, the ignition transient can be quite severe under some conditions of valve opening and ignition. Particularly high overpressures occur when the igniter has not been placed in all baffle compartments. If a compartment must await ignition from another compartment where an igniter is located, the buildup of unreacted propellants can be large. This condition often results in a large ignition spike.

Typically, pressure waves generated by bombs and pulse guns have very short pulse widths. The (positive) overpressures produced by such devices have lifetimes on the order of 300 microseconds with half-amplitude times on the order of 100 μsec. The decay of overpressure behind the wave front of engine instabilities is even more rapid; as shown in figure 14, the half-amplitude time is on the order of 25 to 50 μsec (ref. 34).
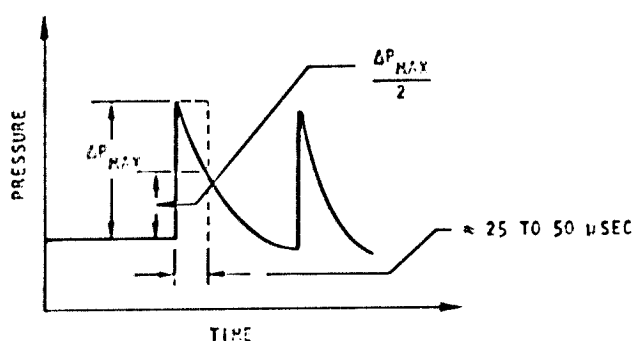
Figure 14. -- Overpressure decay behind wave front.

2.1.3.3 ATTACHMENT

Baffles have been attached both to the injector face and to the combustion chamber wall. Those attached to the injector face have been bolted, brazed or welded, keyed into slots, or made integral with the injector. Baffles have been attached to the chamber wall by being either bolted or keyed and recessed into the wall material. The method of attachment has been strongly influenced by the cooling method. For instance, if the chamber is regeneratively cooled, baffles are seldom attached to the chamber wall, because of the complexity caused by interference with the chamber coolant. If the baffles are to be dump cooled, the coolant can most easily be obtained from the injector; thus these baffles usually are made integral with or brazed to the injector face.

Attachment problems have been minimal for injectors that had short lifetimes or few firings. When long life or many firings were required, severe problems with attachments have resulted from thermal fatigue, thermal creep, and thermal stress.

34

A particularly severe attachment problem was encountered on the LMAE. The aluminum injector had a three-bladed aluminum baffle, electron-beam welded to the injector face. It was found that after several firings the baffle would progressively rip loose, the tear starting at the edge of the injector. Although the original diagnosis attributed the failure to poor welding, later analysis showed that the differential heating of the baffle tip and base (the base is better cooled than the tip) caused tip compressive yield and subsequent failure (see also ref. 35).

Similar problems were experienced on the F-1 engine. Until a high-strength braze joint was developed, baffles would often come loose from the injector face. After the braze joint became sufficiently strong to hold the ring and injector, the deformation described in section 2.1.3.2.1 occurred.

2.1.4 Thermal Control

A baffle is cooled to prevent its being heated to temperatures that endanger its structural integrity. Effective cooling of a baffle normally is achieved by a sequence of steps as follows:

(1) Analytical determination of the thermal and chemical environment of the baffle

(2) Evaluation and selection of the most suitable cooling technique for the conditions established in (1)

(3) Experimental evaluation of the effectiveness of the cooling method.

2.1.4.1 ANALYTICAL BASIS

The most important parameter of the baffle's environment is the adiabatic wall temperature, i.e., the temperature that an uncooled baffle would approach if allowed to remain in the environment for a very long time. The adiabatic wall temperature has been found to vary greatly with distance from the injector face as well as with radial and tangential position (ref. 14). An analysis that assumes that the adiabatic wall temperature of a baffle is equal to the equilibrium gas temperature corresponding to an overall mixture ratio is likely to be grossly in error. The error in adiabatic wall temperature arises because the partially burned combustion gases near the injector face are cooled by the rapidly vaporizing propellant and because the baffle is cooled by liquid propellant splashing on the baffle surface. On the basis of the data in references 14, 29, 30, and 36, the local value of adiabatic wall temperature is unlikely to rise above 3000° F (1922 K) in the first 2 in. (5 cm) downstream of an injector. Methods outlined in references 1 and 14 give a good representation of the environment outside the baffle surface.

Thermal analyses of baffles to determine internal temperatures usually have been based on one- or two-dimensional conduction models (ref. 37) and gas-side boundary conditions calculated from the simplified correlation of Bartz for heat-transfer coefficient (ref. 38). Digital computer calculations (ref. 37) allow prediction of the net of isothermal and adiabatic lines throughout a baffle that may or may not have regenerative-cooling passages.

Use of the simplified gas-side boundary conditions results in conservative calculations that do not adequately predict the benefits of refractory coatings or mixture-ratio biasing[1] by appropriate element placement. The shortcomings of heat-transfer analysis based on the bulk gas flow field have been pointed out in reference 14. Thus, the detailed influences of injector design, propellant mass and mixture-ratio distributions, transverse gas flow, and combustion parameters must be considered.

2.1.4.2 COOLING METHODS

2.1.4.2.1 Regenerative and Dump Cooling

Baffles usually are cooled with the rocket fuel, although oxidizer and bipropellant cooling occasionally have been used. A typical design, showing coolant passages used on the F-1 qualification injector, is presented in figure 15.

Coolant flowrate through regenerative or dump-cooled baffles is established to satisfy two requirements:

(1) The total heat absorbed by the coolant must be equal to the integrated gas-side heat flux, and if the coolant is liquid this heat must be absorbed without producing net vaporization of any of the coolant. In addition, if the coolant temperature is allowed to exceed its decomposition temperature, deposits (e.g., carbon deposits from kerosene) may clog the coolant passages. Both vaporization and decomposition of coolant occurred during development of the F-1 engine.

(2) At the same time, the liquid velocity in the coolant passages must be kept sufficiently high to prevent the peak heat flux to the coolant, at any local point where the gas-side heat transfer is highest, from exceeding the nucleate-boiling heat flux. Calculations of allowable nucleate-boiling heat fluxes follow procedures outlined in references 39 and 40.

Fully regenerative cooling with baffle coolant flow re-entering the main propellant flow and being injected by the main injector is not often used; one successful example is the Titan Transtage engine (ref. 35). This cooling method was tried during the development of the F-1 engine as an aid to performance and stability; however, limited testing showed no effect on either. Because of its complexity, the system was dropped in favor of fuel dump cooling.

----

[1]Reduced mixture ratio near the chamber wall or baffle surface

OUTER RING
BAFFLE

A   A

INNER RADIAL
BAFFLE (OUTER RADIAL
SIMILAR IN DESIGN)

INNER RING
BAFFLE

INJECTOR C
L

SECTION A-A
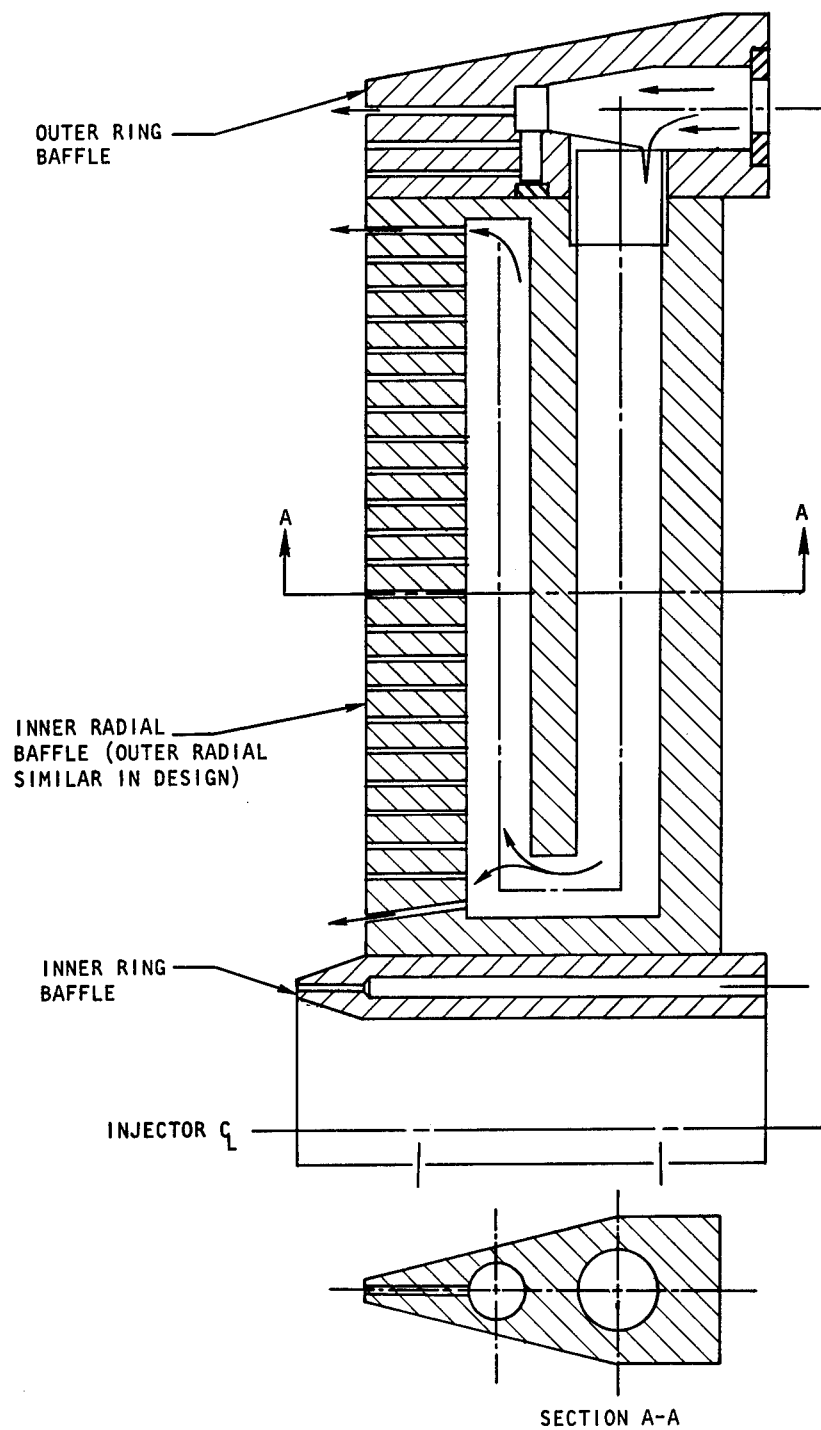
Figure 15. — Coolant passages in baffle on F-1 engine injector.

37

Most cooling methods involve axial (or more complicated) flow of propellants through the baffle assembly, the coolant flow being injected from the downstream tip of the baffles into the combustion space. A baffle assembly of this type is illustrated in figure 16. Several
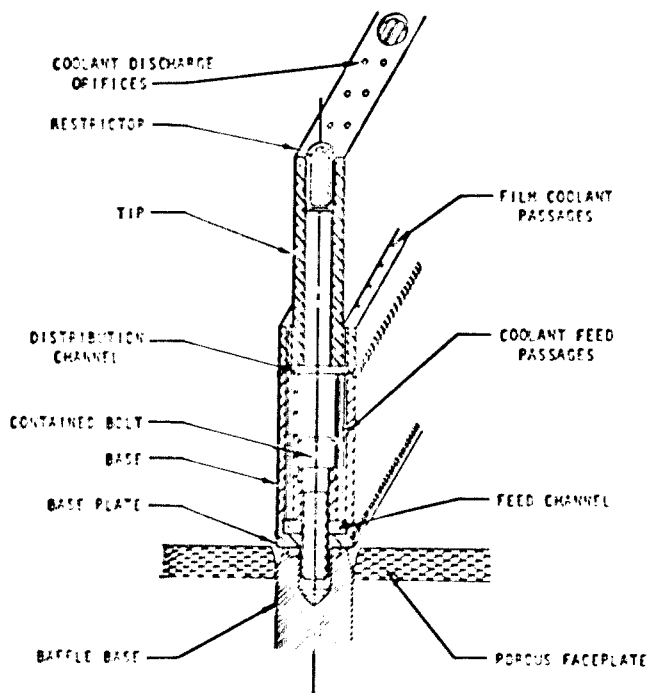
Figure 16. — Bolt-on through-flow copper baffle assembly.

techniques have been used to promote efficient combustion of baffle coolant thus injected: small-diameter closely spaced injection orifices to effect uniform distribution; impinging stream orientations to hasten atomization and aid in distribution; moderately high injection velocities to produce fine sprays; and spatial distribution of mixture ratios (produced by the main propellant injector) biased near the baffles to offset the tendency toward persistence of fuel-rich streaks downstream of the cooled baffles.

Although dumping at the baffle tip of the propellant used for baffle cooling initially was thought to influence combustion stability, detailed investigation showed that this assumption was untrue. In fact, baffle configurations with no propellant tip injection, single-propellant tip injection, and bipropellant tip injection — all exhibited the same stability characteristics. An interesting example of the result of excessive heating of the dump coolant is shown in figure 17. The enlargement of the passage was attributed to

38

SECTION THROUGH BAFFLE ORIFICE
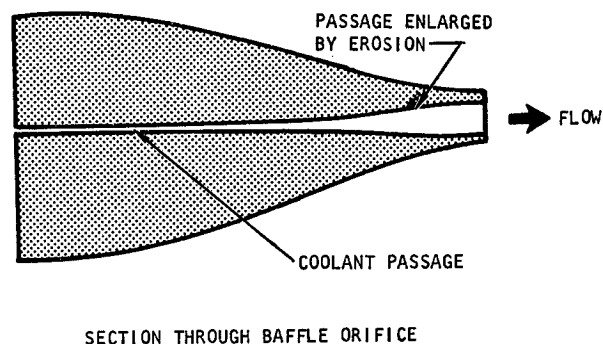
Figure 17. — Coolant-passage enlargement caused by erosive
cavitation of heated coolant.

erosive cavitation. An increase of pitting along the port is characteristic of cavitation, and is probably caused by coolant exit temperature near the boiling temperature. The condition depicted in figure 17 occurs after extensive testing on all baffles exposed to high temperature.

Occasionally, difficulties in fabrication and assembly of the hardware involved in dump cooling may introduce problems. For example, the Bell LMAE incorporated bipropellant (N_2O_4/50:50) dump-cooled baffles. These aluminum baffles had relatively complicated cooling manifolds machined into them. Because of the complex passages, it was necessary to machine from the side of the baffle and subsequently cover these passages with a cover plate. The cover plate was in turn electron-beam welded in place. At one time in the development, an oxidizer leak through a faulty weld apparently triggered an instability. In subsequent tests with leaks intentionally drilled into the oxidizer passages, the engine did indeed run unstably.

2.1.4.2.2 Mass Transfer Cooling

Nearly all baffles have some sort of film, transpiration, or mixture-ratio-bias cooling. In many cases, this form of cooling is not employed by design but simply happens because liquid propellants are splashed on the baffle by the injector orifices. In other cases, as mentioned above, a quickly vaporizing propellant such as hydrogen in a LOX/LH_2 engine quickly surrounds the baffle and forms a cool gas layer before significant oxygen can vaporize and react with the LH_2 to raise the surrounding gas temperature.

In many development programs, chronic hot spots in baffle surfaces have been cooled simply by enlarging a nearby injector fuel port so that it furnished additional film or mixture-ratio-bias cooling.

39

Transpiration cooling is similar to film cooling in that one of the propellants is bled continuously through pores or interstices in the baffle surface. Potentially, this cooling method is precise, since the flowrates can be well controlled by graded porosity of the baffle surface. However, although they have not occurred in baffle cooling, instabilities of the flow through porous media, as a result of excessive heat load, have been reported. It is possible that, as the heat load at a spot on the baffle surface increases, the porous medium is heated to a relatively high temperature, the result being a lower coolant density and a greater pressure drop for a given mass flow. This combination then causes a reduction of coolant capacity that allows the surface to get even hotter, and eventually failure results.

Transpiration-cooled baffles to date have not been used on operational engines. This kind of baffle was used in the early development work on the J-2 engine. Since the J-2 injector face was cooled by a hydrogen flow through a Rigimesh face, it was considered practical to cool the baffles similarly. As it developed, baffles were not deemed necessary on the J-2 engine and were not used in the production engines.

In the case of either film or transpiration cooling, some consideration has been given to the possibility that the coolant passages could act as apertures for acoustic resonators that could be incorporated into the baffles. So far as is known, this technique has not been verified experimentally.

2.1.4.2.3 Insulating Coatings

Insulating coatings have been applied to uncooled (or film-cooled) heat-sink baffles. Typical coatings are flame-sprayed ceramics such as zirconium oxide and alumina. Coatings reduce the rate of increase of baffle surface temperature, so that for "uncooled" baffles (cooled only by conduction to the injector) firing duration may be increased. In addition, with a coating, high-strength materials such as stainless steel may be used in situations where their low thermal conductivity and consequent susceptibility to burning at local hot spots might rule them out.

An important consideration in use of insulating coatings is their structural integrity. In the past, coating adherence has been unreliable, particularly when repetitive thermal cycling over a number of firings was involved. Two relatively new coatings show promise in this regard: the gradated metal ceramic coating (ref. 41), which has given good results, even though its ultimate temperature limit is lower than that of the pure ceramic coating; and a slurry zirconium coating (ref. 42), which has shown good adherence in limited testing.

For some time, aluminum-oxide-coated steel baffles were used on the XRI booster engine. Recently, however, these baffles were replaced with ablative baffles that incorporate a steel matrix for rigidity and strength.

40

2.1.4.2.4 Composite Baffles

Two types of composite baffle structures built up from unlike metals have been used. In one type, a "backbone" of a strong metal is covered completely with a thin sheath of metal that has more desirable baffle surface properties (e.g., high thermal conductivity and resistance to chemical attack, as in gold-plated copper). The other composite, used for internally cooled baffles (ref. 29), has a high-conductivity core (rather than surface) material to distribute the average heat flux to the baffle coolant passages and thus maintain the entire baffle structure at a lower temperature. A more common composite, metal/ablative, is discussed below.

2.1.4.2.5 Ablative Baffles

For applications that have relatively short lifetime and few restarts, an alternative to an uncooled baffle (i.e., conduction cooled) is a baffle made of ablative materials. Ablative materials for baffles have been limited to fiber-glass-reinforced phenolics, but other ablatives such as carbon-cloth/phenolics or nonreinforced materials such as nylon or Teflon could be used equally well, especially if the thrust chamber wall is made of these materials.

Occasionally, baffles have been fabricated entirely of the ablative material, but low structural strength and lack of ductility have resulted in poor performance. Several attempts to use ablative baffles in the F-1 engine always resulted in baffle failure and ejection through the nozzle. A more successful approach has been the use of a surface layer of ablative material over a metal structure.

This approach was used in the XRL engine. There, an ablative-coated stainless steel baffle assembly was attached to the ablative chamber walls. The metal baffle-support structures were recessed into the chamber walls and covered with ablative inserts that restored the cylindrical wall contour. The baffles themselves were strengthened by a metal structure. These baffles, even in lengths up to 7 in. (18 cm), have proven durable for short ($<$ 10 sec) durations.

During the development of these baffles, the ablative material frequently was subject to cracking, breaking, and delaminating. The difficulty was eliminated by increasing the rigidity of the metal structure to reduce deflection and elongation. Ablative material, although reasonably strong, does not have a high allowable elongation.

Thermal design of ablative material follows that of ablative combustion chambers (ref. 43). The most important design parameter is the adiabatic wall temperature of the combustion environment. Since this temperature is generally low for the region near the injector face (sec. 2.1.4.1), thinner ablative materials or longer life may be expected for baffles than for comparable combustion chamber walls.

41

2.1.4.3 EXPERIMENTAL EVALUATION

Baffle designs ultimately are evaluated by experimental means. The success of thermal control is determined by observation of results during engine firing. Often during the development program it is necessary to gather quantitative data on heat fluxes, baffle temperatures, and the other variables involved in thermal control. When few if any problems are anticipated, because of the similarity of design to existing engines, quantitative measurements are not taken, and gross observations are relied upon to show up potential trouble. These qualitative measurements usually include observation of discoloration pattern, surface pitting or melting, erosion (particularly at the baffle tip), peeling of coatings or ablative materials, cracked braze joints, and similar phenomena.

More quantitative experimental characterization may be obtained by measuring local surface temperatures and heat transfer rates at several points of a baffle assembly. Local surface temperature measurements have been made with thermocouples. The requirement for external access and seals for leadwires (to measuring and recording systems) generally limits the number of measurements that can be made. Further, times for thermocouples to reach steady state may be greater than the test duration.

Three generations of thermocouple installations were used during the F-1 engine program in the pursuit of improved reliability through accurate measurements of ring and baffle temperatures. Typical installations are shown in figure 18. The most successful method of thermocouple installation has been furnace brazing the element in place at time of injector assembly. The variations of this method include "through" or "blind" drilled holes to receive the thermocouple. If the holes are drilled through to the external surfaces of the baffles or rings, a seal of braze material must cover the tip of the thermocouple to prevent burnout and leakage. The advantage of furnace brazing the thermocouple in a blind drilled hole is that the surface of the parent material at the point of measurement is not disturbed.

Limited numbers of temperature measurements have also been made by installing Templugs[1], from which surface temperature reached during test is inferred by post-test measurement of the material's hardness. In use, the plugs are flush mounted into prepared tapped holes in the hardware at the point where the temperature measurement is desired. The accuracy of a Templug is on the order of $\pm 50°$ F (± 28 K).

A more or less complete characterization of maximum baffle temperature can be obtained by means of temperature-sensitive paints, although chemical reactions with propellants or adherent coatings of combustion products may prevent their use with some propellants. This approach is preferable to measurements with only a few thermocouples, until specific troublesome locations have been identified, because a few local surface temperatures may be highly dependent on spray splash and hot-gas recirculation patterns, particularly near the injector face.

---

[1] Small machined screws of precisely hardened carbon steel that respond to the maximum temperature to which they are exposed by a change in material hardness. "Templugs" are a product of Shell Research, Ltd., Chester, England.

42

ELECTROFORMED
COPPER SHROUD

TIG BRAZED

0.020 IN.
(0.51 MM)
SHEATH

VOID

(a) ORIGINAL METHOD

LOW-TEMPERATURE
BRAZE ALLOY

0.040 IN.
(1.02 MM)
SHEATH

GOOD CONTACT

(b) IMPROVED METHOD

BRAZE ALLOY RESERVOIR

THERMOCOUPLE SHEATH PLATED
TO IMPROVE BRAZE JOINT

0.040 IN.
(1.02 MM)
SHEATH

(c) FINAL METHOD
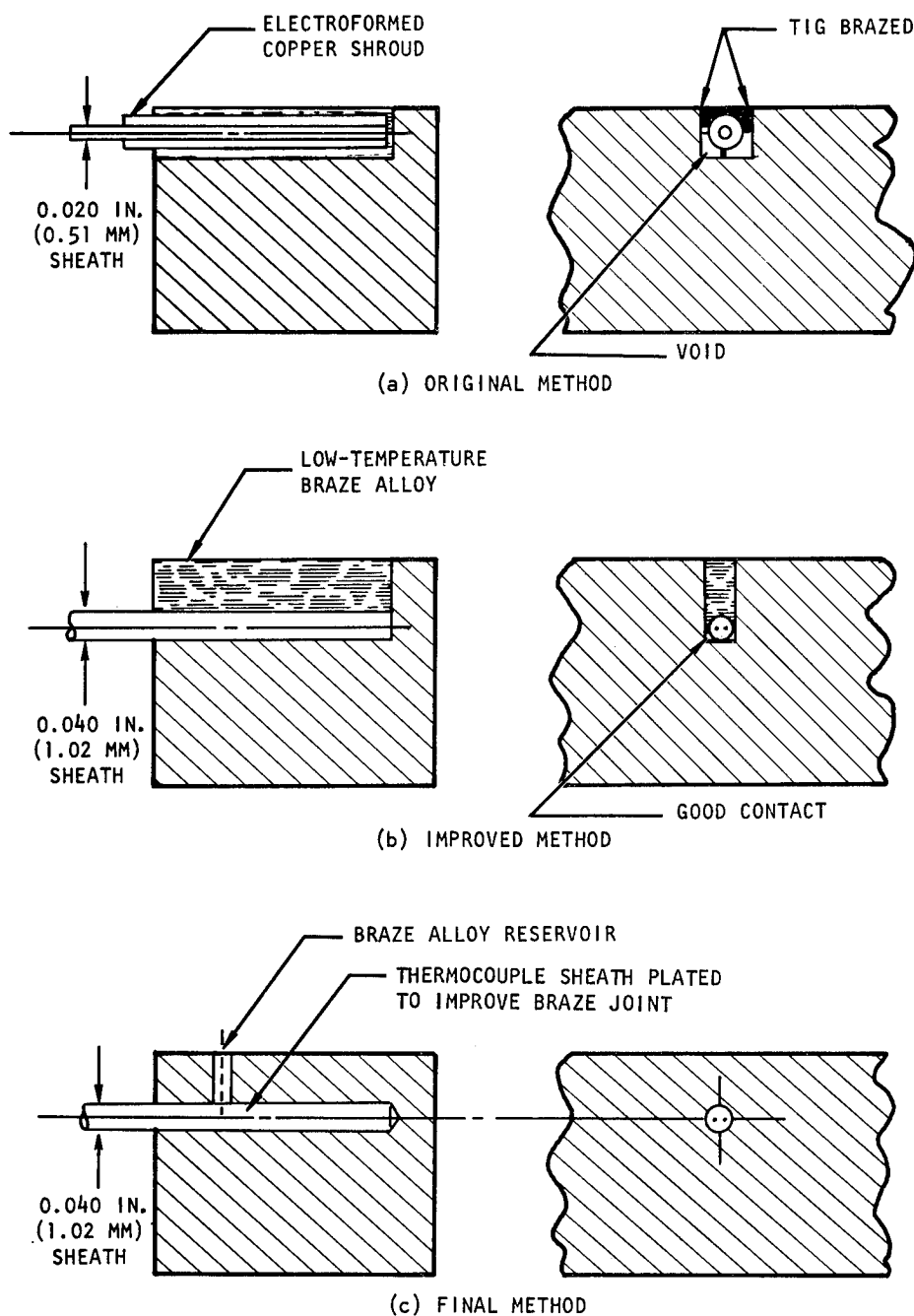
Figure 18. — Methods used to install thermocouples during development of baffles on F-1 engine injector.

43

Qualitative information also may be derived from discoloration of ceramic coatings. During the F-1 engine development, flows of combustion gas and particles were clearly shown by carbon streaks remaining on baffle surfaces after a test. A novel method for measurement of adiabatic wall temperature for ablative materials is discussed in reference 14.

Local heat-transfer rates have been measured by means of heat-flux transducers; overall average rates, by calorimetric measurements of baffle coolant flowrate and bulk temperature rise. Heat-flux transducers, based on measurement of temperature gradient along a one-dimensional conduction path, are subject to the same local influences of spray and recirculation patterns as thermocouples. Generally, however, gross thermal problems can be expected near the downstream ends of baffles, where such injector-imposed irregularities are not nearly so prominent and where heat flux measurements are more generally valid and also of more interest. Baffle heat fluxes measured by calorimetry have greater value, therefore, when local measurements are made in zones along baffle length rather than when they are simply integrated measurements for the entire baffle.

Valuable guidance for the placement, calibration, recording, and interpretation of results from experimental thermal measurements can be provided by concurrent thermal analysis (sec. 2.1.4.1).

2.1.5 Baffle/Engine Interactions

Baffles have often been fitted to injectors as necessary afterthoughts. This inadequate planning has caused severe problems in other aspects of the engine operation.

2.1.5.1 INJECTOR

The prime purpose of a propellant injector is to attain high combustion efficiency and good engine performance by proper mass and mixture-ratio distribution and sufficient atomization of the propellants. This objective is compromised severely when baffles are added to an existing flat-face design. The accompanying necessity to plug injection orifices is one of the major causes of lowered performance. Since the injection ports are initially designed to give a uniform mixture ratio and mass distribution, the removal of orifices in an arbitrary manner (usually in the form of hub-and-spoke baffle configuration, sec. 2.1.2.3.2) results in considerable maldistribution of propellant.

In addition to the effect of maldistribution upon injector performance, the inclusion of baffles into an already designed injector often results in splash of propellants upon the baffles. Although it may be desirable to film cool the baffles, uncontrolled propellant splash has resulted in large globs of propellant rolling off the baffle tips, the result being poor atomization and vaporization that, in turn, result in poor performance (ref. 1).

44

The interference of baffles with normal spray development was partially circumvented in the case of the annular engine for the XRL by making the baffles curved and radial (fig. 7). In this way, the spray fans were made approximately parallel to the baffle surface, and direct impingement of spray on the baffles was avoided.

Another facet of the effect of baffles on mixture-ratio uniformity arises from the hydraulic pressure losses associated with the baffle coolant. Two distinct effects have been observed. The first is caused by removal of injection orifices when baffles are installed. The propellant flow through the removed injector orifice is much larger than the coolant flow through the baffles. This relative reduction of propellant flow causes an increased flow in the injector orifices near the baffle, thus destroying an otherwise uniform mixture-ratio and mass distribution.

The other effect is the opposite of that discussed above. When baffles are installed, coolant flow for the entire baffle may be drawn from the injector in only a few locations. This withdrawal consumes grossly more fluid at these points than would have been used otherwise. As a result, the adjacent orifices are starved, and mixture-ratio distributions are no longer uniform (ref. 1).

Mechanical interaction effects have also caused some problems when baffles were added after the injector was designed. From a stability standpoint, the most serious problem that has arisen is that of propellant accumulation in cracks or crevices.

During a development program, or even in field service, it is often necessary to replace baffles. In most cases, replacement is very difficult because the baffles have been made integral with the injector. In the case of the F-1 engine with the baffles brazed to the face, the only satisfactory way to replace the baffles is to physically machine the baffles from the injector face. New ones are rebrazed by using a braze with a lower melting point than the braze holding the injector rings.

Baffles operate at a higher temperature than the injector face and thus expand more during hot firing. A variety of problems have been encountered because of expansion of the baffles (sec. 2.1.3.2).

2.1.5.2 COMBUSTION CHAMBER

Rigid attachment of baffles to the combustion chamber walls has been used for uncooled solid-wall or ablative-lined chambers, but this method is impractical for regeneratively cooled chambers. If the attachment method extends to the outside of the chamber (e.g., bolts or external coolant-supply tubes), positive seals are provided to prevent leakage (even in the event of baffle failure).

In many baffle installations, the combustion chamber walls downstream of baffles (which extend to the wall) have exhibited signs of abnormally high heat transfer and, sometimes, wall erosion (ref. 36). This effect presumably is caused by the wall boundary layer being thinner and more turbulent downstream of a baffle tip than in the normal flow along the wall. This phenomenon appears to result from flow separation and vortex motion (eddy-shedding) at downstream edges of baffles, and its magnitude can be reduced by tapering or rounding the trailing edges. However, this process makes the baffle itself more susceptible to excessive heat transfer, so the designer must compromise between the two effects. Additional reduction in heat transfer rate may be achieved by providing excess film coolant at the baffle/wall intersection regions to reduce the local combustion gas temperatures.

2.1.5.3 IGNITION

For nonhypergolic propellants, injector compartmentalization with baffles often introduces substantial ignition delays and results in excessively hard engine starts (sec. 2.1.3.2.2). This problem has been avoided (or solved) by providing multiple ignition sources, by machining small vent holes through baffles to speed the convective spread of ignition energy, and by reducing the propellant flowrates during the start transient so that less propellant has accumulated before ignition is completed. An ignition source for each compartment may be needed, but frequently one in every second or third compartment has been found to be adequate. Vent holes are undesirable because they may change stabilization characteristics of the baffles.

2.1.5.4 STABLE OPERATION

Introduction of baffles to effect recovery to stable operation following instability-initiating disturbances has sometimes been observed to increase the incidence of disturbances that occur naturally during normal stable engine combustion. Called "spikes" if observed during transition to mainstage or "pops" if observed during mainstage operation, these pressure surges are most prevalent when the fuel contains hydrazine. Although it might be argued that these short-lived disturbances are not harmful and in fact simply demonstrate that dynamic stability has been achieved, they are usually causes of concern, and efforts are made to eliminate them. Most approaches have been attempts to reduce (1) spray splash of propellant on cold baffle, chamber, or injector surfaces; (2) accumulation of propellant in crevices, corners, pressure taps, and other cracks; and (3) uncontrolled leakage of propellant.

2.1.5.5 STABILITY RATING DEVICE

Transient overpressures behind the initial waves that result from explosive bombs and pulse guns may be considerably higher than those that occur during combustion instability.

46

Amplitudes an order of magnitude higher occasionally are seen, but values on the order of 3 to 5 times chamber pressure are typical. If the rating device is close to a baffle and if the initial blast wave can trigger much release of combustion energy from transient spray, it may be necessary to strengthen the baffle design.

Fragments of a bomb's outer case, a pulse gun's burst diaphragm, or other explosion debris sometimes impact the injector, chamber walls, and baffles at high velocities and have caused severe shrapnel damage. The kind of damage likely to be incurred from different rating devices is discussed in reference 34. The kind of rating device, its size, location in the chamber, orientation, and the design parameters for the device itself — all affect the baffle damage potential, particularly with regard to seals, coolant passages, and injection orifices.

Stability rating bombs sometimes are most conveniently mounted on the downstream edge of a baffle. The baffle design may be required, therefore, to include provision for one or more bomb attachment provisions. Good bomb port design provides for access external to the chamber, so that bombs can be installed quickly and easily and the port can be easily freed of residual debris between tests. Electrical initiation requires lead-wire passages through the baffle, lead-wire seals, and external (to the engine) access for connection to an initiation source. In the preferred bomb design, the lead-wire passages do not communicate with the combustion chamber, either before or after bomb detonation, because they may offer acoustic-cavity damping and thus make the stability of rating tests untypical (ref. 34).

2.1.5.6 THRUST VECTOR CONTROL (TVC)

The combustion gas flow in the wakes of baffles may carry appreciable transverse nonuniformities in composition and temperature all the way through the rocket exhaust nozzle. It has been shown (ref. 44) that injection of a thrust vector control jet into a baffle wake may produce substantially lower side thrust than does injection into neighboring nonwake gases. Therefore, the baffle design and TVC injection site design are coordinated to avoid the effects of baffle wake.

2.2 ABSORBERS

Although acoustic absorbers were shown to be useful in the early nineteen fifties (ref. 45), they were not subjected to substantial analytical and experimental investigation until recently. Several different types of acoustic absorbers have been effective in suppressing acoustic modes of combustion instability in a variety of liquid propellant rocket engines. In fact, acoustic absorbers currently are being used either alone or as a supplement to baffles to maintain stable combustion in several production engines (LM Ascent, RS-14, and XRL booster and sustainer). Absorbers probably will be used in several of the engines involved in the Space Shuttle.

47

Absorbers may affect combustion stability both by removing oscillatory energy from the system (damping) and by interacting with the overall oscillatory combustion process; the extent of this interaction has not been determined. Currently, absorbers are designed by considering only the damping phenomena (believed to be due primarily to viscous jet losses). The amount of damping needed to produce stability thus is not predicted, because such a prediction would require consideration of all gain and loss mechanisms. Some recent analytical methods do allow for all gain and loss processes; these methods are discussed in section 2.2.4.1.

2.2.1 Configuration

Acoustic absorbers generally are comprised of an array of acoustic resonators distributed along the walls of the combustion chamber. Three common types of resonators are the Helmholtz, quarterwave, and intermediate (fig. 19).
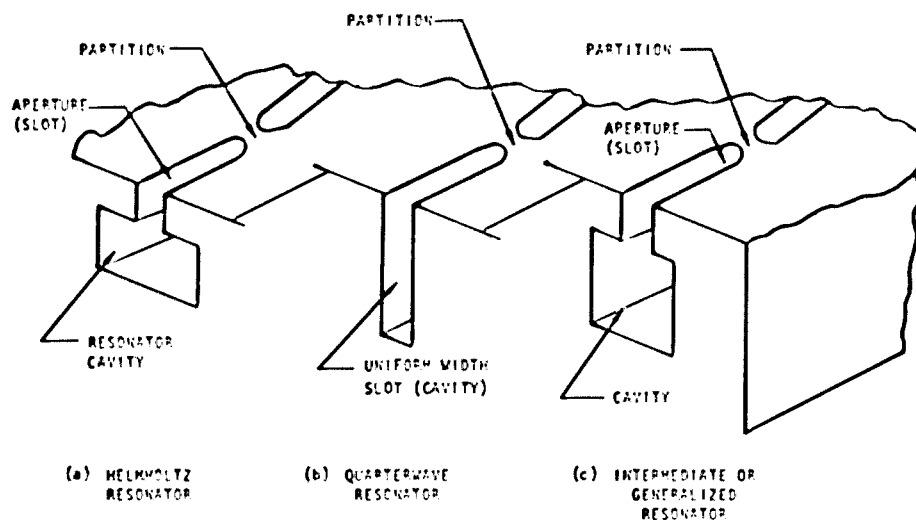
Figure 19. — Three common types of resonators.

A Helmholtz resonator (fig. 19(a)) consists of a small passage connecting the combustion chamber to a resonator cavity; the cavity dimensions are large compared with the passage width but small compared with a wavelength. A quarterwave resonator (fig. 19(b)) is a closed slot or tube (usually straight) with a uniform cross-sectional area. The intermediate or generalized resonator (fig. 19(c)) is similar to a Helmholtz resonator except that the cavity

dimensions are not necessarily small compared with a wavelength. The Helmholtz and quarterwave resonators are simply special cases of the generalized resonator.

The acoustic absorber may be comprised of either a large number of resonators distributed along the thrust chamber wall from the injector to the beginning of nozzle convergence (full-length acoustic liner) or, conversely, a limited number of resonators used over a limited portion of the chamber (usually along the injector periphery or near the injector face). A typical acoustic liner configuration illustrating basic construction principles as well as basic nomenclature appears in figure 20 (ref. 1).
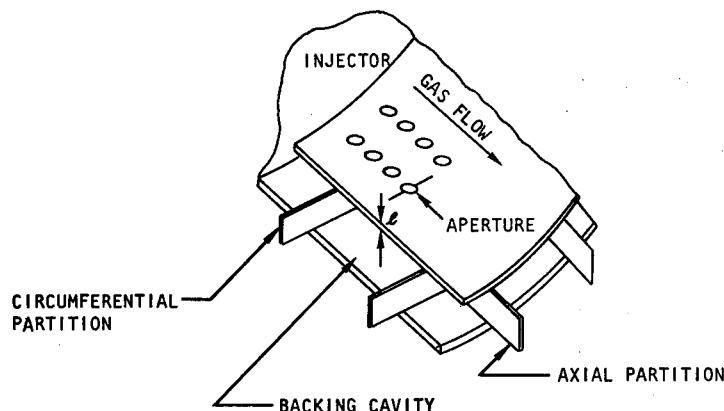
Figure 20. — Typical acoustic liner configuration (ref. 1).

2.2.1.1 LOCATION

The most effective location of a single-row or partial-length absorber is adjacent to the injector face. In some cases, the exact location has been highly critical, whereas in other cases it has been less important. For example, a single-row absorber that stabilized the LMAE when it was adjacent to the injector was no longer effective when moved only ½ in. (1.27 cm) downstream (ref. 21). Later tests with the same hardware showed that stability was regained readily with a slightly larger absorber (ref. 46). Garrison (ref. 1, secs. 8.3.4 and 8.3.5) found that the pressure amplitudes doubled when a partial-length liner adjacent to the injector was moved 3 in. (7.62 cm) downstream (the engine was classified as stable in both cases).

2.2.1.2 PARTITIONS

Partitions usually are placed in the backing cavity of an acoustic absorber to provide structural support and to prevent hot-gas circulation in the cavity. If an acoustic liner has any appreciable length along the chamber axis, partitions are especially important for preventing hot gas from entering upstream apertures and exiting downstream. Although not required for stability, partitions for prevention of tangential gas motion often are used to aid in minimizing overheating and wall erosion. Phillips (ref. 47) has found that the temperatures in the backing cavity can be significantly reduced by including partitions for prevention of the circumferential gas motion. Similar partitions were also found useful for thermal control in slot-type absorbers.

Unfortunately, there are few analytical guidelines presently available for the design of partitions in acoustic absorbers. The effect of the partitions on the acoustic damping is considered in the calculational procedures (sec. 2.2.4), but on the whole the design and use of partitions are based almost entirely on structural and thermal considerations.

2.2.2 Construction

Acoustic absorbers are subjected to structural requirements quite similar to those for injectors and combustion chambers, and structural design is based on the design practices for these basic structures.

2.2.2.1 CHAMBER LINERS

Chamber liner acoustic absorbers generally are located in the combustion chamber between the injector and some downstream position. One design uses a perforated chamber wall enclosed by annular or toroidal rings; examples of this design are given in figures 21 and 22 (refs. 48 and 49). Another type of chamber liner acoustic absorber uses a perforated cylinder inserted in the thrust chamber primary structure (ref. 48). In both cases, liner design is dictated by the requirements of cylindrical shell theory (ref. 50). The problems of stress concentration at the apertures and of differential thermal expansion between inner and outer surfaces must be considered.

2.2.2.2 SLOTS OR ACOUSTIC CAVITIES

An acoustic-slot type of absorber usually consists of a partitioned annular cavity oriented either perpendicular or parallel to the injector face. Most recent test and development work has been done with the cavity configurations shown in figure 23. The acoustic absorber
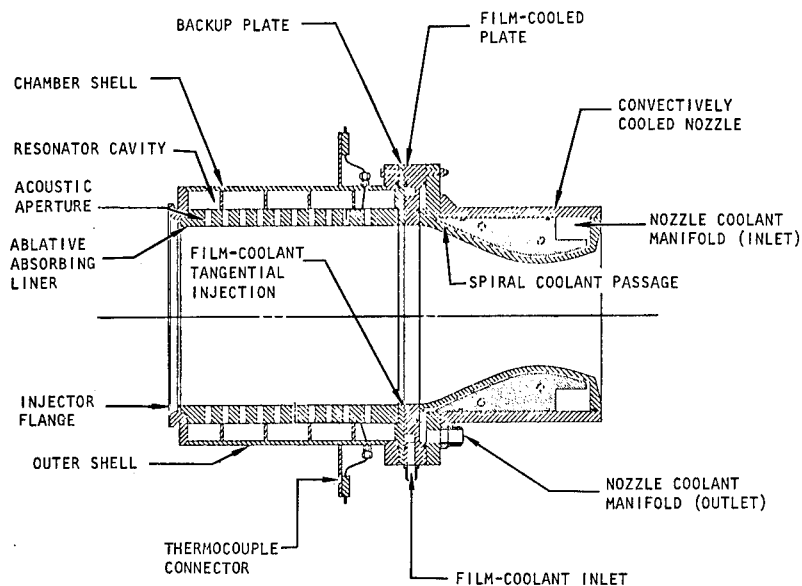
Figure 21. — Chamber liner acoustic absorber assembly for
test and development (ref. 48).
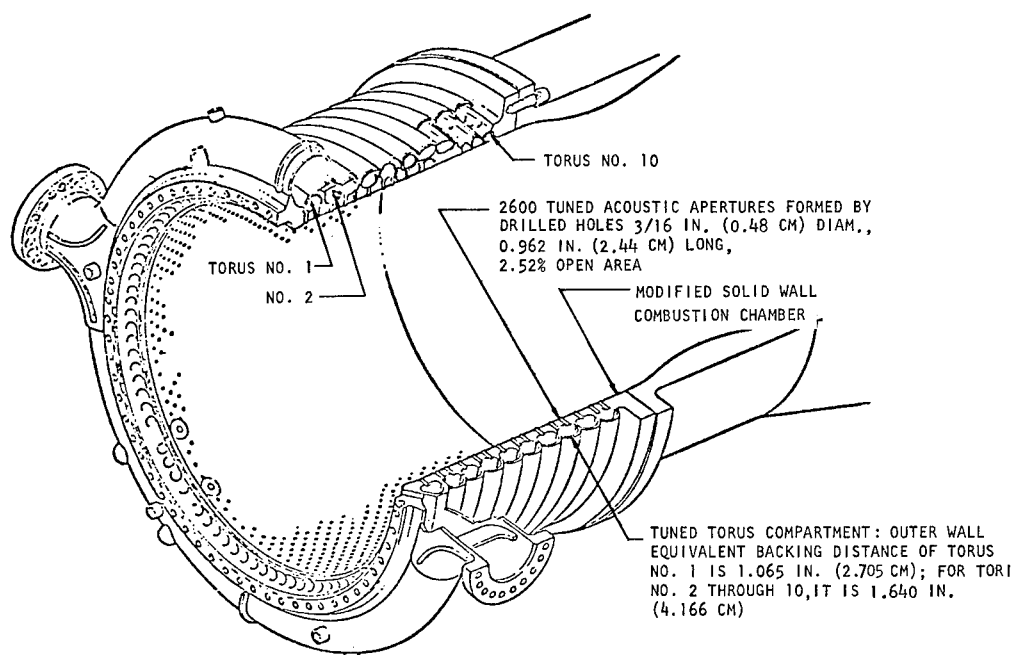
Figure 22. — Acoustic liner design for F-1 engine (ref. 49).

51
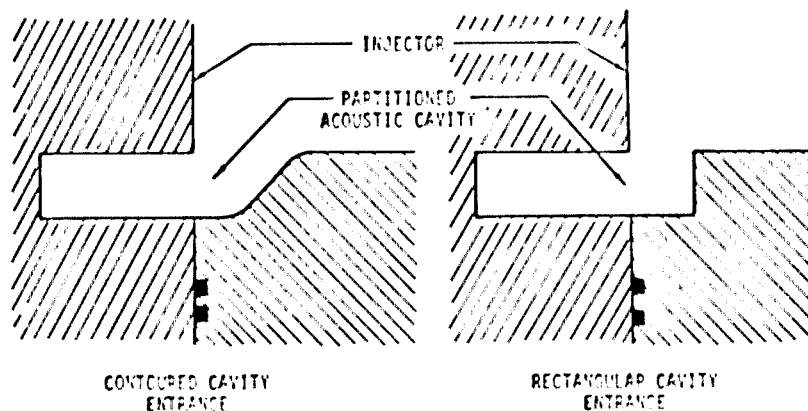
Figure 23. — Acoustic cavity configurations used for recent test and development work.

located adjacent to the injector usually is formed at the injector/chamber interface, part being machined into the injector and part being machined into the chamber. Three production engines that employ acoustic absorbers adjacent to the injector are shown pictorially or schematically in figures 24, 25, and 26. Acoustic absorber structural design near the injector involves only minor modifications to the injector/chamber interface; thermal design considerations are discussed in a subsequent section.

2.2.3 Thermal Control

Few special cooling or materials requirements are unique to acoustic absorbers. Generally, combustion chamber design techniques (refs. 51 and 52) are effectively applied with minimal design complications. Often, no special cooling provisions are required for single-row absorbers mounted in or near the injector. In one case, a thin layer of ablative material on the combustion side of the absorber was sufficient to maintain absorber integrity.

The principal experience with cooling and thermal protection of chamber liners is described in reference 1, secs. 8.3.4 and 8.3.5; general studies of cooling techniques are discussed in references 48, 53, 54, 55, and 56.

Stability-related problems have occurred with both film-cooled and transpiration-cooled liners. For example, the coolant flow was found to decrease the stability of one acoustically

52
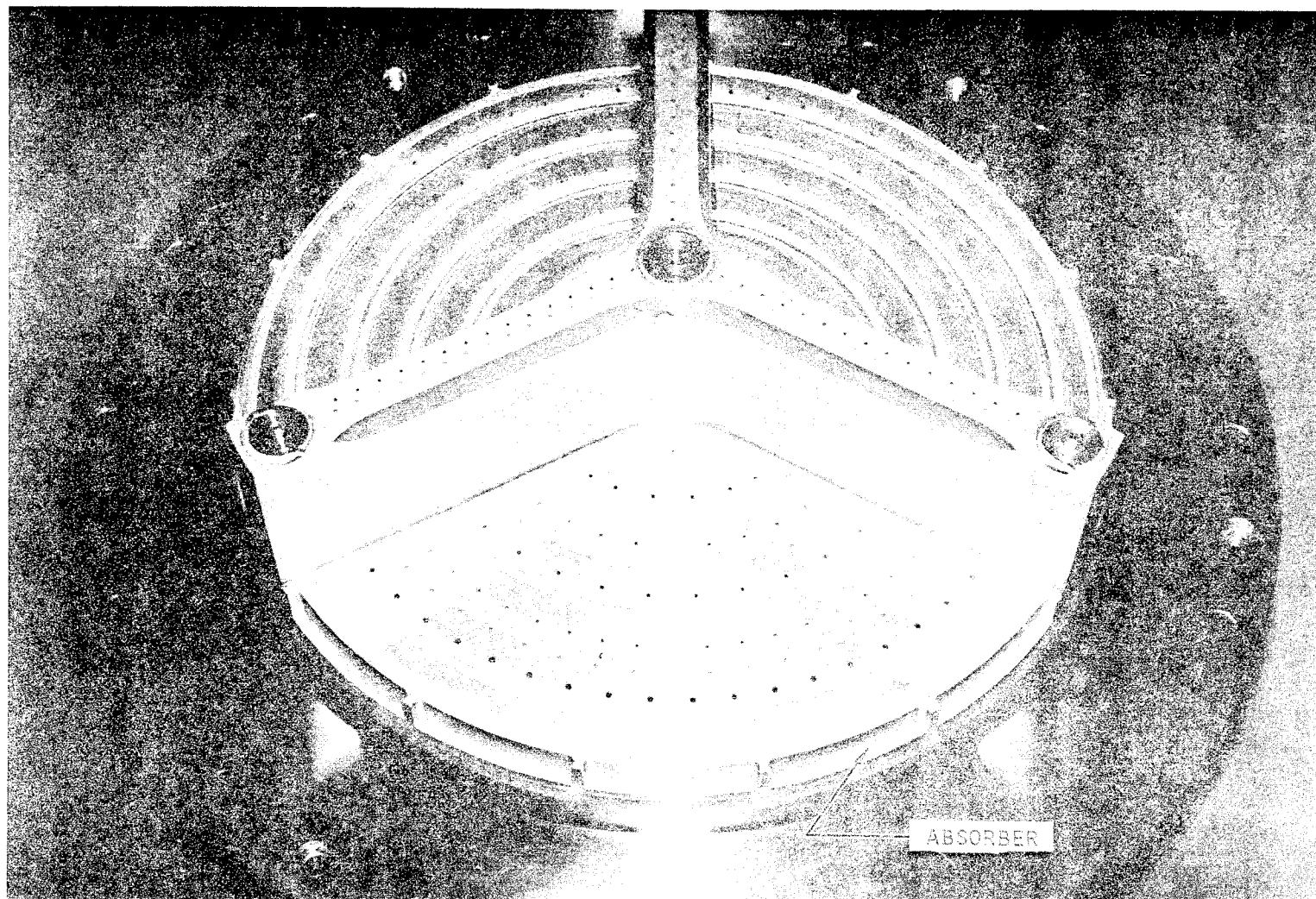
Figure 24. — Baffled injector with acoustic absorber slots on periphery (LMAE).

53
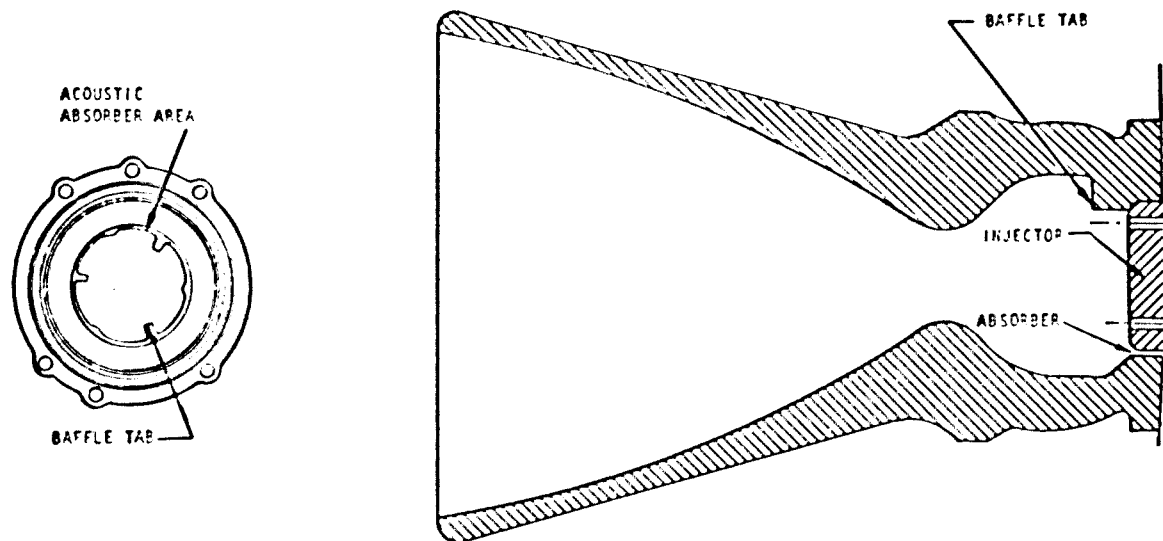
Figure 25. — Quarterwave absorber in RS-14 engine.
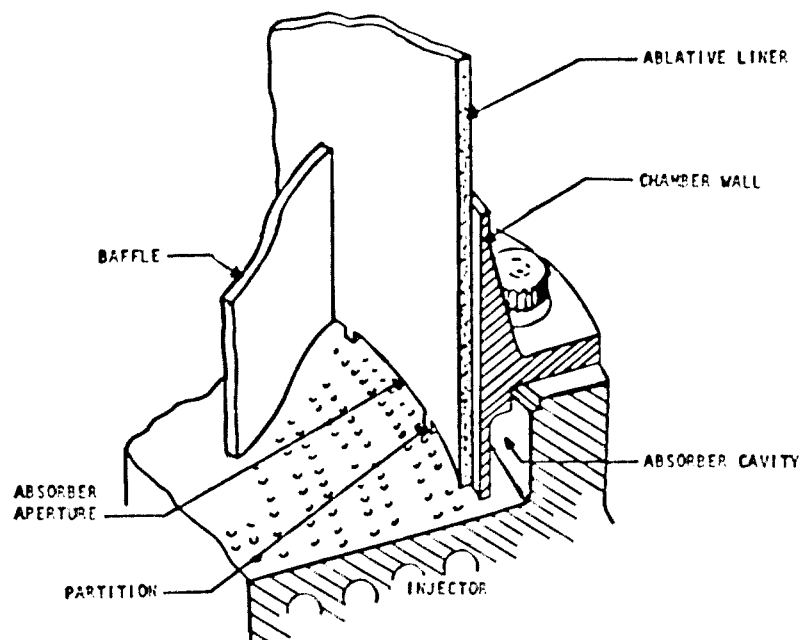
Figure 26. — Absorber configuration in the XRL booster engine.

54

lined engine (ref. 57). This effect is still not understood but may be associated with a convection of acoustic energy into the system by the coolant flow (ref. 58). In the case of the LMAE, stabilization with slot or acoustic-cavity absorbers was found to be unaffected by film-coolant flowrate (ref. 46). However, in the case of a development combustion chamber, stability decreased with increased film-coolant flowrate; the increased instability could be controlled by acoustic cavities (ref. 59).

The use of ablative liners is restricted by several problems: loss of strength resulting from charring; changes in acoustic properties during burn (due to erosion of the apertures); and off-design acoustic behavior caused by changes in gas properties. Nevertheless, ablative liners have been tested successfully (refs. 57 and 60).

2.2.3.1 THERMAL ANALYSIS

Initial calculation of the gas-side heat flux to a regeneratively cooled liner usually is made with the simplified correlation of Bartz (ref. 38), despite the fact that this correlation is more nearly applicable to the nozzle portion of a rocket engine. The equation assumes that the gas is at the equilibrium temperature of the fully reacted gas at the appropriate bulk mixture ratio. Experimental results show that the predictions of the Bartz correlation may be low by as much as a factor of 2 or high by a factor of 3, the deviation depending on injector configuration and mixture ratio (refs. 14 and 61). However, in a large number of cases, the correlation has given satisfactory predictions of heat flux to chamber surfaces (at surface temperatures below $1000°$ F [811 K]).

Bartz-correlation calculations often fail to predict the reduced cooling requirements that result from the use of refractory materials. Measurement of the local adiabatic wall temperature in the combustion chamber indicates that the effective gas temperature is limited by the local equilibrium gas temperature (which corresponds to the local mixture ratio and local proportion burned) (refs. 14, 43, and 61). Therefore, the gas-to-surface driving force for heat transfer in the upstream portion of the chamber can be reduced by a factor of 2 or 3 by use of refractory coatings.

The reduced effective gas temperature near the injector also must be considered in the design of ablative liners, because both char rate and erosion rate of phenolic/Refrasil are controlled primarily by the adiabatic wall temperature (rather than by the heat-transfer coefficient) at chamber pressures above 150 psi (1.03 MN/m^2) (ref. 14). A number of recent analyses (refs. 36, 62, 63, and 64) permit estimation of the local adiabatic wall temperature near the injector. The analyses are based upon both the injector element configuration and the spray combustion of the propellants. Description of the propellant-spray mass and mixture-ratio distributions can be determined either from injector cold flows or from cold-flow characterization of the individual injector elements.

55

Temperature measurements in apertures and cavities indicate that the conditions therein are considerably different from those in the main gas stream. Methods developed for treating flow and heat transfer in slots and holes (ref. 65) have been used to interpret temperatures in slot-type absorbers in combustion chambers (ref. 46). Entrance temperatures in excess of 2800° F (1811 K) have been measured (ref. 21), with the cavity bottom temperatures as much as 1400° F (1033 K) cooler. Heat-flux measurements have shown (ref. 60) that heat loads are modest because there is little or no absorber hot-gas throughput during steady combustion. However, some large openings may encounter cyclic erosive hot-gas flows. The shape of the acoustic absorber, particularly the slot type, is much like a weld relief and behaves like an expansion/contraction space except at the partitions. During a hot firing, the gap might close as much as 0.010 to 0.020 in. (0.25 to 0.51 mm) (not enough to affect the absorber impedance seriously). Although thermal loads to acoustic absorbers cannot be ignored, they are often of little importance. However, the periphery of an injector has been damaged as a result of thermal stresses on the partitions in a slot-type absorber.

2.2.3.2 COOLING METHODS

Convective and nucleate boiling correlations (ref. 51) generally are used in the calculation of flowrates for regenerative cooling. If the thrust chamber wall consists of bundles of thin-walled tubes, the acoustic liner may be made by swedging individual tubes to produce slotted apertures that lead to a backup cavity. In this way, the regenerative cooling capabilities of the thrust chamber are used with minimal conduction complication of the design. If the acoustic liner consists of ports between milled coolant passages, then a three-dimensional conduction analysis is needed to determine the proper spacing between cooling slots. Thermal protection of regeneratively cooled surfaces (located near the injector) is often enhanced by coating such surfaces with refractory materials.

If film cooling is used, then the correlation developed by Hatch and Papell (ref. 66) may be used to determine the amount of film coolant required to maintain the allowable wall temperature downstream of film-coolant injection ports. Liquid accumulation in absorber apertures and cavities due to film cooling is prevented by one of several techniques (e.g., canting the resonator apertures downstream as discussed in ref. 60). In some cases, both film and transpiration cooling have worsened combustion instability (refs. 57 and 59).

In general, either regenerative cooling or transpiration cooling alone requires complex fabrication procedures (ref. 60); in addition, regenerative cooling alone can require excessive pressure drop. Some film cooling used with regenerative cooling, transpiration cooling, or high melting point metals can result in an acceptable system design. State-of-the-art ablative materials used with film cooling ($\approx$ 3 percent of fuel) can also result in an acceptable system design (ref. 60).

The rates of char formation and erosion of ablative liners have been predicted, in terms of local gas temperature and heat-transfer coefficient, by computerized analyses (refs. 37 and

43). Some potential problems with ablative liners along with possible solutions are detailed in table III, which is based on material in reference 60. Maintaining the surface dimensions

Table III. — Ablative Liner Materials: Problems and Solutions

Potential Problem	Possible Solution
Delamination	Small-angle wrap; rosette wrap Precharred material
Strength loss due to local ablation	Carbonaceous materials Precharred materials
Chemical attack (oxidation environment)	Oxidation-resistant coating (Al_2O_3) or reenforcing fillers

Thermal shock	Materials with appropriate combinations of
	   High conductivity
	   High ductility
	   Low coefficient of thermal expansion
	   High ultimate strength

of an ablative acoustic liner (particularly the dimensions of the apertures) in order to maintain the acoustic properties of the liner may be a crucial factor in absorber effectiveness. Consequently, injectors that are compatible with an unlined chamber have, in some cases, been found to be unacceptable in ablative-lined chambers; in other cases, compatible configurations have been designed and tested (ref. 60).

If the absorber apertures are confined to the region just downstream of the injector, the adiabatic wall temperature often is low enough to allow the use of refractory materials on uncooled surfaces (e.g., molybdenum or tungsten alloys protected by disilicide or sprayed ceramic coatings). A low wall temperature allowing use of coatings is more often the case if mixture-ratio bias is built into the injector. It should be noted, however, that the structural integrity of the coatings must be carefully considered.

57

2.2.4 Acoustic Damping Analysis

Several methods have been developed and used to predict the stabilizing capability of acoustic absorbers. None of these methods is universally accepted as clearly superior, despite the implications of some of the literature. Therefore, the designer must assess the relative merits of each before choosing a particular method. The basic purpose of each method is the same but, because different assumptions are employed, the results and corresponding hardware produced by the various methods often differ substantially.

One method involves calculation of an absorption coefficient for an acoustic liner or a "resonator" coefficient (similar to absorption coefficient) for limited numbers of resonators. Another method involves calculating, from a partial stability analysis of the combustion chamber, a temporal-damping-coefficient contribution. The third method involves a complete stability analysis but with restrictive simplifying assumptions.

Each of these methods is analytical in nature. A fourth method is based on simple correlations of absorber configurations that have been found to be adequate or inadequate in producing stability.

For each of the analytical methods noted above, the acoustic impedance of the absorber is required. Methods of calculating this impedance Z and its components R and X are described in Appendix A.

2.2.4.1 ANALYTICAL METHODS

Absorption coefficient. -- The most widely used measure of full-length liner effectiveness is the absorption coefficient. This coefficient, defined as the fraction of the oscillatory energy incident on a wall that is absorbed at the wall, is expressed as

$$A = \frac{4\Theta}{(1 + \Theta)^2 + \chi^2} = \begin{array}{l}\text{absorption coefficient} \\ \text{due to an array of acoustic absorber elements}\end{array} \tag{11}$$

where

$\Theta = R/\bar{c\rho}c = $ specific acoustic resistance of absorber

$\chi = X/\bar{c\rho}c = $ specific acoustic reactance of absorber

$R = $ acoustic resistance of resonator

$X = $ acoustic reactance of resonator

$Z = R + iX = $ acoustic impedance of resonator, $i = \sqrt{-1}$

$\epsilon = $ fraction of surface with acoustic impedance Z (fractional open area of absorber related to liner area)

$\overline{\rho} = $ time-averaged gas density in chamber

$c = $ sound speed in chamber

Details on the use and calculation of the absorption coefficient calculation are given in reference 67; the methods therein are improvements over those presented in the widely used reference 54.

Resonator coefficient. — The calculation and use of the resonator coefficient are described in reference 68. Equations for the resonator coefficient are derived for a single resonator in a manner similar to that used for obtaining the absorption coefficient. This coefficient was developed for the design of limited numbers of resonators.

Damping coefficient. — The temporal-damping-coefficient approach is based on the observation that the time dependence for low- to moderate-amplitude oscillation in the combustion chamber is of the form

$$\widetilde{P} \approx [\exp(-\alpha_N t)] (\cos(\omega_N t)) \qquad (12)$$

where

$\widetilde{P} = $ oscillatory pressure

$\alpha_N = $ damping coefficient

$\omega_N = $ angular frequency of oscillation

$t = $ time

Subscript N denotes the mode as designated m, n, and q in equation (1).

According to the arguments of references 21 and 69, a contribution to α_N due to the absorber may be adequately estimated by solving the wave equation for the combustion chamber (neglecting combustion, flow, and nozzle effects). Thus, the method corresponds to a partial stability analysis. Further description of this approach may be found in references 21, 46, 58, 59, 69, and 70.

59

Calculation of the damping coefficient for a full-length liner is simpler than that for partial-length or single-row types. If the acoustic impedance of the liner is assumed to be uniform, the wave equation can be solved in a straightforward fashion. Actually, the impedance is not entirely uniform, because (1) the local impedance depends on the local oscillation amplitude (a nonlinear effect) and (2) the liner is made up of a finite number of holes. Nonetheless, the assumption of a uniform impedance is a reasonable approximation and has been employed for full-length liners.

For this case, solution of the wave equation by separation of variables leads to a characteristic equation in terms of both the Bessel functions for transverse modes and the specific acoustic impedance of the liner ($\zeta = Z/\bar{c}\bar{\rho}c$). The various temporal damping coefficients may be determined by solving the characteristic equation for the complex eigenvalues; the real part of each eigenvalue specifies the resonant frequency and the imaginary part specifies the damping coefficient for that mode (ref. 69).

Obtaining an expression for the nonuniform impedance case is more difficult because the wave equation cannot be solved by separation of variables. However, reference 71 describes a variational technique that is appropriate for this case. This technique has been used to calculate the damping coefficient for a single row or a few rows of resonators (refs. 21, 46, and 59).

Stability analysis including effects of combustion and flow processes. – Several analyses developed to predict stability of an engine containing an absorber include the effects of steady flow, combustion, and the nozzle.

Priem and Rice (ref. 72) developed an analysis for full-length acoustic liners including steady flow, localized combustion (assumed to all occur at the injector face), and a simple nozzle loss. The liner acoustic impedance was not allowed to vary with frequency.

Mitchell, et al. extended the basic approach used by Priem and Rice to allow for partial-length liners (ref. 73) and distributed combustion (ref. 74).

Oberg, et al. (ref. 75) developed an analysis somewhat similar to that of Mitchell (ref. 73), but for slot-type absorbers.

Sirignano (ref. 1, pp. 139-146 and 154-156) and Smith (ref. 18) developed approximate stability analyses that include several flow and combustion processes, including allowance for an acoustic absorber. Tonon (ref. 1, pp. 408-410) uses the method developed by Sirignano and, also, results from an analysis by Cantrell (ref. 58) in his discussions on acoustic absorber design. The work of Sirignano, Smith, and Tonon leads to the conclusion that the real part of the acoustic admittance (inverse of the impedance) of the absorber should be maximized to create maximum damping.

60

<u>Comparison of analytical methods.</u> — Detailed comparisons of the stability trends predicted by the methods described above have not been made. However, some partial comparisons are discussed below.

The methods described by Sirignano, Smith, and Tonon in the references cited above lead to expressions for the overall damping (or growth) coefficient comprising additive contributions. The influence of the absorber appears in one term that is proportional to the real part of the acoustic admittance of the absorber. Consequently, their approach is based on maximizing this part of the admittance. However, this entire additive term is the damping coefficient contribution by the absorber, the same contribution sought in the damping coefficient method.

Thus, the principal difference between these methods (Sirignano, Smith, and Tonon) and the damping-coefficient method is the way in which this contribution is estimated. With the methods of Sirignano, Smith, and Tonon, the effect of the absorber has been assumed to be sufficiently small that a set of approximations is valid. With the damping-coefficient method these approximations are not made, so that it is not necessary to verify their validity, even though the overall additive nature of the damping coefficient contributions probably is lost when the approximations are not valid. Nevertheless, the damping coefficient method appears superior because it relies less on the validity of the approximation.

The methods of Sirignano, Smith, and Tonon attempt to allow for combustion and steady-flow effects but use a set of simplifying approximations to obtain a tractable result. The methods of Priem (ref. 72), Mitchell (refs. 73 and 74), and Oberg (ref. 75) attempt to retain these effects with fewer assumptions. Therefore, the latter methods appear superior, but they are more complicated and difficult to use. If conditions are such that the additive result obtained by Sirignano, Smith, and Tonon is valid, the results from all analyses should be equivalent in terms of absorber configurations.

Much of the analysis that has been done with these various methods has regarded the absorber impedance to be independent of frequency. However, as shown in figure 27, significantly different results may be obtained if the actual frequency dependence is included. For the calculation of frequency-dependent reactance, the liner was assumed to be tuned for the unlined first-tangential frequency. Note that the results of these calculations indicate a mode splitting that results in two "first-tangential" modes, one of which may be regarded as the first-tangential-first-radial mode with its frequency shifted near to that of the normal first-tangential mode. These results show that the lower mode would be highly damped at a specific acoustic resistance greater than eight. Conversely, the upper (higher frequency) branch is more strongly damped than the lower at specific resistance values less than about six. Thus six would be the optimum value to use. Figure 27 also shows that the optimum is underestimated by a factor of at least two when a constant-reactance value of zero or -3.0 is used.

61
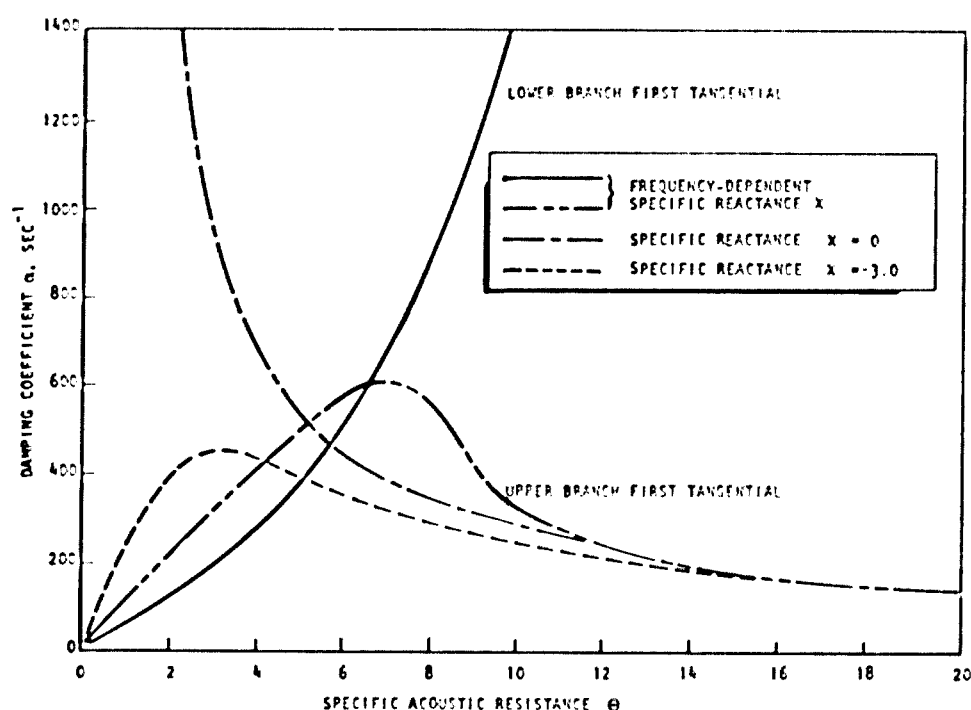
Figure 27. — Comparison of damping predictions for constant reactance and frequency-dependent reactance (full-length acoustic liner).

Although the absorption coefficient method is more accurate than might be expected (considering the assumptions required in its derivation [ref. 71]) and has been used to design a number of successful acoustic liners, it appears to have substantial weaknesses. Tonon (ref. 1, p. 410) concludes that its use may lead to designs that are substantially less than optimum. The absorption coefficient normally is used in the description of room acoustics for wavelengths that are small in comparison with the room dimensions (not the case in rocket engine combustion chambers). Phillips (ref. 47) found the trends predicted by his damping-coefficient calculations when $\Theta/c > 1$ to be the same as those predicted by the absorption coefficient for full-length liners. The absorption coefficient exhibits the same trends as the damping coefficient if the liner reactance is treated as a constant (independent of frequency). However, the liner reactance is known to be strongly dependent on frequency for frequencies near the resonant frequency. As shown in figure 28, when the frequency dependence of the liner reactance is included in the damping calculations, the

62
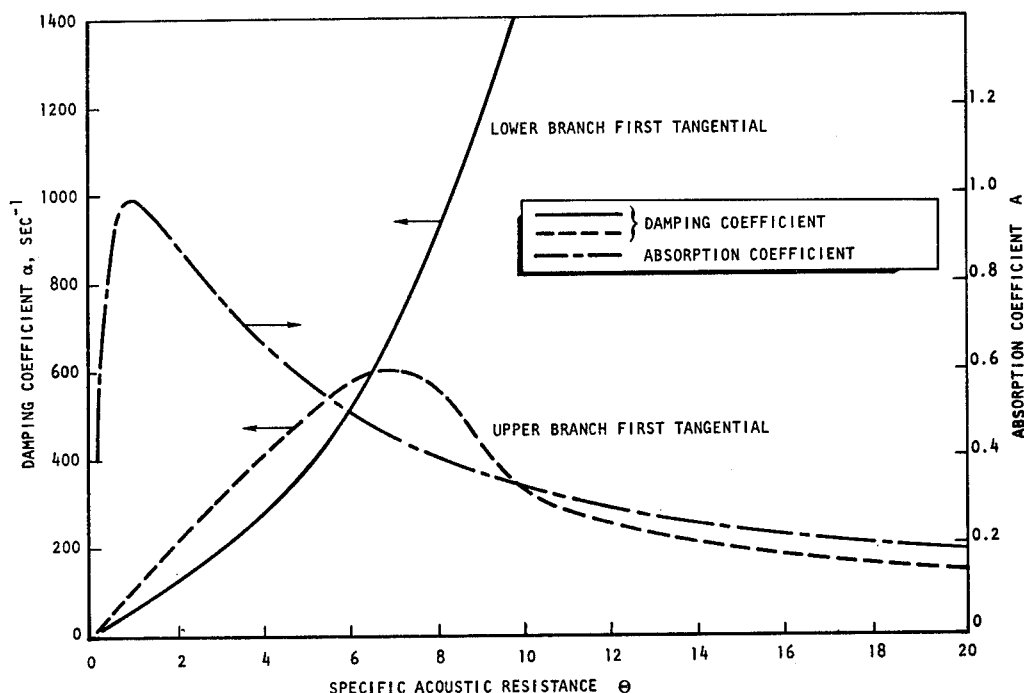
Figure 28. — Comparison of damping predicted by absorption and damping coefficients (full-length acoustic liner).

absorption-coefficient approach causes the optimum resistance to be underestimated by a factor of about six. Thus, the absorption-coefficient approach is less desirable for predicting optimum damping than is the more rigorous damping-coefficient approach.

The damping-coefficient method, the only other analytical method that has been used in hardware design, has been employed in the design of the absorbers in the RS14, RS21, Lunar Module Ascent, and XRL booster and sustainer engines, all of which are production engines. In addition, the method has been used to design hardware for a number of technology programs and the three combustion chambers for the Space Shuttle Main Engine. This method has also been used in recent work to develop the Space Shuttle Orbit Maneuvering Engine (ref. 59).

Figure 29 presents a comparison of measured and predicted stability trends for the LMAE, the predicted trends having been obtained with the damping-coefficient method. The

63
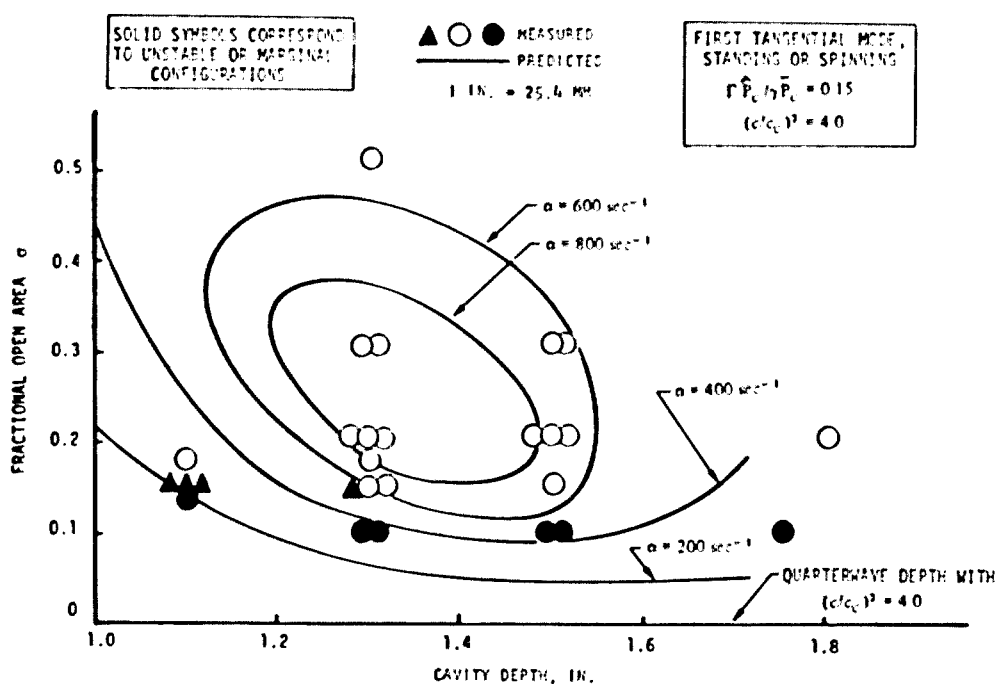
Figure 29. — Comparison of measured and predicted stability trends for the LMAE absorber configurations (ref. 46).

experimental results, which show the effective cavity depth and fractional open area σ (absorber area expressed as a fraction of injector face area) for stable, unstable, and marginal acoustic-cavity or slot-type absorber configurations, were obtained in LMAE type of hardware with an unbaffled injector (ref. 46). This figure summarizes results from ≈ 100 motor firings with 25 conventional acoustic-cavity configurations and ≈ 190 bomb disturbances. The analytical results suggest that when the absorber damping exceeds some level (the experimental data suggest $\alpha \approx 600 \text{ sec}^{-1}$), the combustion should be stable. Clearly, the experimental results do no completely follow the predicted pattern; nevertheless, the agreement is sufficient to justify continued use of the method. No similar comparison for other absorber types or analytical methods is available.

Optimization of the damping for a particular application must be governed by the needs of that application. Often, maximum damping is required; however, if multiple instability modes have been experienced or are expected, a compromise is often required. At times, absorbers designed to eliminate one mode have removed that mode but a new mode occurred (ref. 76); thus, maximum overall damping for a series of modes is often required. For an acoustic liner, it has been suggested that the optimum open area is the area that

64

results in the maximum absorption coefficient with the widest bandwidth (ref. 1, secs. 8.3.4 and 8.3.5).

It is also desirable to include temperature sensitivity in the optimization, because the temperatures in the absorber usually vary greatly.

For a volume-limited system, maximum damping is not necessarily obtained when the resonant frequency of a liner is equal to the frequency of the instability (ref. 69). Thus, in this case, the liner open-area fraction is optimized on a damping basis rather than on a tuning or resonant frequency basis.

2.2.4.2 EXPERIENCE GUIDELINES

Successful absorbers can be designed on the basis of available experience without the use of analytical design methods. For example, figure 29 indicates that a slot-type absorber with an open area of about 15 percent or greater and roughly the proper depth will stabilize the LMAE. The use of such simple guidelines has led to working designs.

McMillion and Nestlerode (ref. 77) have developed similar guidelines by summarizing and correlating much of the available experience with acoustic absorbers. The summaries are shown in tables IVA and IVB, and the correlations are shown in figures 30 and 31. These tables and figures have been revised from those presented in reference 77 in order to reflect the results of a recent review of the original data sources. Some of the information has been changed to incorporate necessary corrections, but the overall conclusions presented in reference 77 remain unchanged. The results indicate that stability can be obtained if σ, the fractional open area of the absorber, exceeds the value $3/f^2$, where f is the frequency of the mode being suppressed.

2.2.4.3 DESIGN PRESSURE AMPLITUDE

Some uncertainty and confusion exists concerning the amplitude of the oscillatory pressure for which an absorber should be designed. Because of impedance nonlinearities, predicted damping varies with amplitude. Most early liner calculations were made with an arbitrarily assumed "incident" amplitude of 190 decibels. The incident amplitude was assumed to be half the local amplitude; thus, the 190-decibel level corresponds to a local amplitude of 56 psi (386 kN/m^2) peak-to-peak.

It is unreasonable to design an absorber for peak-to-peak amplitudes less than a few percent of chamber pressure. For amplitudes greater than 20 percent of chamber pressure, the validity of the acoustic equations becomes questionable. Thus, peak-to-peak oscillation of 20

Table IVA. – Summary of Absorber Effectiveness in Operational and Development Engines – Part I*

[Modified from table II in ref. 77]

Absorber Program[1]	Dominant Instability Without Absorber		Absorber Effectiveness[3]	Fractional Open Area σ percent	Injector Pattern	Propellants	Comments
	Frequency, Hz	Mode[2]					
AFRPL (ref. 78)	2000	1T	No (1T) ↓ Yes (1T)	20.9 28.9 35.1 35.1	Triplet ↓ Like doublet	N₂O₄/50-50	With aperture through-flow No through-flow ↓
PAW-12 in. motor (ref. 79)	3300	1T	Yes (1T, No (7400 Hz)) Yes (1T, No (7200 Hz))	28. 44.	Triplet		Dual array Wide band
PAW-AGENA (ref. 79)	2500, 3200	1T, 1T-1L	No (1T, 1T-1L) Yes (1T, 1T-1L) ↓	4.8 9.5 19.1 10.1			Uncooled ↓ Regeneratively cooled liner
PAW-12 in. motor (ref. 80)	2300, 3600, 4700	1T, 2T, 1R	Yes (2T), No (1T, 1R) Yes (2T, 1R), No (1T) Yes (2T, 1R), No (1T, 7600 Hz) Yes (1T, 2T, 1R), No (Pops) Yes (1T, 2T, 1R), No (7600 Hz)	3.1 7.9 19.2 12.9 17.4			Ablative Film cooled Transpiration cooled Dual ablative Dual steel
NASA-Lewis (ref. 81)	5000, 9000	1R, ?	Yes (1R, 9000 Hz), No (1T) Yes (1R, 1T, 9000 Hz) ↓	7.4 14.8 29.7 59.4			
NASA-Lewis (ref. 82)	3300, 5600	1T, 2T	Marginal (1T, 2T) Yes (1T, 2T)	5.5 14.6	Coaxial	LO₂/LH₂	Individually tuneable resonators
Aerojet-LMA (ref. 60)	3500, 5700	1T, 2T	Yes (1T), Marginal (2T) No (1T), Yes (2T)	8.5 8.5	Triplet	N₂O₄/50-50	Ablative liner Dual resonator, cooled liner[4]
Aerojet-Transtage[5]	3800 to 4800	2T, 3T, 1R	No (1R, 2T, 3T) Yes (1R, 2T, 3T)	5.3 6.5	Quadlet (2 on 2)		
Bell-LMA[6] (ref. 83)	7000	1R, 3T	No (1R, 3T)	~2.	Triplet		
NASA-C1 (ref. 84)	17 000	1T	Yes (1T)	6.0	Unlike	N₂O₄/MMH	Occasional instability without absorber

*Work conducted at places indicated in column 1

[1]Unbaffled chamber except as noted

[2]1T = first tangential mode, 1R = first radial mode, etc.

[4]Water-cooled simulation of regenerative cooling

[5]Five-bladed injector baffle   [6]Three-bladed injector baffle

[3]Absorber effectiveness: Yes (nT, mR, xxxx Hz) implies that the indicated modes (i.e., the nth tangential, mth radial, and undefined mode of frequency xxxx Hz) were judged to be suppressed; No (nT, mR, xxxx Hz) implies that the indicated modes were not suppressed or appeared with the use of the absorber. In some cases, modes or frequencies were observed with the absorber that had not been observed without it.

99

Table IVB. – Summary of Absorber Effectiveness in Operational and Development Engines – Part II*

[Modified from table I in ref. 77]

Absorber Program[1]	Dominant Instability Without Absorber		Absorber Effectiveness[3]	Fractional Open Area σ, percent	Injector Pattern	Propellants	Comments
	Frequency, Hz	Mode[2]					
F-1	500	1T	No (1T)	5.7	Like doublet	LO_2/RP-1	
XRL Booster[4]	1300	Feed system coupled	No (1300 Hz)	0.7	Unlike doublet	IRFNA/UDMH	Combined feed system and chamber mode
J-2 (basic)	1800	1T	No (1T)	5.0	Coaxial	LO_2/LH_2	
Rocketdyne-LMA (unbaffled)	3300	1T	No (1T) / Marginal (1T) / Yes (1T)	4.6 / 9.3 / 18.5	Unlike doublet	N_2O_4/50-50	Unstable without absorber
XRL Sustainer[5]	3500 to 4500	1T	Marginal (1T)	10.0	Unlike doublet (pintle)	IRFNA/UDMH	Marginal to unstable at 3500 to 4500 Hz without absorber. Occasional 3500 Hz with absorber
FLOX/LPG	4000	1T	Marginal (1T)	12.5	Unlike 4 on 1	FLOX/LPG	Unstable without absorber Rapid burning pattern
XRL Booster[4]	4600 / 4600 / 8700	4T / 4T / 7T	Yes (4T) / Yes (4T) / Yes (7T)	4.5 / 6.0 / 1.4	Unlike doublet	IRFNA/UDMH	Unstable without absorber
Spartan[6]	5000	IT, w[7]	Marginal (1T, w)	10.7	Unlike doublet	ClF_3/N_2H_4	Very fast burning patterns — small injection orifices (0.020")
	5000 / 8300	IT, w / IT, h	Marginal (1T, w) / Marginal (1T, h)	10.7	Like doublet		
Flexem[5],[8]	6500	1T	Yes (1T)	8.0	Like and unlike doublet (pintle)	ClF_5/MHF-7	Unstable with unlike pattern and no absorber
Rocketdyne-LMA[9] (baffled)	7000	1R, 3T	Yes (1R, 3T)	4.6	Unlike doublet	N_2O_4/50-50	Unstable without absorber
RS-14/21	9500	1T	Yes (1T)	7.0	Unlike doublet	N_2O_4/MMH	5% of pulse firings unstable without absorber

*Work conducted at Rocketdyne Div., Rockwell International Corp.

[1],[2],[3]See footnotes (1), (2), and (3) for Part I

[4]Annular combustion chamber with four radially directed baffles

[5]Throttleable pintle-type injector

[6]Rectangular combustion chamber

[7]Transverse modes in height (h) or width (w) directions

[8]Acronym for flexible energy management; see ref. 85

[9]Injector had three equally spaced radial baffles.

67
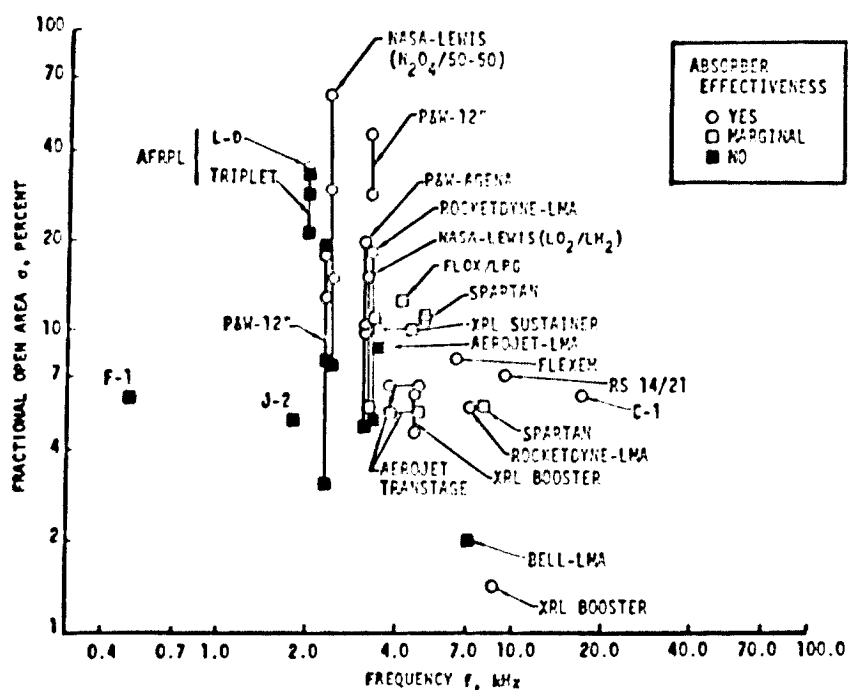
Figure 30. – Absorber effectiveness as a function of frequency f and absorber fractional open area σ (data from tables IVA and IVB) (adapted from ref. 77).
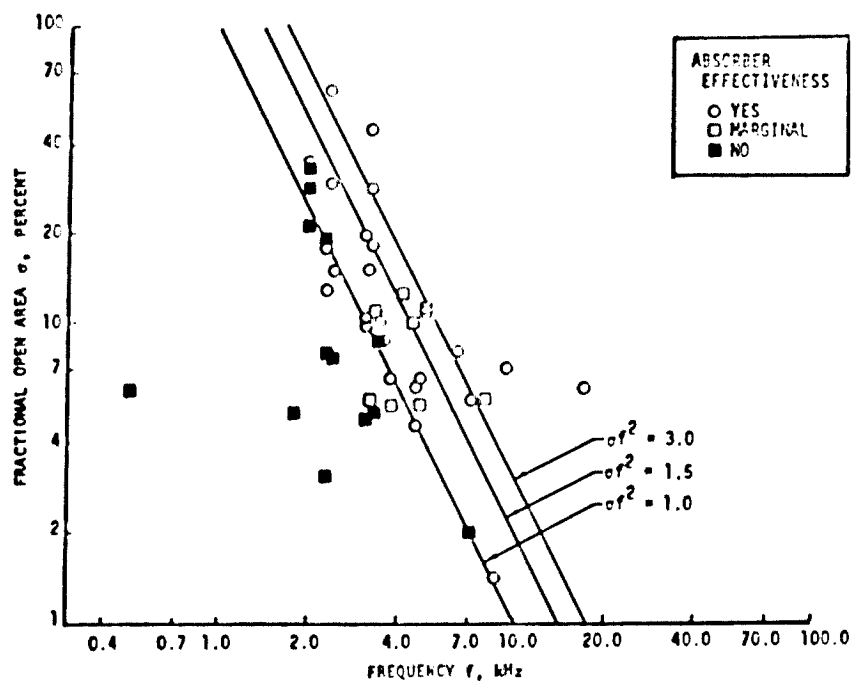
Figure 31. – Abosrber effectiveness related to the product σf² (adapted from ref. 77).

68

percent of chamber pressure has been used for some design calculations (refs. 21 and 69). However, best agreement between measured stability and predicted trends has been obtained for amplitudes $\approx$90 percent of chamber pressure (refs. 46 and 59).

2.2.4.4 BANDWIDTH

In the usual sense, bandwidth refers to frequency range over which an absorber is effective. A related characteristic is the temperature range over which an absorber is effective. Generally, it is considered desirable that an absorber design have sufficient bandwidth to damp all instability modes that might occur. Similarly, it is desirable that the absorber have sufficient damping over the entire temperature range that the absorber might experience. However, there is some danger that overall damping will be sacrificed in favor of bandwidth to the extent the absorber will not be adequate in any range.

The bandwidth characteristics of Helmholtz and intermediate resonators tend to be better than those of quarterwave resonators. Very good bandwidth can be obtained from Helmholtz resonators by adjusting the relative resonator dimensions (particularly, short aperture lengths), but at the expense of greater total resonator volume. Another way of getting good bandwidth is to use several absorbers, each tuned to a different frequency.

An interesting case of an absorber designed for several acoustic frequencies is reported for the Lance booster engine (ref. 86). An absorber that was effective over the frequency range 4000 to 9000 Hz was obtained with a sequence of absorbers for which predicted damping coefficients are shown in figure 32. The initial absorber (config. 1) suppressed the principal instability mode at 4600 Hz, but oscillation in the range of 7000 to 9000 Hz persisted. Therefore, approximately one-fourth of the resonators were retuned to give more damping at the higher frequency (config. 2), some improvement in stability resulting. Subsequently, the absorber was enlarged (open area and cavity size were increased) and tailored by analytical techniques for broad bandwidth. The latter configuration incorporating a single resonator size (config. 3) was successful.

2.2.4.5 HOT-FIRING MEASUREMENTS

In several programs (refs. 21, 47, 49, 67, 69, and 82), oscillatory pressure in the acoustic absorber was measured in order to determine, insofar as possible, the acoustic impedance that actually existed during test firings of an engine; related measurements were made by Crocco, et al. (ref. 19). The technique is essentially that described by Sivian (ref. 87). With this technique, oscillatory pressure measurements are made at the open end and at the closed end of the absorber. These data are used to infer the absorber impedance. Although results from these measurements tend to be widely scattered because of difficulties in making the appropriate measurements, they tend to correlate with the cold-flow results discussed in Appendix A. The technique provides data ultimately useful for design purposes

69
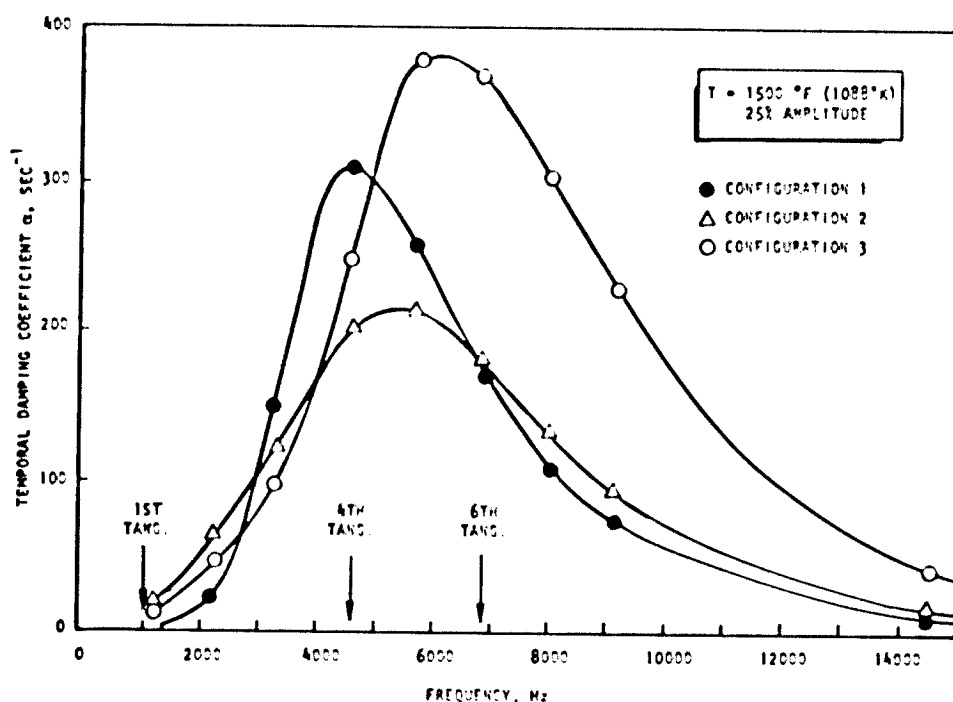
Figure 32. — Calculated damping coefficient vs frequency for absorber in Lance booster engine (ref. 86).

because the information is obtained on the actual behavior of the absorber during use. Otherwise, cold-flow impedance data must be extrapolated to combustion-chamber conditions.

Temperature measurements and gas sampling. – The acoustic impedance and, in turn, the damping of an absorber are strongly dependent on the time-averaged temperature distribution within the absorber. The variations in temperatures measured in cavities and apertures are often rather large, the spread indicating that these temperatures are far from uniform and that they are difficult to measure. With acoustic liners, the temperature varies with open-area fraction. With quarterwave resonators, temperature often varies with open area, and frequently but not always there is a steep temperature gradient from the open to closed ends of the cavity. And, as might be expected, the temperature varies with the propellant combination.

70

In the design of quarterwave-type absorbers, the use of measured absorber temperatures, assumed to be representative of the absorber gas temperature (ignoring temperature gradients), often may be interpreted to indicate improper absorber tuning when the absorber is clearly suppressing an instability. The reason for this discrepancy is not known, but it may be caused by measurement errors resulting from chemical reaction on the surface of the thermocouple used for the measurement.

Temperature data from acoustic liner test firings with LOX/LH$_2$ may be found in references 48, 82, and 88. Temperature data from test firings with quarterwave-type absorbers and the LOX/LH$_2$ propellant combination may be found in reference 89. Similar data from LOX/RP-1 test firings may be found in references 49 and 55, and data from N$_2$O$_4$/50:50 propellant combination appear in references 21, 47, and 53. Temperature data from quarterwave-type absorbers with the N$_2$O$_4$/50:50 and N$_2$O$_4$/MMH propellant combinations are given in reference 21; typical data from these measurements are shown in figures 33 and 34. These data are reasonably reproducible from run to run and are different for different configurations. Some degree of temperature control can be exercised by purging the absorber with cold gas (ref. 47).

Gas sampling has been used to determine the gas composition within the absorber (an important measurement for design calculations). Garrison (ref. 1, secs. 8.3.4 and 8.3.5) used a sampling technique for ablative liners. Sampling measurements were made in the absorbers in the F-1 and LM Ascent engines (refs. 49 and 90) and in the quarterwave absorbers of a LOX/LH$_2$ engine (ref. 89). Phillips (ref. 82) employed gas sampling in his work with the LOX/LH$_2$ propellant combination. In each of these cases, the gas composition was found to reflect the gas composition along the chamber wall. Pressure probes were used in the F-1 engine to measure local gas velocity (ref. 49).

Measurement of gas temperature and composition in the resonator is essential for accurate determination of sound speeds and densities necessary for liner design.
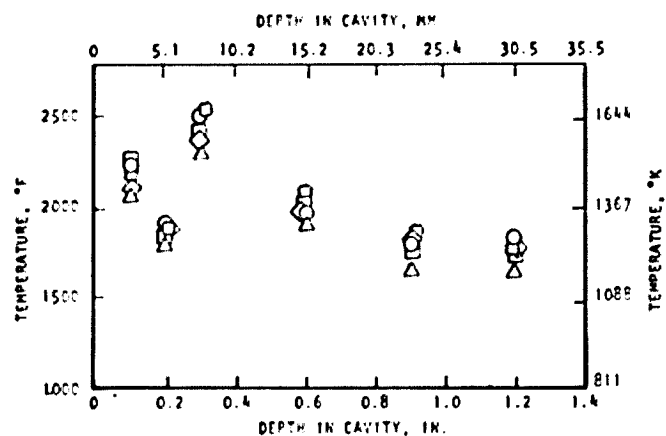
Figure 33. — Typical data on temperature distributions in acoustic cavities, different runs (ref. 21).
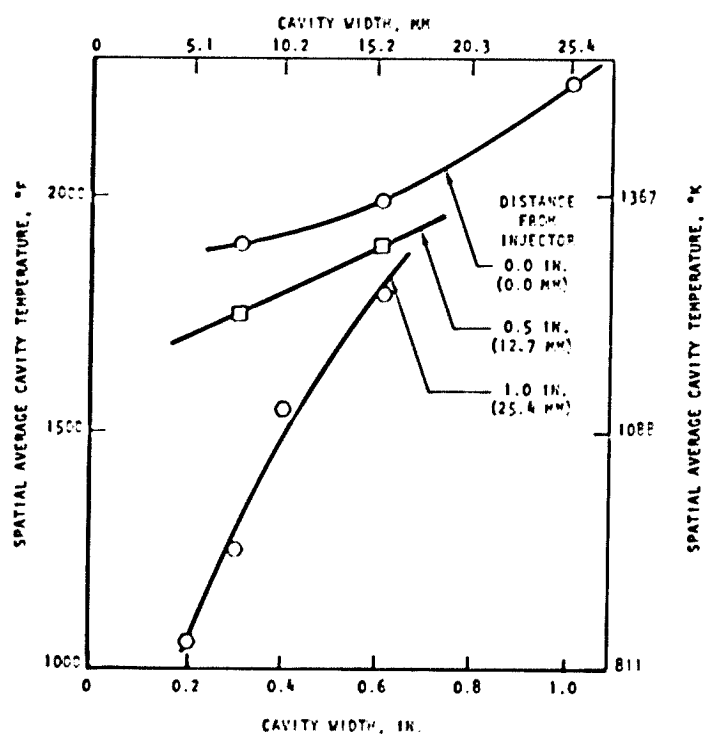
Figure 34. — Measured average cavity temperature vs cavity width, three distances from injector (ref. 21).

72

3. DESIGN CRITERIA and

Recommended Practices

3.1 BAFFLES

3.1.1 Combustion Chamber Acoustics

The probable acoustic modes of the combustion chamber shall be known before baffle design is initiated.

A simple acoustic analysis should be made for the chamber. The procedures for this analysis are outlined in section 2.1.1. Even for complicated chamber geometries with baffles, this simple analysis is recommended as a starting point, but if the chamber is very large or digresses considerably from simple cylindrical or annular shape, acoustic-model tests should be made. These tests should determine the frequencies of the instabilities that may occur. High-amplitude testing with the model can determine effect of baffles (or absorbers) on the damping rate of the chamber. During the testing with these acoustic models, care should be taken to assure that the proper equipment and techniques are used to prevent spurious effects and inaccurate results (ref. 91).

As an alternate to model testing, the acoustic analysis described in reference 2 should be considered.

3.1.2 Baffle Geometry

3.1.2.1 TRANSVERSE COMPARTMENT DIMENSIONS

Baffle spacing in the transverse dimension shall prevent sustained transverse oscillations in the compartments.

When the chamber and injector are very similar to those of a proven design, the baffle compartments should be sized from experience with that proven engine. However, it should be kept in mind that even small changes in injector pattern, hole size, and fluid velocity may make radical changes in stability and thus may require changes in baffle compartment size. A change in propellants is not an important change per se, but because the physical properties of propellants differ, a propellant change usually results in changes in other parameters (e.g., injection velocity) that must be taken into account.

When the changes from a proven design are significant, a detailed analysis (refs. 13, 15, and 64) of the steady-state and transient combustion expected in the combustion chamber should precede the definition of baffle compartment sizes. The referenced analyses consider the detailed combustion and fluid dynamic processes occurring in the combustion chamber and provide much better bases for baffle spacing than rule-of-thumb practices based upon experience. The analysis should proceed as follows: (1) Determine the steady-state operational parameters of the engine including burning rate, liquid and gas velocities, and combustion-gas mixture ratio — all as functions of distance from the injector. (2) Use an instability model such as that in reference 13 to determine a maximum-size baffle compartment. (3) Use the inputs from the steady-state model at locations in the instability model that correspond to the baffle tips and verify the adequacy of the baffle length.

When the new design is so radical as to be beyond the capabilities of the existing analyses, the simple acoustic analysis discussed in section 2.1.1 should be used as a starting point. All modes with frequencies less than approximately 3000 Hz should be prevented by keeping baffle compartment size small (an odd number of radial baffles should be used). Generally, modes with higher frequencies can be effectively controlled by acoustic absorbers with less weight, structural, and cooling penalties than will be incurred with corresponding baffles. Thus, it is recommended that chambers smaller than about 10 in. (25.4 cm) in diameter need use only radial baffle spokes (i.e., radial combustion instability modes would not be expected to be a severe problem). Larger chambers should utilize circular can-type baffles to eliminate radial acoustic instability modes. Similarly, for chambers less than 10 in. (25.4 cm) in diameter, three spokes probably are sufficient; larger chambers will require more. Refer to section 3.1.2.3 for additional guidance.

3.1.2.2 BAFFLE LENGTH

Baffles shall be long enough to prevent full chamber modes from occurring downstream of the baffles.

An analysis (see. 3.1.2.1) of the steady-state and transient combustion at all engine operating conditions should be made to determine the axial region of maximum combustion rate (ref. 64). Generally, a curve such as that shown in figure 35 will be found. Baffles should be made to extend continuously beyond the region of most intense combustion as shown in the figure.

The practical limit on baffle length (due to cooling requirements becoming excessive) is about 5 in. (12.7 cm). Thus, it is recommended that baffles longer than about 4 in. (10.2 cm) be avoided (it may require a basic change in the injector to achieve this objective). If baffles longer than about 4 in. (10.2 cm) are believed to be required, the feed-system oscillations should be carefully scrutinized to determine that resonances outside the chamber are not responsible for the observed chamber oscillations.

74
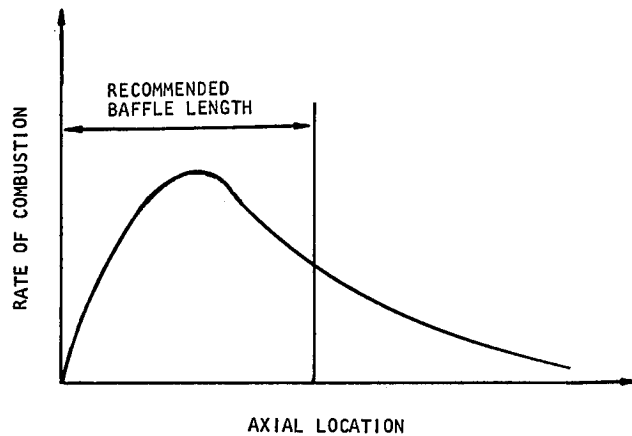
Figure 35. — Baffle length related to axial location of maximum rate of combustion.

As in the case of baffle compartment size, empirical correlations are recommended only if injector and chamber are very similar to a proven design.

Finally, experimental verification of the adequacy of the baffle length is recommended (sec. 3.1.2.4).

3.1.2.3 CONFIGURATION

The baffle configuration shall prevent interaction of the acoustic modes of the chamber and the modes in the injector feed passage.

Possible acoustic modes in the hydraulic side of the injector should be calculated, and pressure nodes located (ref. 1). If these possible nodes are similar to possible nodes in the combustion chamber, it is recommended that a baffle not be placed in a location that would be a pressure node in the feed system. Thus, baffles should be designed to straddle such possible node locations as the injector dome inlet, main ring groove passages, and other passages or passage endings. It is further recommended that, since most hydraulic systems are symmetrical and consist of 2, 4, 6. 8, etc. symmetrical portions, an odd number of baffles should be used.

Hub-and-spoke baffle configurations should be used unless severe interaction problems are encountered.

75

3.1.2.3.1 Profile

The baffle profile shall obstruct acoustic particle displacement and shall maintain continuity with adjacent surfaces.

In very small chambers (D < 4 in. [10 cm]), it may be permissible to use only baffle tabs (fig. 8) to prevent tangential oscillatory gas motion on the periphery of the chamber.

Spaces no more than 0.010 in. (0.254 mm) thick may be allowed between a baffle and the injector or chamber wall. An attachment should be carefully designed to avoid (1) crevices where unreacted propellants may accumulate and possibly detonate and (2) narrow cracks that may allow erosive oscillatory hot-gas flow through them.

If the baffles cannot be sealed tightly to adjacent surfaces, place the baffles such that each baffle compartment has equal mass flow density, i.e., equal propellant injection per unit injector area. This practice will minimize flow between compartments during stable combustion.

3.1.2.3.2 Cross Section

The baffle cross section shall satisfy the requirements for cooling and for structural strength but shall not interfere with propellant injection.

To minimize baffle interaction with injected propellant and combustion-gas acceleration, the baffle should be as thin as possible and should be the simplest cross-sectional shape that can be used. There is no specific cross-sectional shape that appears to have advantages from a stability standpoint, and therefore the shape should be selected for other reasons.

3.1.2.4 DESIGN CONFIRMATION AND RATING

Hot-firing and stability rating tests shall confirm the effectiveness of the baffles.

For designs of low confidence level, hot firing coupled with a stability rating device should be used to sequentially determine minimum baffle length, maximum baffle compartment dimension, and the interaction of those dimensions. Even if the confidence in the stability analysis is low, the analysis should be used in concert with the hot-firing tests to reduce costs and minimize required testing.

Rocket engines that are designed for vehicles that carry human cargo, i.e., man-rated engines, should be known to be dynamically stable. For these engines, the following program (refs. 29 and 30) is recommended:

76

(1) Dynamic stability requirements should be specified at the onset of the engine development program in the initial engine model specification.

(2) Stability demonstration requirements for development, qualification, and production should be specified at the onset of the development program.

(3) A detailed stability history should be maintained throughout the entire development program. The stability history from initial feasibility and development testing will provide the basis for the specific demonstration requirements for the qualification test series.

(4) Potential injector designs and patterns should be evaluated with respect to dynamic stability characteristics as soon as the injectors become available for testing. Stability testing should be accomplished as parasite tests during early component and engine testing to obtain maximum testing at minimum cost. Various techniques for artificially inducing combustion instability should be tried. Initial stability testing should explore the stability margin of candidate designs. At this stage, marginally stable designs should be scrutinized for means to increase their stability margin. Subject to overall development considerations, the designs with the greatest stability margin should be selected for further development.

(5) Stability testing during extended development should be conducted to demonstrate that the preferred combustion-chamber design meets the specified stability requirements and has an adequate design margin. The majority of the tests should be conducted with the most effective rating device at the most sensitive location.

(6) Qualification and subsequent stability testing should be minimal and conducted only to provide confidence that some unknown production factors or minor hardware changes have not reduced the stability margin of the production engine below specification levels. Engine-to-engine variability requires that several engines be tested to establish a confidence level for the design. Engines with different accumulations of test time should be tested to determine whether engine stability degrades with time.

Engines designed for other purposes should also be stability rated, but the extent and requirements of the rating program should not be as strict as those for man-rated systems.

Either a bomb mounted inside the combustion chamber or a pulse gun mounted on the periphery of the combustion chamber should be chosen as a stability rating device.

3.1.3 Structural and Mechanical Design

3.1.3.1 MATERIAL SELECTION

Baffle material shall be suitable for the structural loads and for the chemical and thermal environments.

OFHC copper and aluminum alloys are suitable baffle materials for use with cryogenic propellants and storable propellants, respectively. For short firings, the use of refractory-coated baffles or composite baffles with an ablative outer layer should be considered. Any materials other than those used previously in similar service should be tested carefully for chemical, structural, and thermal suitability, with both combustion gases and raw propellants and with careful attention to engine duty cycle. Whatever material is selected, inspection and quality control measures should be adequate to ensure that the material does not deviate from specifications.

3.1.3.2 STRESSES

3.1.3.2.1 Thermal Stresses

Baffles shall not experience unacceptable permanent distortion from thermal stresses.

If baffles are to be welded or brazed to the injector face, the baffle material should have a coefficient of thermal expansion slightly lower than that of the injector face. The recommended practice is to make the baffles integral with the injector. Other practices to avoid permanent distortion include additional film or mixture-ratio-bias cooling near the baffles and good internal baffle cooling. For instance, regeneratively cooled baffles have shown increased cooling capability over dump-cooled baffles. The improved cooling has not incurred the performance penalty that would result from excessive dumping of baffle coolant downstream of the baffle.

Some baffle distortion would appear to be inevitable for long-duration and repeated firings, but the extent can be controlled by baffle cooling.

3.1.3.2.2 Dynamic Stresses

Baffles shall withstand effects of engine ignition transients and overpressures from the stability rating device.

Prevent excessive dynamic loads due to ignition transients by locating at least one ignition source in each baffle compartment. Even with this precaution, repeated starts can result in

78

permanent baffle distortion. Therefore, the expected lifetime or number of restarts should be considered in the stress calculations. In the case of stability rating devices (e.g., bombs or pulse guns), dynamic overpressures up to five times the steady-state chamber pressure may be expected. Repeated pulsing as well as restarting can cause baffle distortion to become significant and should be considered in the structural design.

3.1.3.3 ATTACHMENT

> *Effects of baffle thermal expansion shall not cause failure of the injector or the injector/baffle joint.*

During repeated engine firings, the baffle tip must be cooled sufficiently (sec. 3.1.4) to prevent compression beyond the elastic limit during firing if the baffles are rigidly attached (i.e., brazed, integral, or welded) to the injector.

3.1.4 Thermal Control

3.1.4.1 ANALYTICAL BASIS

> *Analytical studies shall accurately predict the thermal and chemical environment surrounding the baffles near the injector face.*

The adiabatic wall temperatures, gas mixture ratios, and liquid propellant splashing on the baffles as a function of position should be determined by an analysis similar to that in reference 14. This analysis gives an accurate estimate of propellant and gas velocity vectors, gas mixture ratios, and percent of propellants burned. Injector locations, angles, and orifice sizes; propellant velocities; and propellant properties must be known to obtain the required data.

The calculated adiabatic wall temperature coupled with a heat-transfer coefficient calculated either from the simplified methods of Bartz (ref. 38) or the more accurate methods of Hines (ref. 36) should be used to obtain the heat transfer to the baffles. This heat-transfer analysis forms the boundary conditions and the starting point for subsequent internal thermal analysis of the baffles.

If the analysis indicates severe mixture-ratio inhomogeneities, chemical corrosion of the baffles by highly oxidizer-rich combustion gases at local areas should be prevented either by modifying the injection characteristics or by introducing film coolant.

79

3.1.4.2 COOLING METHODS

The baffle cooling method shall maintain the temperature of the baffle at or below allowable limits during the lifetime of the engine.

The simplest cooling method (cooling by heat sink and conduction of heat to the injector face) is recommended. This method should be strongly considered when the engine lifetime is short, the baffles are less than 2 in. (5.1 cm) long, and the baffles are attached to the injector by a means that ensures good thermal contact (welding or brazing). It is further recommended that all possible simple extensions of this method be investigated. These extensions include the application of coatings or laminations to uncooled baffles to protect them from hot combustion gases and to reduce heat transfer.

Particularly in the case of conduction cooling of baffles, and to a lesser degree in other cooling techniques, conduction analyses such as those in reference 37 should be used to determine the temperature distribution in the baffle. These temperatures are then used to determine thermal stress and allowable material stress.

Coolant flow through dump-cooled or regeneratively cooled baffles must be sufficient for the coolant to absorb the total heat transferred to the baffles from the hot conduction gases without boiling or reaching its decomposition temperature. Further, the coolant velocity must be sufficiently high to prevent local heat fluxes from exceeding the allowable nucleate-boiling heat flux. Generally, the methods used for design of regeneratively cooled thrust chambers (ref. 52) should be followed for design of dump and regeneratively cooled baffles.

Film- and transpiration-cooled baffles should be designed according to procedures established for similarly cooled thrust chambers. Particular attention should be paid to local hot spots caused either by a dearth of coolant or by a localized high burning rate in the combustion gases. Progressive heating of this hot spot can cause failure of the baffle system. Either furnish these hot spots more coolant or reduce the heat input to these points by locally reducing the mixture ratio from the injector. The choice between these methods depends on relative effects on performance of the engine.

Baffles made entirely of ablative materials have not proven successful and are not recommended, but metal baffles covered by ablative material are often appropriate for short-duration firings. Care must be taken in the design of these composite baffles to ensure that the ablative material is not expected to take large strains or deflections (i.e., the metal structure must be designed to be more rigid than might be normal practice without the ablative lamination).

80

3.1.4.3 EXPERIMENTAL EVALUATION

Experimental methods shall provide data adequate for evaluation of the effectiveness of thermal control.

During hot firing, observe discoloration pattern, surface pitting or melting, erosion, peeling of coatings or ablative materials, cracked braze joints, and other evidence of inadequate cooling. These occurrences point out the need for corrective baffle cooling measures.

When insufficient cooling is suspected at a particular position on the baffles, measurements of local surface temperature, heat flux, or overall heat input should be made to assess quantitatively the problem of baffle overheating. These measurements should be integrated closely with an analysis effort such as that discussed in section 3.1.4.1.

3.1.5 Baffle/Engine Interactions

3.1.5.1 INJECTOR

Baffles shall not interact with injected propellants to cause low performance, overheating, or accumulation of unburned propellants.

Baffle design should be an integral part of the manifold/injector design. To minimize the effect of baffles on uniformity of distribution of mass and mixture ratio across the injector face, the number, thickness, and length of baffles should be minimized. Further, the techniques outlined in section 2.1.5.1 should be used to prevent nonuniformities in mixture-ratio and mass distribution. Propellants splashing against the baffles can also cause low performance and should be avoided by placement of baffles away from spray fans.

When baffles are dump or regeneratively cooled, make sure that the removal of the coolant from the injector manifold does not affect (starve) the adjacent injection ports. Similarly, the injection of film coolant for the baffles must be such that it creates minimum perturbation in the overall injection spray pattern. Dump cooling of baffles can also adversely affect the overall mixture-ratio distribution in the region of the baffles. Therefore, the sprays adjacent to the baffles must attempt to level the effect of the coolant dumped from the baffles.

81

3.1.5.2 COMBUSTION CHAMBER

Baffle wake effects shall not cause erosion of the combustion-chamber wall or create gross discontinuities in gas flow.

Baffle tips should be made as thin as possible to minimize vortex motion and flow separation along the chamber wall at the baffle tips. If structural or cooling considerations prevent utilization of sufficiently thin baffle tips, additional film cooling should be provided for the chamber at those points where the boundary layer is disrupted by the flow in the wake of the baffles. Another practice that will prevent erosion of the combustion chamber at these locations is to overcool the baffle in this region by dump cooling such that the coolant dumped from the baffle tip near the wall will also act as a film coolant for the chamber.

3.1.5.3 IGNITION

Baffles shall not increase the likelihood of damage by hard starts.

Provide multiple ignition sources within the chamber, so that any combustion wave progressing through raw propellants cannot build to a strong detonation wave.

Vent holes through baffles are not recommended because they subvert the intended purpose of the baffle.

3.1.5.4 STABLE OPERATION

Baffles shall not contribute to the frequency or magnitude of large-amplitude pressure perturbations in the combustion chamber.

Avoid any baffle design that would allow propellant to accumulate in crevices. Minimize any part of the combustion chamber/injector design that would cause raw propellant to spray on cold surfaces of baffles, chamber, or injector.

3.1.5.5 STABILITY RATING DEVICE

Baffles shall not be subject to damage by stability rating devices.

The bomb or pulse gun used to rate the stability of a combustion chamber should be located and oriented to minimize damage to baffles (and to the combustion chamber and injector) by shrapnel from the device. Particularly sensitive areas such as dump-cooling orifices, thin walls used for cooling, or fragile seals in the baffles should be protected from shrapnel damage.

82

The baffles should be sufficiently strong to withstand the overpressures generated by the combustion-stability rating devices. If the stability rating device is to be mounted to the baffle, easy access (from outside the chamber) to the mounting point and, if electrical initiation is to be used, access to the actuating wires must be provided.

Whatever type of rating device is used, it is essential that the baffle configuration not be changed by the rating device; for example, extra openings caused by exposed lead-wire ports may act as acoustic absorbers that make the chamber more stable than one without the lead-wire port.

3.1.5.6 THRUST VECTOR CONTROL (TVC)

The baffles shall not interfere with normal operation of the thrust vector control system.

The design of baffles and TVC injection sites should be coordinated. The TVC injection site should be located away from the wakes of combustion chamber baffles.

3.2 ABSORBERS

3.2.1 Configuration

3.2.1.1 LOCATION

The location of the acoustic absorber shall provide optimum damping.

In most cases, maximum damping can be obtained by locating the acoustic absorber as close to the injector face as possible. This rule holds for partial chamber acoustic liners as well as for acoustic slots. In all cases the absorber should be as short as possible consistent with adequate damping.

3.2.1.2 PARTITIONS

Acoustic absorber partitions shall provide structural support for the absorber and prevent hot-gas circulation within it.

To maintain structural integrity, support acoustic liner inserts in cylindrical chambers by partitions located between the chamber wall and the insert. The number and location of

83

such partitions may be determined by a stress analysis that assumes a differential pressure of four times the steady-state chamber pressure acting across the liner; this pressure differential corresponds to combustion-chamber overpressures of five times the steady-state chamber pressure. For quarterwave absorbers, twelve equally spaced partitions are recommended.

To prevent hot-gas circulation (and attendant erosion) in the absorber, the number of partitions should be two or three times the number of injector face baffles. Thus, if an injector incorporates three baffles in its design, nine partitions are used to prevent hot-gas circulation in the absorber.

3.2.2 Construction

3.2.2.1 CHAMBER LINERS

Chamber-liner acoustic absorbers shall withstand stress due to both steady-state chamber pressure and impulsive chamber overpressures

Chamber-liner acoustic absorbers may be designed in two basic ways: (1) a perforated chamber enclosed by annular rings, and (2) a perforated cylinder inserted in the chamber primary structure.

In both cases, the components of the chamber-liner acoustic absorber should be designed to withstand high stress levels at high temperatures by methods such as those used for the design of combustion-chamber walls (refs. 40 and 50). Allowance should be made for differential thermal expansion (in both axial and radial directions) between the absorber component and the backup structure (ref. 60).

3.2.2.2 SLOTS OR ACOUSTIC CAVITIES

Slot acoustic absorbers shall have minimal impact on the structural integrity of the injector and combustion chamber wall

Slot acoustic absorbers should be located near the injector face either by machining the slot into the injector face or thrust chamber wall or by judicious machining of the injector/chamber interface region. In both cases, the basic structural designs can be determined from methods used for combustion-chamber and injector design (refs. 52 and 92).

84

3.2.3 Thermal Control

3.2.3.2 COOLING METHODS

The thermal analysis shall accurately predict heat loads on the acoustic absorber.

Calculations of local heat flux should be made with analyses based on both the injector element configuration and the combustion pattern resulting from the propellant spray distribution (refs. 36, 52, 53, and 63).

3.2.3.2 COOLING METHOD

The cooling method shall enable the acoustic absorber to withstand chamber heat loads without loss of damping properties.

In general, acoustic absorbers can be designed to withstand chamber heat loads by employing cooling methods such as those used for the design of combustion chambers and injectors (refs. 52 and 92). In particular, acoustic-absorber cooling requirements can be reduced by making use of existing combustion-chamber cooling capabilities (e.g., swedge apertures between tubes in regeneratively cooled thrust chambers); avoiding regions of extremely high heat flux (e.g., the nozzle region); and locating the absorber in regions of low heat flux (e.g., the injector region). The last two recommendations suggest the use of short absorbers located adjacent to the injector face. If the absorber is short enough and the heat flux in the injection region low enough, then the required cooling can be obtained through the use of refractory metal coatings on the absorbers. Test results (ref. 60) indicate that acceptable acoustic-liner cooling can be achieved by combining film cooling with either regenerative cooling, transpiration cooling, ablative materials, or high-melting-point metals.

If either film or transpiration cooling is used, care must be taken to avoid coolant flow into the cavities; for example, cant the absorber apertures downstream. Liquid accumulation could both reduce the damping of the absorber and cause an explosion in the absorber cavity. If ablatively cooled absorbers are used, erosion of the aperture entrances must be considered, because such erosion could reduce the absorber damping (ref. 60). Special materials might be needed in this region.

85

3.2.4 Acoustic Damping Analysis

3.2.4.1 ANALYTICAL METHODS

Acoustic-absorber damping coefficient shall be a maximum within constraints imposed by hardware and geometry.

The absorber damping coefficient can be optimized without tuning to the frequency of instability. Since new chamber resonances can occur with the absorber present and since temperature variations change tuning of the absorber, the absorber damping coefficient is the critical design parameter. Therefore, the absorber open area can be made to provide optimum damping rather than exact tuning.

The damping coefficient for an acoustic absorber can be calculated by the methods described in section 2.2.4.1. Although the absorption coefficient is easier to calculate (and can be used for preliminary design), the damping coefficient is the better measure of absorber stabilization.

Although results of the damping-coefficient calculations provide no absolute measure of absorber performance, a reasonable value for α should lie in the range 100 to 1000 sec^{-1}. The decision in this range must rest on heuristic evaluation of the "sensitivity" of the instability (qualitatively indicated by damage, pressure amplitude, frequency of occurrence, rating device size required to initiate, growth rate, etc.).

The calculation of absorption/damping coefficients should be based on the calculated absorber acoustic impedance. The overall surface acoustic impedance can be calculated as an area-weighted average by the methods given in Appendix A. Only if dimensions of the resonators are small compared with a wavelength may the simple cavity impedance and aperture reactance be used. Calculations of aperture resistance should be based on the maximum oscillatory velocity in the aperture. These calculations also include the effects of cross and through flows.

3.2.4.2 EXPERIENCE GUIDELINES

Design guides based on experience shall define minimum open area for a tuned absorber.

Empirical results such as those presented in figure 29 and in section 2.2.4.2 show that a minimum open area of the absorber necessary to achieve stability is often found when the available data are assembled and studied. It is recommended that this procedure, based on demonstrated absorber effectiveness in producing stability, be used whenever possible to

determine minimum open area and/or absorber damping coefficient required for stability. To enhance the likelihood of successful design on this basis, the designer should exploit every opportunity with new test, development, and production engines to enlarge the store of knowledge presented in tables IVA and IVB and in figures 29, 30, and 31.

3.2.4.3 DESIGN PRESSURE AMPLITUDE

Acoustic-absorber design calculations shall be based on oscillatory pressure amplitudes that are related to the steady-state chamber pressure.

Calculations of damping coefficient for an acoustic absorber should assume overpressure amplitudes 10 to 100 percent of the steady-state chamber pressure. The use of arbitrary, all-purpose pressure amplitudes for design calculations is not recommended, since they represent negligible disturbances at high chamber pressures and nonlinear, nonacoustic disturbances at low chamber pressures.

3.2.4.4 BANDWIDTH

Acoustic absorbers shall have acceptable side-damping bandwidth.

The frequency range over which an acoustic absorber provides effective damping can be optimized (consistent with structural, spatial, and thermal limitations) by methods described previously. Care must be taken so that effective damping at the primary frequency of instability is not sacrificed.

87

88

APPENDIX A

CALCULATION OF ACOUSTIC IMPEDANCE

The acoustic impedance of a surface is given by

$$Z = \frac{1}{Y} = R + iX = \frac{\tilde{P}}{\vec{n} \cdot \vec{\tilde{u}}} \qquad (A-1)$$

where, as before, $i = \sqrt{-1}$ and

Z = acoustic impedance

Y = acoustic admittance

R = acoustic resistance

X = acoustic reactance

$\tilde{P}$ = oscillatory pressure

$\vec{\tilde{u}}$ = oscillatory velocity

$\vec{n}$ = outwardly directed unit normal vector

An alternate definition of Z is used by Tonon (ref. 1, p. 408).

Generally, the acoustic impedance is a function of both position and frequency. For simplicity, however, it is often assumed to be constant over some region of space. At high amplitudes, the acoustic resistance R is strongly dependent on the local pressure amplitude, but the reactance X is weakly dependent.

Calculations of absorber impedance (especially for acoustic liners) usually are based on an area-weighted average acoustic impedance given by

$$\frac{1}{Z_{av}} = \epsilon_1 \frac{1}{Z_1} + (1 - \epsilon_1) \frac{1}{Z_2} \qquad (A-2)$$

89

where

Z_{av} = the average surface impedance

ϵ_1 = the fraction of the surface with impedance Z_1

$(1 - \epsilon_1)$ = the fraction of the surface with impedance Z_2

For many calculations, specifically calculation of absorption coefficient (eq. (11)), Z_{av} and Z are taken as the same.

Equation (A-2) holds for absorber elements whose separation is small compared with the wavelength λ (spacing less than $\lambda/(2\pi)^{\frac{1}{2}}$, according to Ingard (ref. 93)).

Equation (A-1) generally is used for acoustic liners (with the assumption $Z_2 >> Z_1$). For more than two kinds of absorber elements, equation (A-2) can be generalized to

$$\frac{1}{Z_{av}} = \sum_{i=1}^{n} \epsilon_i \frac{1}{Z_i} \qquad (A-3)$$

where

n = number of different types of absorber elements

ϵ_i = fraction of surface occupied by the ith type of absorber element

Z_i = impedance of the ith type of absorber element

The spacing between each type of element should be less than $\lambda/(2\pi)^{\frac{1}{2}}$

Two kinds of fractional areas have been employed in liner calculations: one, ϵ, based on the total chamber-side surface area, and the other, a, based on the cavity-side surface area (a is defined as (aperture area)/(resonator area)). The chamber-side basis ϵ is the appropriate one for calculating the liner impedance since, without changing either the open area of the resonator or the natural resonant frequency, the internal cavity area could be varied to give a value for a very near zero or one.

The acoustic impedance of an absorber element itself can, particularly in the case of a Helmholtz resonator, be approximated by

$$Z = Z_C + Z_A \qquad (A-4)$$

90

where

Z_C = cavity acoustic impedance = $R_C + iX_C$

Z_A = aperture acoustic impedance = $R_A + iX_A$

R_C = cavity acoustic resistance

X_C = cavity acoustic reactance

R_A = aperture acoustic resistance

X_A = aperture acoustic reactance

A.1 CAVITY ACOUSTIC IMPEDANCE

The impedance of a simple resonator cavity alone (region V_C in fig. A-1) is purely reactive (i.e., $R_C = 0$) and is given by the well-known expression

$$Z_C = iX_C = -i\frac{\gamma_C \overline{P}_C A_A}{\omega V_C} \qquad (A\text{-}5)$$
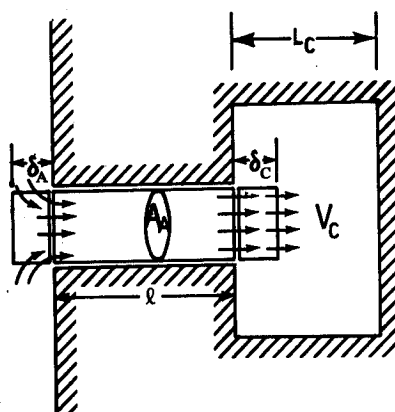
Figure A-1. — Sketch illustrating parameters involved in calculation of acoustic impedance (adapted from ref. 1).

91

where

γ_c = ratio of specific heats of gas in the cavity

$\overline{P}_c$ = time-averaged pressure in cavity

A_A = cross-sectional area of aperture

ω = angular frequency of oscillation

V_c = volume of cavity

This equation is valid if all cavity dimensions are small compared with the wavelength $\lambda = 2\pi c_c/\omega$. Terms involved are illustrated in figure A-1.

If the cavity depth is not small compared with the wavelength, but the cavity cross-section is either rectangular or cylindrical in shape, equation (A-5) may be replaced by the expression

$$Z_c = -i \, \frac{\overline{\rho}_c \, c_c \, A_A}{A_c} \, \cot\left(\frac{\omega l_c}{c_c}\right) \qquad (A\text{-}6)$$

where

A_c = cross-sectional area of the cavity

l_c = cavity depth

c_c = isentropic speed of sound in the cavity = $\left(\dfrac{\gamma_c \overline{P}_c}{\overline{\rho}_c}\right)^{\frac{1}{2}}$

This equation is readily obtained by solving the wave equation with boundary conditions appropriate to the cavity. The particular form given here results from a long-wavelength approximation: correction terms can be obtained with variational approximation. It should be noted that, for small $\omega l_c/c_c$ (i.e., $l_c \ll c_c/\omega \approx \lambda$), equation (A-6) reduces to equation (A-5).

Acoustic liners frequently are made with an annular resonator cavity around the circumference of the chamber (figs. 20 and 21); i.e., a perforated cylinder with an outside diameter somewhat smaller than the inside diameter of the combustion chamber is inserted into the chamber. The perforated cylinder is centered in the chamber with several circumferential struts. The annular space between the combustion-chamber wall and the perforated cylinder forms the resonator cavity. The acoustic impedance of this kind of

92

resonator cavity is different from that given in equation (A-6), because the length of the cavity in the annular direction is not small compared to a wavelength. A suitable expression is easily obtained by solving the wave equation with boundary condtions for the annular cavity. Since the thickness of the cavity usually is small, the Bessel function expression that results can be reduced by a Taylor-series expansion around the outer radius to give

$$Z_C = -i \frac{\gamma_C \overline{P}_C A_A}{\omega A_C \Delta r} \frac{\left(\dfrac{\omega r_o}{c_C}\right)^2}{\left[\left(\dfrac{\omega r_o}{c_C}\right)^2 - m^2\right]} \tag{A-7}$$

where

A_A = aperture cross-sectional area (per aperture)

A_C = cavity cross-sectional area (per aperture)

Δr = radial depth of resonator cavity

r_o = radius of outer shell of resonator cavity

m = angular index of the mode excited in the main chamber

Equation (A-7) reduces to equation (A-5) if $m = 0$, a radial or longitudinal mode. Also, equation (A-7) is valid only if the radial cavity dimension Δr is small compared with the wavelength.

A.2 APERTURE ACOUSTIC IMPEDANCE

Acoustic resistance. – The resistance of absorber elements is affected substantially by both the local pressure amplitude and the steady-flow environment. In the amplitude range of interest for absorber design, the resistance of Helmholtz and quarterwave resonators is dominated by high-amplitude effects, the viscous losses generally being negligible in comparison.

The high-amplitude acoustic resistance of acoustic resonators often may be adequately expressed as

$$R_A = \Gamma \overline{\rho}_A \hat{u}_A \tag{A-8}$$

93

where

Γ = coefficient that varies with resonator type

$\bar{\rho}_A$ = time-averaged gas density in the resonator open end (aperture)

$\hat{u}_A$ = peak velocity amplitude in the open end (aperture)

Values for the resistance coefficient Γ may be obtained from the theoretical studies of Zinn (ref. 1, pp. 400-405), Sirignano (ref. 76), Tonon (ref. 1, pp. 405-408), and Oberg (ref. 94). For Helmholtz resonators, the value

$$\Gamma = 0.37/C_f^2 \tag{A-9}$$

where C_f is an empirical flow coefficient for steady flow, provides good correlation with experimental data (ref. 1, p. 404). For quarterwave resonators, values of Γ ranging from about 0.6 to about 0.3 have been obtained (refs. 21 and 46).

In absorber-design calculations, the value of Γ often may be combined with the value for the assumed design pressure amplitude to give a single design parameter (ref. 46).

The effects of steady flow through the resonator have been studied by several investigators (ref. 1, pp. 405-407; refs. 47, 48, 94, 95, 96, and 97). The results suggest the use of

$$R_A = \Gamma \bar{\rho}_A (\hat{u}_A + 3.5\, U_A) \tag{A-10}$$

where U_A is the steady-flow velocity through the aperture.

The effects of steady cross flow (perpendicular to the axis of the aperture) are even less well known. Most cross-flow liner designs have been based on the work of Meyer, Mechel, et al. (refs. 98 and 99). They found both components of the impedance to be affected by the flow. In particular, aperture resistance was found to increase with cross-flow velocity. An interesting feature of this work is that amplification was encountered in some regions of operation, but this does not appear to be a problem in absorber work (ref. 88).

More recent work by Garrison (ref. 96) led to the empirical expression

$$R_A = (1 + 1.9\, M_\rho)\, R_{A(v = 0)} \tag{A-11}$$

94

where M_p is Mach number of the steady flow past the orifice and $R_{A(U=0)}$ is the no-flow aperture resistance. This expression is based on data obtained in the range $0.05 < M_p < 0.25$. Phillips' results (ref. 100) appear to obey a similar relationship with a somewhat greater slope.

Garrison (ref. 48) also measured the aperture resistance with simultaneous through and cross flows. He concluded the resistance was dominated by the through-flow effect and was adequately described by the through-flow expression except for very low through-flow velocities.

The effect of steady flow on the resistance of quarterwave resonators has not been measured. It appears reasonable to assume, however, that the effects are similar to those found with Helmholtz resonators.

Acoustic reactance. – The reactance of a Helmholtz resonator aperture that is short compared with a wavelength may be written as

$$X_A = \overline{\rho}_A \omega \ell_e \qquad\qquad (A\text{-}12)$$

where ℓ_e is the effective aperture length. The effective aperture length is obtained by adding a mass end correction δ to the physical length ℓ, i.e., $\ell_e = \ell + \delta$.

The mass end correction δ is composed of contributions from each area change, i.e., from each end of an aperture (fig. A-1):

$$\delta = \delta_A + \delta_C \qquad\qquad (A\text{-}13)$$

The contributions from each end may be different but usually are assumed to be equal. In addition, the parameter δ depends on both oscillatory velocity amplitude and steady-flow velocity. Table A-I presents some recommended equations for δ for the conditions cited. These equations are based on the assumption that $\delta_A = \delta_C$. When this assumption is not valid, the same equations can be used to determine δ_A and δ_C by halving the coefficient of D_A or $A_A^{\frac{1}{2}}$ and assigning an appropriate value to a for each end of the aperture; δ then is the sum of δ_A and δ_C thus determined. For low area ratios ($a < 0.16$), the equation

$$\delta = 0.96 A_A^{\frac{1}{2}} \left(0.5 - 0.7\sqrt{a}\right) \qquad\qquad (A\text{-}14)$$

appears to be most suitable for all conditions.

95

Table A-1. – Recommended Equations for Mass End Correction δ

δ	Limitation	Reference
$0.85 \, D_A \, (1 - 0.7 \sqrt{a})$	a < 0.16 Low amplitude, no flow	93
$0.4 \, D_A \, (1 - 0.7 \sqrt{a})$	High amplitude, high through flow	47, 95, and 97
$3/8 \, (0.85 \, D_A \, (1 - 0.7 \sqrt{a}))$	Sharp edge orifices, moderate amplitude	101
$0.85 \, D_A \, (0.5 - 0.7 \sqrt{a})$	High external cross flow or through flow	This work
$0.877 \, A_A^{1/2} \, (1 - 0.818 \sqrt{a})$	Noncircular apertures, moderate amplitude	53
$0.96 \, A_A^{1/2} \, (0.5 - 0.7 \sqrt{a})$	All conditions a < 0.16	This work

Notes: D_A = diameter of aperture

   A_A = area of aperture

   a = (aperture area)/(resonator area)

A.3 RESONATOR ACOUSTIC IMPEDANCE

When equation (A-4) is rewritten in terms of the resistance and reactance components, the impedance of a simple resonator is expressed as

$$Z = (R_C + iX_C) + (R_A + iX_A) \qquad \text{(A-15)}$$

The preceding discussion has shown that the acoustic resistance of the resonator is simply the resistance of the aperture R_A, so that equation (A-14) becomes

$$Z = R_A + i(X_A + X_C) \qquad \text{(A-16)}$$

The reactance of a Helmholtz resonator thus can be written as the sum of the aperture and cavity reactances:

$$X = X_A + X_C \qquad \text{(A-17)}$$

96

Equation (A-17) rewritten in terms of equation (A-12) and equation (A-5) yields

$$X = \bar{\rho}_A \, \omega \ell_e - \frac{\gamma_A \bar{P}_C A_A}{\omega V_C} \qquad\qquad (A\text{-}18)$$

or

$$X = \bar{\rho}_A \, \omega_o \ell_e \left(\frac{\omega}{\omega_o} - \frac{\omega_o}{\omega} \right) \qquad\qquad (A\text{-}19)$$

where

$$\omega_o = \left(\frac{\gamma_A \bar{P}_A}{\bar{\rho}_A} \frac{A_A}{\ell_e V_C} \right)^{\!\!1/2} = c_A \left(\frac{A_A}{\ell_e V_C} \right)^{\!\!1/2} \qquad\qquad (A\text{-}20)$$

with c_A the sonic velocity in the aperture.

By comparison, the reactance of a quarterwave resonator, for a partitioned cavity, is

$$X = -\bar{\rho}_A \, c_A \, \cot\!\left(\frac{\omega L_C}{c_A} \right) \qquad\qquad (A\text{-}21)$$

where L_C is the depth of the slot or cavity.

The reactance of an intermediate resonator can be calculated from the solution for the wave equation for the inside of the cavity (ref. 7). The expression for this reactance reduces to the Helmholtz expression (eq. (A-18)) when L_C and ℓ_e are small compared to a wave length; it also reduces to the quarterwave expression (eq. (A-21)) when $\left(\dfrac{\bar{\rho}c}{A} \right)_A = \left(\dfrac{\bar{\rho}c}{A} \right)_C$.

Expressions for the reactance of more nearly general resonator configurations may be found in reference 46.

97

98

APPENDIX B
GLOSSARY

Symbol	Definition
A	absorption coefficient
A (with subscript)	cross-sectional area
a	aperture area/resonator area
C_f	empirical flow coefficient for steady flow
C_p	specific heat at constant pressure
c	velocity of sound
D	diameter
f	frequency
h	average baffle height
i	imaginary unit, $i = \sqrt{-1}$
k	thermal conductivity
L	length or depth
$\overline{L}$	mean length
LMA, LMAE	lunar module ascent engine
ℓ	physical length of aperture
ℓ_e	effective aperture length, $\ell_e = \ell + \delta$
M_p	Mach number of the steady flow past the orifice
m	angular index of the mode excited in the main chamber

Symbol	Definition
N_B	number of radial baffles or baffle blades
N_{CC}	number of cylindrical baffle cans
$\vec{n}$	unit normal vector directed outward from surface
o/f	oxidizer-to-fuel weight ratio
P	pressure
$\bar{P}$	time-averaged pressure
$\tilde{P}$	oscillatory pressure
$\hat{P}$	pressure peak amplitude
ΔP	overpressure
R	acoustic resistance
$R_{A(U=0)}$	acoustic resistance of aperture with no steady flow through it
r	radius
r_o	radius of outer shell of resonator cavity
Δr	radial depth of resonator cavity
t	time
U	steady-flow velocity
$\hat{u}$	velocity peak amplitude
$\vec{\tilde{u}}$	oscillatory velocity
V	volume
w	transverse compartment dimension
w_r	compartment dimension in radial direction

100

Symbol	Definition
w_θ	compartment dimension in tangential direction
X	acoustic reactance
XRL	extended range Lance
Y	acoustic admittance
Z	acoustic impedance
Z_i	acoustic impedance of ith kind of absorber element
α	temporal damping coefficient
$\beta_{m,n}$	transverse (tangential and radial) eigenvalues (m = integer indicating tangential mode; n = integer indicating radial mode)
Γ	correlation coefficient for slot resistance
γ	ratio of specific heat of gas at constant pressure to that at constant volume
δ	(1) decay rate (2) mass end correction added to physical length ℓ of aperture (table A-I)
ϵ	fraction of surface with impedance Z
ϵ_i	fraction of surface with impedance Z_i (fraction of surface occupied by the ith absorber element)
ζ	specific acoustic impedance
Θ	specific acoustic resistance of a liner surface
κ	thermal diffusivity, $\kappa = \dfrac{k}{\rho C_p}$
λ	wavelength
ρ	density, usually gas density

101

$\bar{\rho}$	time-averaged gas density
σ	open area of absorber expressed as a fraction or percentage of injector face area
χ	specific acoustic reactance of a liner surface
ω	angular frequency of oscillation

<center>Subscripts</center>

A	aperture
av	average
B	baffle
C	cavity
CC	cylindrical cans
ch	chamber
m	integer indicating tangential mode number
max	maximum
min	minimum
N	mode of oscillation (m, n, or q as in eq. (1))
n	integer indicating radial mode number
opt	optimum
q	integer indicating longitudinal mode number

Material	Identification
50:50, 50-50	50/50 blend by weight of hydrazine and UDMH, propellant grade per MIL-P-27402
Chromel-alumel thermocouple	thermocouple whose elements are nickel-base alloys. The positive element is chromel; the negative element is alumel.

Material	Identification
CTF	chlorine trifluoride
FLOX	mixture of liquid fluorine and liquid oxygen
hydrazine	N_2H_4, propellant grade per MIL-P-26536
IRFNA	inhibited red fuming nitric acid, propellant grade per MIL-N-7254 Type III A
LH_2	liquid hydrogen (H_2), propellant grade per MIL-P–27201
LO_2,LOX	liquid oxygen (O_2), propellant grade per MIL-P-25508
LPG	liquified petroleum gases: 55% CH_4, 45% C_2H_6
MHF-7	mixed hydrazine fuel
MMH	monomethylhydrazine, propellant grade per MIL-P-27404
N_2O_4	nitrogen tetroxide (oxidizer), propellant grade per MIL-P-26539
nylon	a thermoplastic polyamide
OFHC copper	oxygen-free high-conductivity copper
Refrasil	trademark of HITCO (Los Angeles, CA) for fibrous silica of high purity SiO_2; useful as extreme high temperature insulation; resistant to high-frequency vibrations
Rigimesh	trademark of Aircraft Porous Media, Inc. (Glen Cove, NY) for porous plate formed by compressed, sintered stacks of wire screen
RP-1	kerosene-base high-energy hydrocarbon fuel per MIL-P-25576
Teflon	trademark of E. I. duPont Co. for tetrafluoroethylene fluorocarbon resins
UDMH	unsymmetrical dimethylhydrazine, propellant grade per MIL-D-25604

ABBREVIATIONS

Organization	Identification
AFOSR	Air Force Office of Scientific Research
AFRPL	Air Force Rocket Propulsion Laboratory
AGARD	Advisory Group on Aeronautical Research and Development
AIChE	American Institute of Chemical Engineers
AMRL	Aerospace Medical Research Laboratory
ASME	American Society of Mechanical Engineers
CPIA	Chemical Propulsion Information Agency
ICRPG	Interagency Chemical Rocket Propulsion Group
JANNAF	Joint Army-Navy-NASA-Air Force
P&W	Pratt & Whitney Aircraft
WPAFB	Wright-Patterson Air Force Base

REFERENCES

1. Harrje, D. T.; and Reardon, F. H., eds.: Liquid Propellant Rocket Combustion Instability. NASA SP-194, 1972.

2. Oberg, C. L.; Wong, T. L.; and Schmeltzer, R. A.: Analysis of the Acoustic Behavior of Baffled Combustion Chambers. NASA CR-72625, Rocketdyne Div., North American Rockwell Corp., January 1970.

3. Oberg, C. L.; Evers, W. H. Jr.; and Wong, T. L.: Analysis of the Wave Motion in Baffled Combustion Chambers. NASA CR-72879, Rocketdyne Div., North American Rockwell Corp., October 1971.

4. Oberg, C. L.; et al.: Analysis of the Effects of Baffles on Combustion Instability. NASA CR-134614, Rocketdyne Div., Rockwell International, May 1974.

5. Green, L., Jr.; Lipow, M.; and Nall, K. L.: An Experimental Study of Combustion Instability in Solid Propellant Rocket Motors. AFOSR-TN-55-233, Aerojet-General Corp. (Azusa, CA), July 1955.

6. Converse, J. W.; and Hoffman, J. D.: Acoustic Standing Waves in a Rocket Combustion Chamber With Ring and Spoke Baffles. Report No. TM-67-5, Purdue University Research Foundation (Lafayette, IN), August 1967.

7. Morse, P. M.: Vibration and Sound. Second ed., McGraw-Hill Book Co. (New York), 1948.

8. Rosen, B.; and Oberg, C. L.: Acoustic Model Studies of Baffle Configurations for the Extended Range Lance (XRL) Booster Engine. RR67-21, Rocketdyne Div., North American Aviation, Inc., December 1967.

9. Anon.: Gemini Stability Improvement Program (GEMSIP), Final Report. Vol. 5: Development Tools. SSD-TR-66-2, Aerojet-General Corp., August 1965.

*10. Kesselring, R. C.: Spartan Stability Investigation. CSM67-73, Rocketdyne Div., North American Aviation, Inc., December 1967.

11. Kesselring, R. C.; and Powell, M. F.: Stability Scaling Using a Modular Injection Concept (U). Sixth ICRPG Conf. CPIA Publ. 192, Vol. II, CPIA, December 1969. (CONFIDENTIAL)

12. Priem, R. J.; and Guentert, D. C.: Combustion Instability Limits Determined by a Nonlinear Theory and a One-Dimensional Model. NASA TN D-1409, October 1962.

13. Coultas, T. A.; and Kesselring, R. C.: Extension of the Priem Theory and Its Use in Simulation of Instability on the Computer. Second ICRPG Combustion Conf., CPIA Publ. 105, CPIA, May 1966.

---

*Dossier for design criteria monograph "Liquid Rocket Engine Combustion Stabilization Devices." Unpublished. Collected source material available for inspection at NASA Lewis Research Center, Cleveland, Ohio.

14. Hines, W. S.; et al.: Development of Injector Chamber Compatibility Analysis, Final Report. AFRPL-TR-70-12, Rocketdyne Div., North American Rockwell Corp., March 1970.

15. Dickerson, R.; Tate, K.; and Nurick, W.: Correlation of Spray Injector Parameters With Rocket Engine Performance. AFRPL-TR-68-11, Rocketdyne Div., North American Aviation, Inc., January 1968.

16. Hannum, N. P.; Bloomer, H. E.; and Goelz, R. R.: Stabilizing Effects of Several Injector Face Baffle Configurations on Screech in a 20,000-Pound Thrust Hydrogen-Oxygen Engine. NASA TN D-4515, April 1968.

17. Anon.: Design Guide for Stable H_2/O_2 Combustors. Vol. I: Design Application. Report 20672-P2D, Aerojet-General Corp., May 1970.

18. Smith, A. J. Jr.; Reardon, F. H.; et al.: The Sensitive Time Lag Theory and Its Application to Liquid Rocket Combustion Instability Problems. AFRPL-TR-67-314, Vol. 1, Aerojet-General Corp., March 1968.

19. Crocco, L.; et al.: Nonlinear Aspects of Combustion Instability in Liquid Propellant Rocket Motors. NASA CR 72426, Dept. Aerospace and Mechanical Sciences, Princeton Univ. (Princeton, NJ), June 1968.

20. Clayton, R. M.: Baffle Performance with High-Impedance Injectors. 7th JANNAF Combustion Meeting. CPIA Publ. 204, Vol. I, CPIA, February 1971, pp. 797-809.

21. Oberg, C. L.; et al.: Lunar Module Ascent Engine Acoustic Cavity Study. Rep. R-7935, Rocketdyne Div., North American Rockwell, August 1969.

22. Sirignano, W. A.; and Strahle, W. C.: A New Concept in Rocket Engine Baffles. AIAA J., vol. 3, no. 5, May 1965, pp. 954-6.

23. Fontaine, R. J.; Levine, R. S.; and Combs, L. P.: Secondary Non-Destructive Instability in Medium Size Liquid Fuel Rocket Engines. Advances in Tactical Rocket Propulsion, AGARD Conf. Proc. No. 1, S. S. Penner, ed., Technivision Services (Maidenhead, England), 1968, pp. 383-402.

24. Waugh, R. C.; McCallister, D. A.; and McBride, J. M.: A Mathematical Model for Transverse Mode Instability with Feed System Coupling for Titan III. Fifth ICRPG Combustion Conf., CPIA Publ. 183, CPIA, December 1968, pp. 59-64.

25. Waugh, R. C.; and Reardon, F. H.: Feed System Effects on Combustion Instability. Bulletin of the Fifth Liquid Propulsion Symposium, CPIA Publ. 37, Vol. II, CPIA, December 1963, pp. 843-862.

26. Anon.: Gemini Stability Improvement Program (GEMSIP), Final Report. Vol. 1: Summary. SSD-TR-66-2, Aerojet-General Corp., August 1965.

27. Levine, R. S.: Experimental Status of High-Frequency Liquid Rocket Combustion Instability. Tenth Symposium (International) on Combustion, The Combustion Institute (Pittsburgh, PA), 1965, pp. 1083-1089.

28. Clapp, S. D.; Nurick, W. H.. and Arbit, H. A.: Definition of Thrust Chamber-Injector Design Criteria for High Performance with the CTF/Gelled Boron Fuel Propellant Combination (U). Paper presented at the 10th Liquid Propulsion Symposium (Las Vegas, NV), November 19-21, 1968. (CONFIDENTIAL)

29. Anon.: Gemini Stability Improvement Program (GEMSIP), Final Report. Vol. 4: Baffle Design Studies. SSD-TR-66-2, Aerojet-General Corp., August 1965.

30. Reardon, F. H.: Guideline for Combustion Stability Specifications and Verifications Procedure for Liquid Propellant Rocket Engines. CPIA Publ. 247, CPIA, October 1973.

31. Harrje, D. T.: Navy Case 31127 Patent, Recorded Oct. 17, 1963.

32. Schmidt, H. W.: Handling and Use of Fluorine and Fluorine-Oxygen Mixtures in Rocket Systems. NASA SP-3037, 1967.

33. Perlee, H. E.; and Christos, T.: Summary of Literature Survey of Hypergolic Ignition Spike Phenomena, Phase I, Final Report. NASA CR-78986, December 1965.

34. Combs, L. P.; et al.: Improvement of Bombs and Pulse Guns as Combustion Stability Rating Devices. AFRPL-TR-68-18, Rocketdyne Div., North American Aviation, Inc., March 1968.

35. Weiss, R. R.; and Klopotek, R. D.: Experimental Evaluation of the Titan III Transtage Engine Combustion Stability Characteristics. AFRPL-TR-66-51, Air Force Rocket Propulsion Laboratory, March 1966.

36. Hines, W. S.; et al.: Extension of a Thrust Chamber Compatibility Model. AFRPL TR-72-19, Rocketdyne Div., North American Rockwell Corp., March 1972.

*37. Dray, B. J.: Thermophysics Note No. 57: Thermal Analysis Program (TAP) User's Manual, Fortran II Version. NAA-SR-TDR-11812, North American Aviation, Inc., January 1966.

38. Bartz, D. R.: A Simple Equation for Rapid Estimation of Rocket Nozzle Convective Heat Transfer Coefficients. Jet Propulsion, vol. 27, 1957, pp. 49-51.

---

*Dossier for design criteria monograph "Liquid Rocket Engine Combustion Stabilization Devices." Unpublished. Collected source material available for inspection at NASA Lewis Research Center, Cleveland, Ohio.

39. Seader, J. D.; Miller, W. S.; and Kalvinskas, L. A.: Boiling Heat Transfer for Cryogenics. NASA CR-243, June 1965.

40. McCarthy, J. R.; Hines, W. S.; Seader, J. D.; and Trebes, D. M.: Regenerative Cooling Characteristics. Bulletin of the 6th Liquid Propulsion Symposium, Vol. 1, CPIA, Sept. 22-25, 1964.

41. Carpenter, H. W.: Design and Testing of Protective Coatings for the J-2X Film Coolant Ring. Res. Rep. 66-31, Rocketdyne Div., North American Aviation, Inc., September 1966.

42. Carpenter, H. W.: Protective Coating System for a Regeneratively Cooled Thrust Chamber, Tasks I and II, Final Report. NASA CR-72569, January 1969.

43. Anon.: Designer's Guide and Computer Program for Ablative Materials in Liquid Rocket Thrust Chambers. AFRPL-TR-159, Air Force Rocket Propulsion Laboratory, June 1967.

*44. Kusak, L.: Final Report: Lance XRL Thrust Vector Control System Experimental Program. RM1327-343, Rocketdyne Div., North American Aviation, Inc., November 1967.

45. Levine, R. S.; and Lawhead, R. B.: Rocketdyne Engine Vibration Studies – Final Summary Report. Project MX913, Contract AF33(038)-19430, Rocketdyne Div., North American Aviation, Inc., July 1953.

46. Oberg, C. L.; Wong, T. L.; and Ford, W. M.: Evaluation of Acoustic Cavities for Combustion Stabilization. NASA CR-115087, Rocketdyne Div., North American Rockwell Corp., July 1971.

47. Phillips, B.: Recent Advances in Acoustic Liner Technology at the Lewis Research Center. Fifth ICRPG Combustion Conf., CPIA Publ. 183, CPIA, December 1968, pp. 343-350.

48. Garrison, G. D.: A Study of the Suppression of Combustion Oscillations With Mechanical Damping Devices – Phase II Summary Report. PWA FR-1922. Pratt & Whitney Aircraft, Florida Res. and Dev. Center (W. Palm Beach, FL), July 1966.

49. Anon.: F-1 Engine Acoustic Absorber Task, Final Report (U). Rocketdyne Div., North American Aviation, Inc., July 1967. (CONFIDENTIAL)

50. Timoshenko, S.; and Woinowski-Krieger, S.: Theory of Plates and Shells. Second ed., McGraw-Hill Book Co. (New York), 1959.

51. Seader, J. D.; and Wagner, W. R.: Regenerative Cooling of Rocket Engines. Chem. Eng. Prog. Symp. Series, vol. 60, no. 52, AIChE (New York), 1964, pp. 130-150.

---

*Dossier for design criteria monograph "Liquid Rocket Engine Combustion Stabilization Devices." Unpublished. Collected source material available for inspection at NASA Lewis Research Center, Cleveland, Ohio.

52. Anon.: Liquid Rocket Engine Fluid-Cooled Combustion Chambers. NASA Space Vehicle Design Criteria Monograph, NASA SP-8087, April 1972.

53. Garrison, G. D.: Acoustic Liners for Storable Propellant Rocket Chambers—Phase I Final Report (U). AFRPL-TR-67-205, Pratt & Whitney Aircraft, Florida Res. and Dev. Center (W. Palm Beach, FL), July 1967. (CONFIDENTIAL)

54. Garrison, G. D.: Absorbing Liners for Rocket Combustion Chambers. Theory and Design Techniques (U). AFRPL-TR-66-234, PWA FR-1007, Pratt & Whitney Aircraft, Florida Res. and Dev. Center, (W. Palm Beach, FL), August 1966. (CONFIDENTIAL)

55. Bailey, C. R.: An Investigation of the Use of Acoustic Energy Absorbers to Damp LOX/RP-1 Combustion Oscillations. NASA TN D-4210, 1967.

56. Anon.: Advanced Throttling Concept Study. AFRPL-TR-98, PWA FR-1279, Pratt & Whitney Aircraft, Florida Res. and Dev. Center (W.Palm Beach, FL), March 1965.

57. Garrison, G. D.: A Study of the Suppression of Combustion Oscillations With Mechanical Damping Devices — Final Report. PWA FR-2596, Pratt & Whitney Aircraft, Florida Res. and Dev. Center (W. Palm Beach, FL), November 1967.

58. Cantrell, R. H.; and Hart, R. W.: Interaction Between Sound and Flow in Acoustic Cavities: Mass, Momentum, and Flow Considerations. J. Acoust. Soc. Am., vol. 36, 1964, pp. 697-706.

59. Oberg, C. L.; Hines, W. S.; and Falk, A. Y.: High-Temperature Earth-Storable-Propellant Acoustic Cavity Technology. Final Report R-9401, Rocketdyne Div., Rockwell International, May 1974.

60. Anon.: Acoustic Liner Feasibility Program, Final Report. Rep. 8852-FR, Aerojet Liquid Rocket Co., June 1970.

61. Anon..: Chamber Technology for Space Storable Propellants, Task II. R-6028-2, Rocketdyne Div., North American Aviation, Inc., October 1963.

62. Conn, T. E.; Hester, J. N.; and Valentine, R. S.: Environmental Effects Upon Rocket Injector/Chamber Compatibility. J. Spacecraft Rockets, vol. 4, no. 12, December 1967, pp. 1581-1585.

63. Anon.: FLOX-Diborane Technology — Boundary Reactions. Final Report 659-F, Contract NAS7-659, Aerojet-General Corp. (Sacramento, CA), September 1969.

64. Sutton, R. D.; Hines, W. S.; and Combs, L. P.: Comprehensive Analysis of Liquid Rocket Combustion Processes. Paper presented at the 6th AIAA Joint Propulsion Specialists Conf. (San Diego, CA), June 1970.

65. Haugen, R. L.; and Dhanak, A. M.: Momentum Transfer in Turbulent Separated Flow Past a Rectangular Cavity. J. Appl. Mech., Trans. ASME, Series E, vol. 88, 1966, pp. 641-646.

66. Hatch, J. E.; and Papell, S. S.: Use of a Theoretical Flow Model To Correlate Data for Film Cooling or Heating an Adiabatic Wall by Tangential Injection of Gases of Different Fluid Properties. NASA TN D-130, November 1959.

67. Garrison, G. D.; et al.: Suppression of Combustion Oscillations with Mechanical Damping Devices. Interim Report, PWA FR-3299, Pratt & Whitney Aircraft, Florida Res. and Dev. Center (W. Palm Beach, FL), August 1969.

68. Anon.: Supression of Combustion Oscillations with Mechanical Damping Devices. Final Report, PWA FR-4993, Pratt & Whitney Aircraft, Florida Res. and Dev. Center (W. Palm Beach, FL), June 1972.

69. Oberg, C. L.; and Kuluva, N. M.: Acoustic Liners for Large Engines. Rep. R-7792, Rocketdyne Div., North American Rockwell Corp., March 1969.

70. Hart, R. W.; and McClure, F. T.: Theory of Acoustic Instability in Solid Propellant Rocket Combustion. Tenth Symposium (International) on Combustion, The Combustion Institute (Pittsburgh, PA), 1965, pp. 1047-1065.

71. Morse, P. M.; and Ingard, K. U.: Theoretical Acoustics. McGraw-Hill Book Co. (New York), 1968.

72. Priem, R. J.; and Rice, E. J.: Combustion Instability With Finite Mach Number Flow and Acoustic Liners. NASA TM X-52412, 1968.

73. Mitchell, C. E.; et al.: Stability of Combustors with Partial Length Acoustic Liners. NASA CR-120889, Colorado State Univ. (Fort Collins, CO), March 1972.

74. Mitchell, C. E.; and Baer, M. R.: Stability of Lined Combustors with Continuous Combustion Distributions. 10th JANNAF Combustion Meeting, CPIA Publ. 243, Vol. II, CPIA, December 1973, pp. 255-270.

75. Oberg, C. L.; Kesselring, R. C.; and Warner, C. III: Analysis of Combustion Instability in Liquid Propellant Engines With or Without Acoustic Cavities. R-9353, Rocketdyne Div., Rockwell International, June 1974.

76. Sirignano, W. A.; et al.: Acoustic Liner Studies. Third ICRPG Combustion Conf., CPIA Publ. 138, Vol. I, February 1967, pp. 581-585. [Also: Nonlinear Aspects of Combustion Instability in Liquid Propellant Rocket Motors, Rep. 553-f, Dept. Aerospace and Mechanical Sciences, Princeton Univ. (Princeton, NJ) 1966.]

77. McMillion, R. L.; and Nestlerode, J. A.: Design Criterion for Acoustic Absorbers. 8th JANNAF Combustion Meeting, CPIA Publ. 220, Vol. I, CPIA, November 1971, pp. 817-823.

78. Berl, G. O.; and Ensminger, J.: Evaluation of Acoustic Liners in 35,000 lbf Thrust Storable Propellant Rocket Engines. AFRPL-TR-69-212, Air Force Rocket Propulsion Laboratory, October 1969.

110

79. Garrison, G. D.; et al.: Acoustic Liner Design and Demonstration, Final Report (U). AFRPL-TR-71-75, Pratt & Whitney Aircraft, Florida Res. and Dev. Center (W. Palm Beach, FL), August 1971.(CONFIDENTIAL)

80. Anon.: Acoustic Liners for Storable Propellant Rocket Chambers – Phase II, Final Report (U). AFRPL-TR-68-118, Pratt & Whitney Aircraft, Florida Res. and Dev. Center (W. Palm Beach, FL), August 1968.(CONFIDENTIAL)

81. Vincent, D. W.; Phillips, B.; and Wanhainen, J. P.: Experimental Investigation of Acoustic Liners to Suppress Screech in Storable-Propellant Rocket Motors. NASA TN D-4442, March 1968.

82. Phillips, B.: Experimental Investigation of an Acoustic Liner With Variable Cavity Depth. NASA TN D-4492, April 1968.

83. Senneff, J. M.; and Berman, K.: Stability Investigation Relating to Bell/LM Ascent Engine. Sixth ICRPG Combustion Conf., CPIA Publ. 192, CPIA, December 1969, pp. 317-327.

84. Bailey, C. R.: Acoustic Liner for the C-1 Engine. Fifth ICRPG Combustion Conf., CPIA Publ. 183, CPIA, December 1968, pp. 335-341.

85. Briley, G. L.; and Shuster, E. B.: Nonconventional Injector Development for Flexible Energy Management With CPF/MHF-7 (U). 8th JANNAF Combustion Meeting, CPIA Publ. 220, Vol. II, November 1971, pp. 189-216. (CONFIDENTIAL)

86. Nestlerode, J. A.; and Oberg, C. L.: Combustion Instability in an Annular Engine. Proc. Sixth ICRPG Combustion Conf., CPIA Publ. 192, December 1969.

87. Sivian, L. J.: Acoustic Impedance of Small Orifices. J. Acoust. Soc. Am., vol. 7, no. 2, October 1935, pp. 94-101.

88. Phillips, B.; and Morgan, C. J.: Mechanical Absorption of Acoustic Oscillations in Simulated Rocket Combustion Chambers. NASA TN D-3792, 1967.

89. Oberg, C. L.; Hines, W. S.; and Kusak, L.: Advanced Acoustic Cavity Technology. R-9136, Rocketdyne Div., Rockwell International, June 1974.

90. Anon.: Interim Phase Report, Design Feasibility Test Phase of the Lunar Module Ascent Engine Program. R-7460, Rocketdyne Div., North American Aviation, Inc., July 1968.

91. Beranek, L. L.: Acoustic Measurements. John Wiley & Sons, Inc., 1949, pp. 408-9.

92. Anon.: Liquid Rocket Engine Injectors. NASA Space Vehicle Design Criteria Monograph, NASA SP-8090 (to be published).

93. Ingard, U.: On the Theory and Design of Acoustic Resonators. J. Acoust. Soc. Am., vol. 25, no. 6, November 1953, pp. 1037-1061.

111

94. Oberg, C. L.; et al.: Solid Propellant Combustion Instability Suppression Devices. AFRPL-TR-72-21, Vol. I, Rocketdyne Div., North American Rockwell Corp., June 1972.

95. Ingard, U.; and Ising, H.: Acoustic Nonlinearity of an Orifice. J. Acoust. Soc. Am., vol. 42, no. 1, 1967, pp. 6-17.

96. Garrison, G. D.; et al.: A Study of the Suppression of Combustion Oscillations with Mechanical Damping Devices – Interim Report. PWA FR-3299, Pratt & Whitney Aircraft, Florida Res. and Dev. Center (W. Palm Beach, FL), August 1969.

97. Ingard, U.: Absorption Characteristics of Nonlinear Acoustic Resonators. J. Acoust. Soc. Am., vol. 44, no. 4, 1968, pp. 1155-1156.

98. Meyer, E.; et al.: Experiments on the Influence of Flow on Sound Attenuation in Absorbing Ducts. J. Acoust. Soc. Am., vol. 30, no. 3, March 1958, pp. 165-174.

99. Mechel, F.; and Schilz, W.: Research on Sound Propagation in Sound-Absorbent Ducts With Superimposed Air Streams. AMRL-TDR-62-140(II), Biomedical Laboratory (WPAFB, OH) December 1962.

100. Phillips, B.: Acoustic Liner Studies at the Lewis Research Center. Fourth ICRPG Combustion Conf., CPIA Publ. 162, CPIA, December 1967.

101. Westervelt, P. J.: Acoustic Impedance in Terms of Energy Functions. J. Acoust. Soc. Am., vol. 23, no. 3, May 1951, pp. 347-348.

112

NASA SPACE VEHICLE DESIGN CRITERIA
MONOGRAPHS ISSUED TO DATE

ENVIRONMENT

SP-8005	Solar Electromagnetic Radiation, Revised May 1971
SP-8010	Models of Mars Atmosphere (1967), May 1968
SP-8011	Models of Venus Atmosphere (1972), Revised September 1972
SP-8013	Meteoroid Environment Model—1969 (Near Earth to Lunar Surface), March 1969
SP-8017	Magnetic Fields—Earth and Extraterrestrial, March 1969
SP-8020	Mars Surface Models (1968), May 1969
SP-8021	Models of Earth's Atmosphere (90 to 2500 km), Revised March 1973
SP-8023	Lunar Surface Models, May 1969
SP-8037	Assessment and Control of Spacecraft Magnetic Fields, September 1970
SP-8038	Meteoroid Environment Model—1970 (Interplanetary and Planetary), October 1970
SP-8049	The Earth's Ionosphere, March 1971
SP-8067	Earth Albedo and Emitted Radiation, July 1971
SP-8069	The Planet Jupiter (1970), December 1971
SP-8084	Surface Atmospheric Extremes (Launch and Transportation Areas), Revised June 1974.
SP-8085	The Planet Mercury (1971), March 1972
SP-8091	The Planet Saturn (1970), June 1972
SP-8092	Assessment and Control of Spacecraft Electromagnetic Interference, June 1972
SP-8103	The Planets Uranus, Neptune, and Pluto (1971), November 1972

| SP-8105 | Spacecraft Thermal Control, May 1973 |

STRUCTURES

SP-8001	Buffeting During Atmospheric Ascent, Revised November 1970
SP-8002	Flight-Loads Measurements During Launch and Exit, December 1964
SP-8003	Flutter, Buzz, and Divergence, July 1964
SP-8004	Panel Flutter, Revised June 1972
SP-8006	Local Steady Aerodynamic Loads During Launch and Exit, May 1965
SP-8007	Buckling of Thin-Walled Circular Cylinders, Revised August 1968
SP-8008	Prelaunch Ground Wind Loads, November 1965
SP-8009	Propellant Slosh Loads, August 1968
SP-8012	Natural Vibration Modal Analysis, September 1968
SP-8014	Entry Thermal Protection, August 1968
SP-8019	Buckling of Thin-Walled Truncated Cones, September 1968
SP-8022	Staging Loads, February 1969
SP-8029	Aerodynamic and Rocket-Exhaust Heating During Launch and Ascent May 1969
SP-8030	Transient Loads From Thrust Excitation, February 1969
SP-8031	Slosh Suppression, May 1969
SP-8032	Buckling of Thin-Walled Doubly Curved Shells, August 1969
SP-8035	Wind Loads During Ascent, June 1970
SP-8040	Fracture Control of Metallic Pressure Vessels, May 1970
SP-8042	Meteoroid Damage Assessment, May 1970
SP-8043	Design-Development Testing, May 1970
SP-8044	Qualification Testing, May 1970

SP-8045	Acceptance Testing, April 1970
SP-8046	Landing Impact Attenuation for Non-Surface-Planing Landers, April 1970
SP-8050	Structural Vibration Prediction, June 1970
SP-8053	Nuclear and Space Radiation Effects on Materials, June 1970
SP-8054	Space Radiation Protection, June 1970
SP-8055	Prevention of Coupled Structure-Propulsion Instability (Pogo), October 1970
SP-8056	Flight Separation Mechanisms, October 1970
SP-8057	Structural Design Criteria Applicable to a Space Shuttle, Revised March 1972
SP-8060	Compartment Venting, November 1970
SP-8061	Interaction with Umbilicals and Launch Stand, August 1970
SP-8062	Entry Gasdynamic Heating, January 1971
SP-8063	Lubrication, Friction, and Wear, June 1971
SP-8066	Deployable Aerodynamic Deceleration Systems, June 1971
SP-8068	Buckling Strength of Structural Plates, June 1971
SP-8072	Acoustic Loads Generated by the Propulsion System, June 1971
SP-8077	Transportation and Handling Loads, September 1971
SP-8079	Structural Interaction with Control Systems, November 1971
SP-8082	Stress-Corrosion Cracking in Metals, August 1971
SP-8083	Discontinuity Stresses in Metallic Pressure Vessels, November 1971
SP-8095	Preliminary Criteria for the Fracture Control of Space Shuttle Structures, June 1971
SP-8099	Combining Ascent Loads, May 1972
SP-8104	Structural Interaction With Transportation and Handling Systems, January 1973

115

GUIDANCE AND CONTROL

SP-8015	Guidance and Navigation for Entry Vehicles, November 1968
SP-8016	Effects of Structural Flexibility on Spacecraft Control Systems, April 1969
SP-8018	Spacecraft Magnetic Torques, March 1969
SP-8024	Spacecraft Gravitational Torques, May 1969
SP-8026	Spacecraft Star Trackers, July 1970
SP-8027	Spacecraft Radiation Torques, October 1969
SP-8028	Entry Vehicle Control, November 1969
SP-8033	Spacecraft Earth Horizon Sensors, December 1969
SP-8034	Spacecraft Mass Expulsion Torques, December 1969
SP-8036	Effects of Structural Flexibility on Launch Vehicle Control Systems, February 1970
SP-8047	Spacecraft Sun Sensors, June 1970
SP-8058	Spacecraft Aerodynamic Torques, January 1971
SP-8059	Spacecraft Attitude Control During Thrusting Maneuvers, February 1971
SP-8065	Tubular Spacecraft Booms (Extendible, Reel Stored), February 1971
SP-8070	Spaceborne Digital Computer Systems, March 1971
SP-8071	Passive Gravity-Gradient Libration Dampers, February 1971
SP-8074	Spacecraft Solar Cell Arrays, May 1971
SP-8078	Spaceborne Electronic Imaging Systems, June 1971
SP-8086	Space Vehicle Displays Design Criteria, March 1972
SP-8096	Space Vehicle Gyroscope Sensor Applications, October 1972

116

SP-8098	Effects of Structural Flexibility on Entry Vehicle Control Systems, June 1972
SP-8102	Space Vehicle Accelerometer Applications, December 1972

CHEMICAL PROPULSION

SP-8087	Liquid Rocket Engine Fluid-Cooled Combustion Chambers, April 1972
SP-8107	Turbopump Systems for Liquid Rocket Engines, August 1974
SP-8109	Liquid Rocket Engine Centrifugal Flow Turbopumps, December 1973
SP-8052	Liquid Rocket Engine Turbopump Inducers, May 1971
SP-8110	Liquid Rocket Engine Turbines, January 1974
SP-8081	Liquid Propellant Gas Generators, March 1972
SP-8048	Liquid Rocket Engine Turbopump Bearings, March 1971
SP-8101	Liquid Rocket Engine Turbopump Shafts and Couplings, September 1972
SP-8100	Liquid Rocket Engine Turbopump Gears, March 1974
SP-8088	Liquid Rocket Metal Tanks and Tank Components, May 1974
SP-8094	Liquid Rocket Valve Components, August 1973
SP-8097	Liquid Rocket Valve Assemblies, November 1973
SP-8090	Liquid Rocket Actuators and Operators, May 1973
SP-8080	Liquid Rocket Pressure Regulators, Relief Valves, Check Valves, Burst Disks, and Explosive Valves, March 1973
SP-8064	Solid Propellant Selection and Characterization, June 1971
SP-8075	Solid Propellant Processing Factors in Rocket Motor Design, October 1971
SP-8076	Solid Propellant Grain Design and Internal Ballistics, March 1972
SP-8073	Solid Propellant Grain Structural Integrity Analysis, June 1973
SP-8039	Solid Rocket Motor Performance Analysis and Prediction, May 1971

117

SP-8051   Solid Rocket Motor Igniters, March 1971

SP-8025   Solid Rocket Motor Metal Cases, April 1970

SP-8041   Captive-Fired Testing of Solid Rocket Motors, March 1971